Development and Testing of Novel Sensor Systems for Real-Time Automated Data Collection and Monitoring with Focus in Non-Motorized Facilities

Asad Lesani

Department of Civil Engineering and Applied Mechanics

McGill University, Montreal

December 2018

A thesis submitted to McGill University in partial fulfillment of the requirements of the degree of Doctor of Philosophy in Engineering.

TABLE OF CONTENTS

LIST OF FIGURES

LIST OF TABLES

ABSTRACT

Recently, decision makers have tried to develop smart city frameworks that can help optimize infrastructure usage and increase the quality of life for citizens. An intelligent transportation system (ITS) is a key element of any smart city platform. An ITS requires monitoring and data analysis capabilities to better understand the real-time conditions of the road network using different types of sensory systems. Ultimately, an ITS can optimize the network capacity based on the mobility information collected. For traffic monitoring, many technologies have been developed in recent years including traditional magnetic detectors or pneumatic tubes for vehicle or bicycle traffic, infrared- or image-based sensors, etc. Such systems have several limitations, such as high installation and maintenance costs, low accuracy, issues in performance under different weather and lighting conditions, and a lack of detailed information about the mode and class of the object in multi-modal traffic networks. Traditionally, a single mode was considered in vehicle-based traffic network monitoring. More recent studies are analyzing multi-modal networks in which the interaction between all modes (pedestrian, cyclist and vehicle) are considered. However, some elements of multimodal traffic monitoring systems remain missing in the research and development of multimodal traffic monitoring systems.

The general objective of this thesis work is to develop two categories of monitoring technologies, between-point and fixed-point systems, as complementary components of a multi-modal traffic monitoring system. This thesis introduces a between-point monitoring system using an embedded WiFi-Bluetooth scanning system. The detection rate of both technologies has been compared. The results show that, in vehicular networks, the accuracy of travel time estimation can be improved by adding WiFi detected samples to the traditional Bluetooth-based systems. The same system was used to monitor a mixed pedestrian/cyclist network and to classify the objects using WiFi traces captured by sensors. The test results show that with the combined classification model, the algorithm could classify the objects correctly in 96% of the cases. The high correlation between the number of trips detected with WiFi signals and the flow of the pedestrians, as ground truth, demonstrates the potential of using the proposed system in flow extrapolation.

To complement the proposed between-point monitoring system, this thesis introduces two types of fixed-point counting systems based on Lidar technology. The first system functions based on single beam Lidar technology. The system is easy to install, accurate and robust in different

weather and lighting conditions and addresses a shortcoming among commercially available counting technologies. The test results show an average directional count error of less than 5% for pedestrians and 2% for cyclists. All counting technologies that are installed from the side undercount because of occlusion. The problem of occlusion is particularly problematic along wide pedestrian sidewalks with high pedestrian volumes. To address this issue, another counting system, based on 2D Lidar technology, installed above and facing down, was developed in this thesis. This technology has improved performance over the 1D Lidar in environments with high pedestrian volumes. Additionally, this technology can be used in mixed mode networks; the shape of the object can be used in classification. The test results show an average absolute percent error of less than 5% when counting pedestrians on sidewalks with high flows and dense clusters.

RÉSUMÉ

Récemment, les décideurs ont essayé de développer des systèmes de villes intelligentes pouvant aider à optimiser l'utilisation des infrastructures et à améliorer la qualité de vie des citoyens. Un système de transport intelligent (STI), est un élément clé de toutes les plates-formes de ville intelligente. Un STI nécessite des capacités de surveillance et d'analyse des données afin de mieux comprendre les conditions du réseau routier en temps réel, et ce en utilisant différents types de systèmes sensoriels. En fin de compte, un STI peut optimiser la capacité du réseau en fonction des informations de mobilité collectées. Pour la surveillance du trafic, de nombreuses technologies ont été développées ces dernières années, notamment des détecteurs magnétiques traditionnels ou des tubes pneumatiques pour la circulation des véhicules ou des vélos, des capteurs infrarouges ou basés sur des images, etc. Ces systèmes ont plusieurs limitations, telles que des coûts d’installation et d’entretien élevés, un manque de précision, des problèmes de performances dans différentes conditions météorologiques et d'éclairage, et un manque d'informations détaillées sur le mode et la classe de l'objet dans les réseaux de transport multimodal. Traditionnellement, les véhicules étaient le seul mode de transport pris en compte dans la surveillance du réseau de circulation. Les études plus récentes analysent les réseaux multimodaux dans lesquels l’interaction entre tous les modes (piéton, cycliste et véhicule) est prise en compte. Toutefois, certains éléments demeurent absents dans la recherche et développement de systèmes de surveillance du trafic multimodal.

L'objectif général des travaux de cette thèse est de développer deux catégories de technologies de surveillance, un système d’entre-points et un système de points fixes, en tant que composants complémentaires à un système de surveillance du trafic multimodal. Cette thèse présente un système de surveillance d’entre-points utilisant un système de numérisation WiFi-Bluetooth intégré. Le taux de détection des deux technologies a été comparé, et les résultats du test montrent qu'avec le modèle de classification combiné, l'algorithme pourrait classifier les objets correctement dans 96% des cas. La corrélation élevée entre le nombre de déplacements détectés avec des signaux WiFi et le flux de piétons réel observé démontre le potentiel de l’utilisation du système proposé dans le but d’extrapoler des flux.

Pour compléter le système de surveillance d’entre-points proposé, cette thèse introduit deux types de systèmes de comptage de points fixes basés sur la technologie Lidar. Le premier système fonctionne sur la technologie Lidar à faisceau unique. Ce système est facile à installer, précis et

robuste dans différentes conditions météorologique et d'éclairage, et corrige une lacune parmi les technologies de comptage disponibles sur le marché. Les résultats du test montrent une erreur de comptage directionnel moyenne inférieure à 5% pour les piétons et à 2% pour les cyclistes. Toutes les technologies de comptage installées latéralement par rapport à la zone d'analyse obtiennent des sous-dénombrements en raison d'occlusions. Le problème de l'occlusion est particulièrement problématique le long des trottoirs piétons larges avec un volume de passage élevé. Pour résoudre ce problème, un autre système de comptage basé sur la technologie 2D Lidar, installé au-dessus et orienté vers le bas, a été développé dans cette thèse. Cette technologie a amélioré les performances par rapport au Lidar 1D dans les environnements très fréquentés par les piétons. En outre, elle peut être utilisée dans des réseaux à mode de transport mixte, la forme de l'objet pouvant être reconnue et classifiée. Les résultats du test montrent un pourcentage d'erreur absolu moyen inférieur à 5% lors du comptage de piétons sur des trottoirs à débits élevés et avec des groupes denses.

ACKNOWLEDGEMENTS

I would like to thank my supervisor, Luis Miranda-Moreno for his guidance and support. Without his knowledge and support, the completion of my thesis would not have been possible.

I owe thanks to a very special person, my wife, Nasim Moghim for her continued and unfailing love, support and understanding during the pursuit of my Ph.D degree, which made the completion of thesis possible.

There are several other people and agencies I would like to acknowledge, each of which played an important role in my research:

- David Bietel, Lana Samara, Taras Romancyshyn, Ehsan Nateghinia, Joshua Stipancic, Anthony Andreoli, Ting Fu, Marina Jorge Amaral and other McGill Students who helped me with the data collection.
- The "Fonds de recherche du Québec - Nature et technologies » FRQNT, Quebec Ministry of Transportation and The Natural Sciences and Engineering Research Council of Canada (NSERC).
- The City of Montreal for their support in data collection.

CONTRIBUTIONS OF AUTHORS

Please note that this is a manuscript-based thesis consisting of two journal papers (one published and one submitted), a patent-initiated application and several peer-reviewed conference papers. The title of the articles, names of the authors, and journals or conferences are listed below. It is worth mentioning that the author of this thesis is the sole student among the co-authors of the journal papers and patent application. Furthermore, among all papers, the author of this thesis is the first author who was responsible for conducting the research development, the methodology, analyzing the data, and presenting the manuscripts. The author's supervisor Prof. Luis Miranda-Moreno, provided guidance and editorial revisions throughout the entire process. Note that minor changes (edits) have been made to the original published papers.

Asad Lesani, Luis Miranda-Moreno, "Development and Testing of a Real-Time WiFi-Bluetooth System for Pedestrian Network Monitoring, Classification and Data Extrapolation", IEEE Transactions on Intelligent Transportation Systems, Volume:20, Issue: 4, April 2019, DOI: 10.1109/TITS.2018.2854895.

Asad Lesani, Ehsan Nateghinia, Luis Miranda-Moreno, "Designing a 2D Lidar Based Real-Time Pedestrian Counting System for High-Volume Conditions", submitted for publication: Transportation Research Part C: Emerging Technologies

Asad Lesani, Luis Miranda Moreno, "Pedestrian/cyclists counting system using Lidar technology", Patent application, Disclosure Number D2018-0070

Asad Lesani, Ehsan Nateghinia, Luis Miranda-Moreno, "Development and Evaluation of a 2D Lidar Real-Time Pedestrian Counting System for High-Volume Conditions", 97th Annual Meeting of the Transportation Research Board.

Asad Lesani, Anthony Andreoli, Luis F. Miranda-Moreno, "Development and Testing of an Laser-Based Automated Pedestrian/Cyclist Counting System", 96th Annual Meeting of the Transportation Research Board.

Asad Lesani, Luis F. Miranda-Moreno, "Development and Testing of a Real-Time WiFi-Bluetooth System for Pedestrian Network Monitoring and Data Extrapolation", 95th Annual Meeting of the Transportation Research Board, January 2016

Asad Lesani, Taras Romancyshyn, Luis F. Miranda-Moreno, "Arterial Traffic Monitoring Using an Integrated WiFi-Bluetooth System", 95th Annual Meeting of the Transportation Research Board, January 2016

Asad Lesani, Luis F. Miranda-Moreno, Ting Fu, Taras Romancyshyn, "Development and Testing of an Ultrasonic-Based Pedestrian Counting System", 94th Annual Meeting of the Transportation Research Board, January 2015

GLOSSARY OF TERMS

ARM Processor: is one of a family of processing units, which is based on RISC (Reduces Instruction Set Commuters) architecture developed by Advance RISC Machines.

Average Travel Time: The average length of time taken to travel from point A to point B.

Bluetooth: a wireless technology standard for exchanging data over short distances.

Classification: dividing the object into one of the corresponding categories: pedestrian, cyclist or vehicle.

Counting Systems: technologies, which can provide user flow in traffic networks.

Detection rate: the number of identified users divided by a total number of objects in the coverage area of a sensor.

Inductive Loop Detectors: a technology measuring the variation of an electromagnetic field. Inductive loop detectors use that information to detect the presence of an object built from metal.

Infrared: region of the electromagnetic radiation spectrum where wavelengths range from approximately 700 nanometers (nm) to 1 millimeter (mm). Infrared-based sensors monitor the variation of infrared signals and detect the presence of the object based on measured variation.

ITS: intelligent transportation systems include advanced and innovative technologies to better monitor transportation systems and act based on the collected data.

Lidar technology: a technology, which uses the light flight time through the air to measure the distance to objects. There are three types of Lidar sensors: single-beam, which emits one laser beam at a time, 2-dimensional (2D), which emits multiple parallel laser beams to monitor a line rather than a single point, and 3-dimensional (3D), which simultaneously emits multiple beams along two different axes to generate a 3D map.

MAC Address: an identifier assigned to a wireless device by the manufacturers. This address includes six (6) characters for the manufacturer ID and six (6) characters for the device, which are unique for each device.

Multi-Modal Traffic Network: A traffic network in which at least two different classes of objects (pedestrian, cyclist, vehicle) exists.

Non-motorized traffic: any form of transportation that provides personal or mobility goods by methods other than combustion motors.

Occlusion: when two or more objects adjacent to one another (side by side) make it difficult for technologies installed from the side to identify all of them. The closest object effectively masks all objects from being detected.

Origin-Destination Study: a study used to determine travel patterns of traffic during a typical day.

Passive and Active Scanning: During an active scan, the sensor transmits a request signal and listens for a response from a wireless device. During a passive scan, the sensor simply listens for probe signals sent periodically by a wireless device.

WiFi protocol: a technology for radio wireless local area networking of devices based on IEEE 802.11 standard, mainly used in high-speed data transmission and internet.

Wireless Network Scanner: a system that records wireless signals emitted by wireless devices and processes them to extract the unique ID of the wireless device.

Chapter 1: Introduction

This chapter presents a brief introduction of the concept of intelligent transportation systems (ITS) in the context of smart city applications. The chapter focuses on automated data collection for motorized and non-motorized traffic monitoring systems and includes a literature review on ITS as well as the contributions and objectives of this work.

1.1 GENERAL CONTEXT

It is estimated that more than six billion people will be living in urban areas by the year 2050, representing about 75% of the global population. The concentration of individuals in cities creates many opportunities; however, urbanization also creates its own challenges, such as congestion, poor air quality, road injuries, etc. With the significant growth of cities and the issues related to urban mobility, local governments are looking for solutions to improve the quality of life of its citizens. Active transportation, such as walking and cycling, has gained momentum in recent years (Bagloee et al. 2016, Dong et al. 2016, Hipp et al. 2017, Pucher and Dijkstra 2003, Staunton et al. 2003). The cycling ridership and network size have risen sharply in the last decade in many North American cities. With the promotion of non-motorized transportation, the diversity and use of alternative modes has increased, resulting in more complex traffic conditions, with higher volumes, higher traffic mix, and, thus, more dangerous interactions among road users of different modes (Caviedes and Figliozzi 2018, El-Assi et al. 2017, Hamilton and Wichman 2018, Ricci 2015). To deal with the increase of demand of alternative modes of transportation, cities have been looking for innovative strategies to monitor traffic conditions and transportation infrastructure operations using sensing technologies as part of the intelligent transportation systems (ITS) (Brosnan et al. 2015, Lindsey et al. 2015, Nordback et al. 2016, Proulx et al. 2016, Ryus et al. 2014). Depending on the technology and the mode, monitoring technologies typically provide basic traffic parameters such as volumes or counts, speeds, travel times, etc. This information is often required in real-time for traffic operations.

In the search for innovative solutions for traffic monitoring, cities are leveraging the emergence of new technologies and the growth of the Internet of Things movement, (Sherly and Somasundareswari 2015, Singh et al. 2014, Zanella et al. 2014). Technological solutions can help cities understand the temporal and spatial patterns of urban mobility demand in real time not only for motor-vehicle traffic but also for non-motorized traffic. This is critical, not only for the traffic operations but also for the planning and the design of new road infrastructure that accounts for emerging modes (walking and cycling). For example, data on non-motorized mobility can provide essential information for traffic signal operation in real-time, but can also help assess the quality of service of sidewalks, bicycle facilities, streets, intersections, etc. Moreover, greater access to data can assist in the planning and design of new infrastructure, as well as in the ex-post evaluation of the impact of new infrastructure on traffic and air quality. Therefore, automated data acquisition can enable better management of traffic controls, safety, and emergency services, and it is essential in the planning and design process of the urban space and non-motorized facilities.

1.2 PROBLEM STATEMENT

Modern urban transportation networks involve complex traffic dynamics composed of non-motorized (pedestrians and bicycles) and motorized traffic flows. For the development of advanced traffic management and control systems, real-time and accurate traffic monitoring systems are crucial. These systems can collect data on traffic parameters such as flow, speed, density, travel time, etc. These parameters are monitored not only for motorized but for non-motorized modes in the road network and/or in transportation facilities such as airports and terminals. In addition to roads or urban streets, other public spaces (such as parks, university campuses, malls, etc.) need monitoring systems that can provide a comprehensive and detailed account of human activity or flow non only for motorized but also for active modes.

In recent years, we have seen the emergence of new technologies for automated data collection and monitoring of urban transport systems. Generally, traffic monitoring systems (motorized or non-motorized) can be divided into three types:

- **Fixed-point monitoring systems:** These systems provide information based on the detection at a given point (e.g., radar, magnetic, infrared sensors). These systems are designed for vehicular traffic to obtain volumes, speeds, and other parameters at different levels of granularity at a fixed point. For active transportation, these systems mainly provide volume or count data. Magnetic (loop) detectors are very popular for bicycle traffic while counting infrared systems for pedestrian volumes.
- **Between-point monitoring systems**: Systems provide information such as travel time, origin-destination (O-D) matrices, and routes using a network of sensors. They use

technologies such as WiFi, Bluetooth, RFID, plate recognition, or other re-identification sensors. Generally, a signature (unique ID) of the user (for example MAC addresses of the user's wireless device) is detected to identify the path, travel time and origin-destination of the road users among a set of sensors located strategically in a network (Ahmed et al. 2008, Bullock et al. 2010, Malinovskiy et al. 2012, Martchouk et al. 2010).

- **GPS-based monitoring systems:** These systems are used in higher levels of data collection systems in both the real-time and offline modes, with rich information quality (not limited to one or a few point measurements) (Herring et al. 2010). However, the penetration rates and representativity of the data of GPS-based systems can be an issue.

Most of the technological development has been geared towards motor-vehicle traffic monitoring systems. Technologies for monitoring and collecting non-motorized traffic data have emerged more recently. In general, effort on data collection and monitoring systems has gone into reducing costs (acquisition and operation), increasing the granularity of data, increasing the installation flexibility in terms of data collection duration (long term vs. short term), increasing the temporal and spatial coverage, and designing real-time systems.

Of the three types of monitoring systems mentioned above, each has some advantages and shortcomings associated with respect to aspects of spatial and temporal coverage, accuracy, detection rates and efficiency in different weather and traffic conditions, and cost (Bagloee et al. 2016, Hamilton and Wichman 2018, Leduc 2008, Nordback et al. 2016, Ricci 2015). Among the commercially-available traffic monitoring systems, several are touted for their functionality, real-time implementation, and cost-effectiveness.

1.2.1 Fixed-point monitoring systems

Fixed-point monitoring systems are widespread in practice because they can be efficiently installed and implemented at a set of permanent data collection stations in a city to collect data for long periods of time. However, the traffic information collected from these systems has limited spatial coverage (Mitsakis et al. 2015). The systems are too expensive to be deployed at each facility in a large-scale network.

Among the main outcomes from fixed-point monitoring systems, traffic volume (also referred to as flow or counts) and speeds are key parameters that provide information about the network state. Depending on the transportation facility that is being studied, there are various popular fixed-point systems available in the market such as loop detectors (Cheung et al. 2005, Coifman and Kim

2009, Kwon et al. 2003), radar sensors (Davis and Mee 2002, Hutchison et al. 2010), and video-based sensors (Atev et al. 2005, Datondji et al. 2016, Robert 2009, Setchell and Dagless 2001). The accuracy of existing systems has been tested in the literature.

1.2.2 Between-point monitoring systems

Between-point monitoring systems are less expensive economically; hence larger networks can be covered in practice. These systems are often deployed for real-time data collection purposes. However, the detection rate depends on the penetration rates of technology. For instance, in the case of Bluetooth, the system can only report road users with enabled smartphones; the detection rates of Bluetooth MAC (Media Access Control) addresses that can be very low (Bhaskar et al. 2015, Friesen and McLeod 2015, Malinovskiy et al. 2012, Mei et al. 2012, Moghaddam and Hellinga 2014, Wieck 2011).

In Bluetooth monitoring systems, the typical mobility information that is reported includes travel times, paths, O-D matrices, etc. Bluetooth detectors have been widely researched for motor-vehicle traffic applications as a way of detecting Bluetooth devices such as smartphones (Agarwal et al. 2013, Barcelo et al. 2010, Day et al. 2010, Haseman et al. 2010, Omrani et al. 2013, Zoto et al. 2012). Bluetooth-based systems detect road users across multiple detection sites. Only a few applications have been explored the use of Bluetooth for non-motorized traffic; low detection rates have been documented. More recently, systems based on WiFi sniffers have been proposed as an alternative to Bluetooth (Danalet et al. 2014, Hidayat et al. 2018, Vu et al. 2010); however, very few applications have been documented for motorized and non-motorized traffic applications.

1.2.3 GPS-based monitoring systems

As a traditional travel time estimation method, probe vehicles equipped with GPS are used in the literature (Chen and Chien 2001, Li and McDonald 2002, Nantes et al. 2016, Nanthawichit et al. 2003, Wei and Forougi 2016). However, the penetration rate, temporal coverage, and special coverage of this method are limited, and it is very costly.

With the growth and ubiquity of smartphones, recent studies have used the GPS points logged by smartphones for traffic monitoring purposes. The location data can provide precise measurements of the user’s micro-scale activity. While most studies have used smartphone GPS points recorded by drivers for travel time and origin-destination studies (D'Andrea and Marcelloni 2017, Engelbrecht et al. 2015, Hu et al. 2015), a few studies have used the GPS data for monitoring the activity of the cyclists (Dabiri and Heaslip 2018, Martin et al. 2017, Montoya et al. 2015, Strauss et al. 2015). Although GPS data can provide rich micro-level information about user activity and the transportation network, it has the drawback of requiring the user to actively participate in installing the application and recording their location. Privacy issues and the contribution to the battery drain of the device are the two main concerns that users have with smartphone GPS applications. These concerns reduce the penetration rate of this method of data collection.

1.2.4 Non-motorized traffic monitoring systems

Non-motorized traffic monitoring systems are typically categorized as pedestrian or bicycle monitoring systems. There are several pedestrian counting systems that can be placed along sidewalks and at the entrances of public areas (Dharmaraju et al. 2002, Greene-Roesel et al. 2008, Lesani et al. 2015, Lindsey et al. 2013, Proulx et al. 2016). Infrared based systems are the more widely used systems, particularly due to their cost and ease of installation (Ozbay et al. 2010). Although the accuracy of infrared-based systems has been shown to be adequate in the literature, there are circumstances in which the accuracy can drop (Lesani et al. 2015). For bicycle traffic monitoring, traditional technologies such as pneumatic tubes (Brosnan et al. 2015, Nordback et al. 2016) and loop detectors (Jansen et al. 2014) have been widely used by cities. The pneumatic tubes are used mainly for temporary data collection and are easy to install, but the counting accuracy diminishes as the length of the tubes increases. The tubes are easily damaged, which translates into high maintenance cost (Nordback et al. 2016). Loop detectors are primarily used in permanent cyclists counting applications. The accuracy of loop detector systems tends to be high; however, they also typically require high maintenance and installation costs due to cutting into the pavement.

1.2.5 Research needs

Despite the advantages of each technology, some other practical and research needs have yet to be thoroughly addressed including:

- Current technologies typically target one mode, or in the case of active modes, sensors typically provide only counts. For active modes, there is a lack of technology to gather microscopic data. Non-motorized sensors often do not provide information on gap time, density and speeds.
- Current counting systems such as infrared sensors for pedestrian counting, installed from the side, suffer from an occlusion in high-density pedestrian facilities. Additionally, some

other shortcomings of infrared-based counting systems include sensitivity to temperature, short range, and the requirement of facing a wall to avoid over-counting.

- Traditional bicycle counting systems, such loop detectors, have several shortcomings, namely, the high cost of installation due to the need to cut into the pavement. Installation involves road closure. This causes interruption in traffic flow, adds additional cost for the users and makes system maintenance more difficult.
- Methods based on WiFi monitoring systems are lacking in the literature, in particular, for non-motorized networks with pedestrian and bicycle flows. The mode classification and extrapolation of MAC signals have not been addressed in the literature.
- There is a lack of development of multiple-sensor systems with the capability of reporting data in real time while covering entire networks over long periods of time. Moreover, in the current context, requirements for the monitoring of, not only vehicular traffic but also, non-motorized activity (pedestrians and bicycles) are growing. The flexibility (including wireless communication) and monetary costs (including installation and maintenance) associated with these systems are also important elements which can be improved upon.
- Many sensors have their own software and data platform, making integration into the overall system of the city very difficult.
- Many of the more advanced systems, such as video-based and radar-based solutions, require accurate calibration to achieve the claimed performance. This requirement can add human error as a source of performance error. The vision-based systems also require homographic analysis to extract the objects speed.

1.3 OBJECTIVES

This research work is a response to the practical needs and research gaps listed above. More specifically, the general objective of this work is to develop and test innovative monitoring systems using wireless network (WiFi) signatures from mobile devices and emerging Lidar (Light Detection and Ranging) technologies.

The specific objectives of this research are to:

1- Develop a WiFi-Bluetooth based monitoring system for automatically collecting and reporting road user signals in real time through a network of sensors. Such a system could be used to monitor traffic conditions. For this purpose, a real-time wireless network scanning system is developed to capture the MAC addresses of wireless devices and send the data in real-time to the cloud platform for processing. These addresses are unique for each device, and can, therefore, be used to track the activity of the user throughout the network. The designed system combines WiFi and Bluetooth technologies to gain benefits from each technology. The combination of the two technologies enhances the performance of the data analysis algorithms and increases the penetration rate.

2- Develop and evaluate the performance of an integrated WiFi-Bluetooth system to monitor pedestrian and bicycle flows in shared spaces. This includes the development of WiFi classification and extrapolation methods. Comparative analysis of technologies is also carried out.

3- Investigate the performance of WiFi-Bluetooth Scanner for monitoring travel times along urban corridors. The goal is to compare the performance of the two wireless technologies, comparing their penetration rates and evaluating the accuracy of travel time estimation. The benefits of data fusion are also investigated to improve the performance of the Bluetooth monitoring system.

4- Develop and evaluate the performance of a real-time counting system based on single-beam Lidar sensors that measure the distance to the object (road user) and process the distance readings to detect, classify, and count pedestrians and bicycles on non-motorized facilities. The system is evaluated in different traffic conditions and compared to the performance of existing technologies.

5- Propose and test a pedestrian monitoring system that is based on 2D Lidar sensors. The sensors read distances to objects (road users) in two-dimensional space and from above facing down. This sensor is designed to operate under very high pedestrian flow conditions and addresses occlusion and classification issues associated with traditional, side-mounted counting systems.

1.4 ORIGINAL CONTRIBUTION

This thesis contributes to the existing literature by addressing several shortcomings in:

- Designing and testing an integrated WiFi-Bluetooth scanner to detect the MAC addresses of wireless devices and monitor the activity and travel times of road users in different traffic networks.

- Evaluating the performance of WiFi vs. Bluetooth scanning systems in mixed pedestrian and cyclist networks, proposing a framework to classify objects (pedestrian/cyclists) and extrapolating the pedestrian flow using their WiFi traces and counts.
- Evaluating the performance of WiFi vs. Bluetooth scanning systems in terms of detection rate and speed estimation accuracy, and proposing an integrated system to estimate vehicular travel time which benefits from the integration of the two technologies in one system.
- Developing a novel pedestrian and cyclist monitoring system using single-beam Lidar technologies. The proposed solution performs better than existing systems, for temporary or continuous data collection, in terms of accuracy, cost, and installation flexibility. The developed technology provides higher accuracy, more flexibility in different traffic networks, and lower maintenance and installation costs when compared to commercially-available systems.
- Developing a pedestrian counting system using 2D-Lidar technology for high-volume conditions. This sensor addresses occlusion issues associated with traditional, side-mounted counting systems.

1.5 ORGANIZATION OF THE DOCUMENT

This thesis is organized into seven chapters, including the introduction. Since this is a manuscript-based thesis, the following chapters, three through six, are each article for which the author is the primary author. These papers are either published in journals and/or conferences or are reserved for submission after finalizing the provisional patent applications.

Chapter 2 provides a general literature review following the description of the system architecture.

Chapter 3 presents the WiFi-Bluetooth system that is implemented and tested to monitor pedestrian and bicycle activity in a shared space (McGill Campus). The performance of the two technologies is evaluated using ground truth data. A modeling framework is proposed to track, classify, and extrapolate MAC signals.

In Chapter 4, the proposed WiFi-Bluetooth scanning system is evaluated for monitoring traffic flow and travel times of road users in vehicular traffic networks. A comprehensive comparison between WiFi and Bluetooth technologies is conducted to show the advantages of the WiFi system over traditional Bluetooth systems.

Chapter 5 presents the design and development of a novel pedestrian/cyclist counting system based on single beam Lidar sensors. The system can accurately count objects, and detect the direction of the passing object.

Chapter 6 presents a novel pedestrian counting system, based on 2 dimensional (2D) Lidar designed for high pedestrian flow applications. The system functions in real-time and addresses issues associated with side-mounted systems.

Chapter 7 summarises the achieved objectives, concluding remarks, and potential future work.

1.6 REFERENCES

Agarwal, N., Varma, S.R. and Vanajakshi, L.D. (2013) Evaluation of Bluetooth for Traffic Stream Travel Time Estimation Under Indian Conditions.

Ahmed, H., EL-Darieby, M., Abdulhai, B. and Morgan, Y. (2008) Bluetooth-and Wi-Fi-based mesh network platform for traffic monitoring.

Atev, S., Arumugam, H., Masoud, O., Janardan, R. and Papanikolopoulos, N.P. (2005) A vision-based approach to collision prediction at traffic intersections. IEEE Transactions on Intelligent Transportation Systems 6(4), 416-423.

Bagloee, S.A., Sarvi, M. and Wallace, M. (2016) Bicycle lane priority: Promoting bicycle as a green mode even in congested urban area. Transportation Research Part A: Policy and Practice 87, 102-121.

Barcelo, J., Montero, L., Marques, L. and Carmona, C. (2010) Travel time forecasting and dynamic origin-destination estimation for freeways based on bluetooth traffic monitoring. Transportation Research Record (2175), 19-27.

Bhaskar, A., Qu, M. and Chung, E. (2015) Bluetooth vehicle trajectory by fusing bluetooth and loops: Motorway travel time statistics. IEEE Transactions on Intelligent Transportation Systems 16(1), 113-122.

Brosnan, M., Petesch, M., Pieper, J., Schumacher, S. and Lindsey, G. (2015) Validation of bicycle counts from pneumatic tube counters in mixed traffic flows. Transportation Research Record: Journal of the Transportation Research Board (2527), 80-89.

Bullock, D., Haseman, R., Wasson, J. and Spitler, R. (2010) Anonymous bluetooth probes for measuring airport security screening passage time: the indianapolis pilot deployment.

Caviedes, A. and Figliozzi, M. (2018) Modeling the impact of traffic conditions and bicycle facilities on cyclists' on-road stress levels. Transportation research part F: traffic psychology and behaviour 58, 488-499.

Chen, M. and Chien, S. (2001) Dynamic freeway travel-time prediction with probe vehicle data: Link based versus path based. Transportation Research Record: Journal of the Transportation Research Board (1768), 157-161.

Cheung, S.Y., Coleri, S., Dundar, B., Ganesh, S., Tan, C.-W. and Varaiya, P. (2005) Traffic measurement and vehicle classification with single magnetic sensor. Transportation Research Record 1917(1), 173-181.

Coifman, B. and Kim, S. (2009) Speed estimation and length based vehicle classification from freeway single-loop detectors. Transportation Research Part C: Emerging Technologies 17(4), 349-364.

D'Andrea, E. and Marcelloni, F. (2017) Detection of traffic congestion and incidents from GPS trace analysis. Expert Systems with Applications 73, 43-56.

Dabiri, S. and Heaslip, K. (2018) Inferring transportation modes from GPS trajectories using a convolutional neural network. Transportation Research Part C: Emerging Technologies 86, 360-371.

Danalet, A., Farooq, B. and Bierlaire, M. (2014) A Bayesian approach to detect pedestrian destination-sequences from WiFi signatures. Transportation Research Part C: Emerging Technologies 44(0), 146-170.

Datondji, S.R.E., Dupuis, Y., Subirats, P. and Vasseur, P. (2016) A survey of vision-based traffic monitoring of road intersections. IEEE Transactions on Intelligent Transportation Systems 17(10), 2681-2698.

Davis, C. and Mee, G. (2002) Doppler-shift radar transceiver for traffic monitoring system, Google Patents.

Day, C.M., Haseman, R., Premachandra, H., Brennan Jr, T.M., Wasson, J.S., Sturdevant, J.R. and Bullock, D.M. (2010) Evaluation of arterial signal coordination: Methodologies for visualizing high-resolution event data and measuring travel time. Transportation Research Record (2192), 37-49.

Dharmaraju, R., Noyce, D.A. and Lehman, J.D. (2002) An evaluation of technologies for automated detection and classification of pedestrians and bicycles, University of Massachusetts at Amherst.

Dong, H., Ma, L. and Broach, J. (2016) Promoting sustainable travel modes for commute tours: A comparison of the effects of home and work locations and employer-provided incentives. International Journal of Sustainable Transportation 10(6), 485-494.

El-Assi, W., Salah Mahmoud, M. and Nurul Habib, K. (2017) Effects of built environment and weather on bike sharing demand: a station level analysis of commercial bike sharing in Toronto. Transportation 44(3), 589-613.

Engelbrecht, J., Booysen, M.J., van Rooyen, G.-J. and Bruwer, F.J. (2015) Survey of smartphone-based sensing in vehicles for intelligent transportation system applications. IET Intelligent Transport Systems 9(10), 924-935.

Friesen, M.R. and McLeod, R.D. (2015) Bluetooth in intelligent transportation systems: a survey. International Journal of Intelligent Transportation Systems Research 13(3), 143-153.

Greene-Roesel, R., Diogenes, M.C., Ragland, D.R. and Lindau, L.A. (2008) Effectiveness of a commercially available automated pedestrian counting device in urban environments: Comparison with manual counts.

Hamilton, T.L. and Wichman, C.J. (2018) Bicycle infrastructure and traffic congestion: Evidence from DC's Capital Bikeshare. Journal of Environmental Economics and Management 87, 72-93.

Haseman, R.J., Wasson, J.S. and Bullock, D.M. (2010) Real-time measurement of travel time delay in work zones and evaluation metrics using bluetooth probe tracking. Transportation Research Record: Journal of the Transportation Research Board 2169(1), 40-53.

Herring, R., Hofleitner, A., Abbeel, P. and Bayen, A. (2010) Estimating arterial traffic conditions using sparse probe data, pp. 929-936, IEEE.

Hidayat, A., Terabe, S. and Yaginuma, H. (2018) WiFi Scanner Technologies for Obtaining Travel Data about Circulator Bus Passengers: Case Study in Obuse, Nagano Prefecture, Japan. Transportation Research Record, 0361198118776153.

Hipp, J.A., Bird, A., van Bakergem, M. and Yarnall, E. (2017) Moving targets: Promoting physical activity in public spaces via open streets in the US. Preventive medicine 103, S15-S20.

Hu, S., Su, L., Liu, H., Wang, H. and Abdelzaher, T.F. (2015) Smartroad: Smartphone-based crowd sensing for traffic regulator detection and identification. ACM Transactions on Sensor Networks (TOSN) 11(4), 55.

Hutchison, M.C., Pautler, J.A. and Smith, M.A. (2010) Traffic light signal system using radar-based target detection and tracking, Google Patents.

Jansen, S., Hoting, D., Runge, J., Brinkhoff, T., Nicklas, D. and Sauer, J. (2014) 9 Million Bicycles? Extending Induction Loops with Bluetooth Sensing, pp. 113-116, IEEE Computer Society, Los Alamitos, CA, USA.

Kwon, J., Varaiya, P. and Skabardonis, A. (2003) Estimation of truck traffic volume from single loop detectors with lane-to-lane speed correlation. Transportation Research Record: Journal of the Transportation Research Board (1856), 106-117.

Leduc, G. (2008) Road traffic data: Collection methods and applications. Working Papers on Energy, Transport and Climate Change 1, 55.

Lesani, A., Miranda-Moreno, L.F., Fu, T. and Romancyshyn, T. (2015) Development and Testing of an Ultrasonic-Based Pedestrian Counting System.

Li, Y. and McDonald, M. (2002) Link travel time estimation using single GPS equipped probe vehicle, pp. 932-937, IEEE.

Lindsey, G., Hankey, S., Wang, X. and Chen, J. (2013) The Minnesota bicycle and pedestrian counting initiative: methodologies for non-motorized traffic monitoring.

Lindsey, G., Petesch, M. and Hankey, S. (2015) The Minnesota bicycle and pedestrian counting initiative: Implementation study.

Malinovskiy, Y., Saunier, N. and Wang, Y. (2012) Pedestrian Travel Analysis Using Static Bluetooth Sensors. Transportation Research Board: Journal Of The Transpotation Research Board, 1-22.

Martchouk, M., Mannering, F. and Bullock, D. (2010) Analysis of freeway travel time variability using Bluetooth detection. Journal of Transportation Engineering 137(10), 697-704.

Martin, B.D., Addona, V., Wolfson, J., Adomavicius, G. and Fan, Y. (2017) Methods for real-time prediction of the mode of travel using smartphone-based GPS and accelerometer data. Sensors 17(9), 2058.

Mei, Z., Wang, D. and Chen, J. (2012) Investigation with Bluetooth sensors of bicycle travel time estimation on a short corridor. International Journal of Distributed Sensor Networks 2012.

Mitsakis, E., Salanova Grau, J.M., Chrysohoou, E. and Aifadopoulou, G. (2015) A robust method for real time estimation of travel times for dense urban road networks using point-to-point detectors. Transport 30(3), 264-272.

Moghaddam, S.S. and Hellinga, B. (2014) Algorithm for Detecting Outliers in Bluetooth Data in Real Time. Transportation Research Record: Journal of the Transportation Research Board (2442), pp 129–139.

Montoya, D., Abiteboul, S. and Senellart, P. (2015) Hup-me: Inferring and reconciling a timeline of user activity from rich smartphone data, p. 62, ACM.

Nantes, A., Ngoduy, D., Bhaskar, A., Miska, M. and Chung, E. (2016) Real-time traffic state estimation in urban corridors from heterogeneous data. Transportation Research Part C: Emerging Technologies 66, 99-118.

Nanthawichit, C., Nakatsuji, T. and Suzuki, H. (2003) Application of probe-vehicle data for real-time traffic-state estimation and short-term travel-time prediction on a freeway. Transportation Research Record: Journal of the Transportation Research Board (1855), 49-59.

Nordback, K., Kothuri, S., Phillips, T., Gorecki, C. and Figliozzi, M. (2016) Accuracy of bicycle counting with pneumatic tubes in Oregon. Transportation Research Record: Journal of the Transportation Research Board (2593), 8-17.

Omrani, R., Izadpanah, P., Nikolic, G., Hellinga, B., Hadayeghi, A. and Abdelgawad, H. (2013) Evaluation of wide-area traffic monitoring technologies for travel time studies. Transportation Research Record (2380), 108-119.

Ozbay, K., Yang, H. and Bartin, B.O. (2010) Calibration of an infrared-based automatic counting system for pedestrian traffic flow data collection.

Proulx, F.R., Schneider, R.J. and Miranda-Moreno, L.F. (2016) Performance evaluation and correction functions for automated pedestrian and bicycle counting technologies. Journal of Transportation Engineering 142(3), 04016002.

Pucher, J. and Dijkstra, L. (2003) Promoting safe walking and cycling to improve public health: lessons from the Netherlands and Germany. American Journal of Public Health 93(9), 1509-1516.

Ricci, M. (2015) Bike sharing: A review of evidence on impacts and processes of implementation and operation. Research in Transportation Business & Management 15, 28-38.

Robert, K. (2009) Video-based traffic monitoring at day and night vehicle features detection tracking, pp. 1-6, IEEE.

Ryus, P., Ferguson, E., Laustsen, K.M., Prouix, F.R., Schneider, R.J., Hull, T. and Miranda-Moreno, L. (2014) Methods and technologies for pedestrian and bicycle volume data collection, Citeseer.

Setchell, C. and Dagless, E. (2001) Vision-based road-traffic monitoring sensor. IEE Proceedings-Vision, Image and Signal Processing 148(1), 78-84.

Sherly, J. and Somasundareswari, D. (2015) Internet of things based smart transportation systems. International Research Journal of Engineering and Technology 2(7), 1207-1210.

Singh, D., Tripathi, G. and Jara, A.J. (2014) A survey of Internet-of-Things: Future vision, architecture, challenges and services, pp. 287-292, IEEE.

Staunton, C.E., Hubsmith, D. and Kallins, W. (2003) Promoting safe walking and biking to school: the Marin County success story. American Journal of Public Health 93(9), 1431-1434.

Strauss, J., Miranda-Moreno, L.F. and Morency, P. (2015) Mapping cyclist activity and injury risk in a network combining smartphone GPS data and bicycle counts. Accident Analysis & Prevention 83, 132-142.

Vu, L., Nahrstedt, K., Retika, S. and Gupta, I. (2010) Joint bluetooth/wifi scanning framework for characterizing and leveraging people movement in university campus, pp. 257-265, Association for Computing Machinery, Bodrum, Turkey.

Wei, H. and Forougi, S. (2016) GPS and wireless integrated fleet management system and method, Google Patents.

Wieck, M. (2011) Use of bluetooth based travel time information for traffic operations.

Zanella, A., Bui, N., Castellani, A., Vangelista, L. and Zorzi, M. (2014) Internet of things for smart cities. IEEE Internet of Things journal 1(1), 22-32.

Zoto, J., La, R.J., Hamedi, M. and Haghani, A. (2012) Estimation of average vehicle speeds traveling on heterogeneous lanes using bluetooth sensors, Institute of Electrical and Electronics Engineers Inc., Quebec City, QC, Canada.

Chapter 2: General Literature Review and System Architecture

This Chapter consists of a literature review of the technologies and methodologies for traffic network monitoring with a particular focus on non-motorized modes. The literature review is divided into two parts: 1) studies focusing on wireless network sniffing devices that track user activity, known as between-point monitoring systems, and 2) studies focusing on fixed-point monitoring systems for motorized and non-motorized traffic.

2.1 WIRELESS NETWORK SNIFFING FOR TRAFFIC MONITORING

The need for real-time traffic information is becoming increasingly important in urban areas, where large sets of monitoring locations are required. The use of fixed-point sensors is limited in spatial coverage and the high cost of installation and operation of large networks. More importantly, there is a particular interest in real-time monitoring of travel times or speeds (at segments, corridors or networks) and in generating origin-destination matrices, in addition to getting count data. To gather this information, the detection of the same road user across two or more locations is required.

In recent years, the literature in traffic monitoring has expanded to include the use of floating traffic monitoring technologies in addition to fixed location sensory systems. Recent advances in Global Positioning System (GPS) technology have helped make the technology more commercially viable. Floating traffic monitoring systems could complement existing fixed location traffic monitoring systems, which limit spatial coverage in traffic networks. GPS technology can be utilized in three different contexts: i) GPS units on public bus fleets, taxis, car-sharing companies, (Bacon et al. 2011, Balan et al. 2011, Herrera et al. 2010, Schäfer et al. 2002), ii) GPS equipped probe vehicles (Chen and Chien 2001, Li and McDonald 2002, Nanthawichit et al. 2003), and iii) GPS units following regular drivers (typically using smartphones) (D'Andrea and Marcelloni 2017, Engelbrecht et al. 2015, Hu et al. 2015). In a recent study (Dabiri and Heaslip 2018) a convolutional neural network scheme was used to extract the mode of mobility using raw GPS data. An accuracy of 84% was achieved in detecting users who were walking, driving, biking, using the bus and train. Despite many studies that have utilized GPS technology in travel time estimation on motorized networks, few studies have applied this technology to non-motorized networks. For example, Strauss et al. 2012 used GPS points to investigate the link between cyclists volume and air pollution level along bicycle facilities. Martin et al. 2017 developed a framework to classify the users based on GPS points reported by user smartphones. In Strauss et al. 2015, the authors mapped cyclists activity and injury risk in a network by combining GPS traces and fixed-point count data. The study demonstrated that accurate count data is crucial for developing such frameworks.

Despite the high accuracy in GPS-based methods, its use is not widespread because of some significant shortcomings. The greatest potential of this technology is to monitor regular users using smartphones. However, privacy issues and the contribution to battery drainage of smartphones are the two main concerns that users have with smartphone GPS applications. These concerns dramatically reduce the penetration rate of this method of data collection. The difficulty in achieving wide-spread implementation have led researchers to use other, less accurate, sources of data.

To address the challenges of GPS-based monitoring system, alternative approaches have emerged using i) wireless technologies (Bluetooth) (Ahmed et al. 2008, Bullock et al. 2010, Danalet et al. 2013, Malinovskiy et al. 2012, Martchouk et al. 2010, Porter et al. 2013, Saeedi 2013, Tsubota et al. 2011), ii) WiFi access points (Ahmed et al. 2008, Danalet et al. 2013, Musa and Eriksson 2012), and iii) cellular tower data (Caceres et al. 2007, Calabrese et al. 2015, Iqbal et al. 2014, Williams et al. 2015).

The concept behind using cellular tower data (geo-localization of the users with GSM data) is to acquire their location based on knowledge of which Based Transceiver Stations (BTS) they are connected to in specific time spans. This data source, however, creates privacy concerns since the registered phones on networks can be associated with people's identity. Moreover, the low positioning accuracy and ping-pong handover between BTSs represent technical limitations in using cellular data. Low BTS density in some areas makes this data unreliable; the large radius of the BTS cells (approximately 200 m) makes the data very noisy for short trips, (Kalatian and Shafahi 2016).

As an alternative cellular tower data source, Bluetooth and WiFi detectors can detect a unique media access control (MAC) address for each device. Then, each device can be monitored (tracked) as it moves through a network. Bluetooth-based sensors have gained popularity for collecting motor-vehicle traffic data in recent years. Systems based on Bluetooth-enabled devices have been used to collect real-time measures of traffic congestion based on travel times or speeds (Martchouk et al. 2010, Tsubota et al. 2011) and for O-D matrix applications (Laharotte et al. 2015, Michau et al. 2017). Bluetooth-base sensor popularity has been increasing in the last several years because the systems offer portability, and instant, unobtrusive data collection (Wasson et al. 2008). A basic device that collects travel time data is composed of a reader unit, a unit to store MAC addresses, and an antenna. The advantages of Bluetooth methods over conventional technologies include relatively lower costs (hardware and software are inexpensive), the ability to collect large quantities of data over time, and ease of installation. Given their flexibility, Bluetooth data collection devices are suitable for temporary or permanent installation along roadway facilities of interest. These sensors have been demonstrated to work well in vehicular traffic applications, and a few studies have shown that they can be used to monitor pedestrian traffic (Lan et al. 2017, Malinovskiy et al. 2012, Markowitz et al. 2009, Yoshimura et al. 2017). Using multiple detectors throughout a network, the path and approximate speed of each device can be determined and used to generate OD matrices, travel times, and measures of congestion (Martchouk et al. 2010, Saeedi 2013, Tsubota et al. 2011, Wasson et al. 2008). Several applications in which Bluetooth devices have been used to compute travel time and other traffic performance measures have been recently reported. Among earlier works, Wasson et al. 2008, estimated travel times on freeways and arterials in the greater Indianapolis area. In another study Haseman et al. 2010, computed congestion measures to evaluate the impact of highway work zones along rural interstates in Indiana. Among the studies in urban environments, Quayle et al. 2010 measured segment travel time, average running speed, and origin-destination on arterials in Portland, Oregon. In a different application, Day et al. 2010 evaluated signal coordination by combining travel time measurements with detector event data. Other studies have compared alternative methods, such as floating car versus Bluetooth data collection. More recently, Porter et al. 2013, evaluated the use of different antennas and concluded that an antenna with a large gain and a lower sampling rate may provide more accurate travel time samples. Although most of the studies focused on vehicular traffic networks, some recent works have applied Bluetooth scanners to monitor users in mixed mode traffics. For instance, Michau et al. 2017 developed a framework to classify the mode of the object in mixed mode (bike-vehicle) facilities. Some other recent works have used Bluetooth data to monitor activity in pedestrian environments (Lan et al. 2017, Malinovskiy et al. 2012, Yoshimura et al. 2017).

Despite the advantages of Bluetooth listed above, technology has several documented limitations. Among them is the fact that the quantity of collected data depends on the level of market penetration of Bluetooth technology. Sampling rates vary from 3 to 12% on roadways

(Malinovskiy et al. 2012). For instance, Wieck 2011 investigated the technology on an arterial corridor with six intersections and found a matching rate that varied from 3% to 11.4%. While these values can be statistically adequate given a large enough fleet size, higher detection rates between sensors are always preferred to ensure system reliability. Another shortcoming is that Bluetooth devices are often disabled or not "discoverable" on smartphones due to security risks, battery concerns, or lack of use. Moreover, Bluetooth-based systems have difficulty capturing usable data on arterials or facilities with high traffic mix, in particular with high volumes of pedestrians and bikes.

To overcome the issues associated with Bluetooth sensors and increase the detection rate, researchers have considered WiFi access points as an alternative way to capture the MAC address of wireless devices connected to the network. WiFi is another common wireless service, and it has a considerably higher rate of use than Bluetooth. WiFi is typically left enabled by users because doing so allows users to connect to known networks when in range. WiFi has been used in existing networks to track devices that are connected to a specific network. In several studies, the information about connected devices to the network was used to monitor network performance and user activity (Hidayat et al. 2018, Reichl et al. 2018, Weppner et al. 2016). The advantages of using WiFi are particularly evident for networks with a large wireless coverage area and many nodes, e.g., on a university campus. For a device to be tracked, it must be connected to the given wireless network and must be within the coverage area. Therefore, the area studied cannot be expanded without extending the network coverage, which can be difficult as it means expanding the area supporting internet usage to its users. Because of the shortcomings of using WiFi access point data to monitor network traffic using WiFi protocol, there is a growing interest in developing independent WiFi sniffer systems. In these systems, capturing MAC addresses is not limited to the devices that are connected to a specific network.

In the literature, few studies have compared the performance of Bluetooth and WiFi scanners in providing usable and representative travel data (Hidayat et al. 2018, Tufuor and Rilett 2018). In studying vehicle traffic, Abbott-Jard et al. 2013 compared the performance of the two technologies with data collected along a major arterial and freight route in Brisbane, Australia. The results indicated that Bluetooth performed better: 1191 matched MAC-IDs could be identified from the data produced by the Bluetooth scanners compared to 149 from the data produced by the WiFi scanners. In addition, the percentage of usable data from the Bluetooth and WiFi scanners was

81% and 19% respectively. The authors mentioned that WiFi technology might have been affected by interference with other WiFi signals in the area.

For non-motorized monitoring, there are several ongoing studies that have applied WiFi network scanners to pedestrian networks at airports, shopping malls, university campuses (Abedi et al. 2015, Bai et al. 2017, Kurkcu and Ozbay 2017, Schauer et al. 2014, Song and Wynter 2017). The purpose of these studies is to demonstrate how user activity can be monitored to improve in the management of the facilities, services provision, advertisement, and emergency evacuations. As part of the WiFi pedestrian-related applications, Schauer et al. 2014 compared various pedestrian flow techniques using both WiFi and Bluetooth scanners in the Munich Airport. The results showed that WiFi overestimated and Bluetooth underestimated flows compared to the number of boarding pass scans (ground truth). More recently, Kurkcu and Ozbay 2017 proposed an application to estimate the wait time in a bus terminal but the results were not validated with the ground truth data. Du et al. 2017 proposed a method to improve the detection rate and estimation precision of pedestrian flows. Bai et al. 2017 used the WiFi scanning approach to count the number of pedestrians using WiFi traces at public transport stations. In Abedi et al. 2015, the authors empirically assessed the impact of small and large antenna gains on tracking movements of pedestrians and cyclists based on MAC address datasets. Despite the growing body of work, some issues and gaps remain. Firstly, the authors considered a fixed coverage area based on the antenna gain but, in practice, the coverage area is also dependent on the type of device and network characteristics. Secondly, the proposed speed estimation approach was only validated for pedestrians (and not for cyclists). Thirdly, pedestrians, runners, and cyclists are classified only based on speed; the applicability of which is limited to large networks with large distances between sensors.

Despite the growing body of literature, research gaps remain in the monitoring of multi-modal and non-motorized transportation networks. More specifically, their significant gaps related to methods for mode detection or classification of signal (MAC) and the extrapolation of the traffic flows based on WiFi signatures persist. Additionally, more validation on the performance of the Bluetooth and WiFi-based wireless scanning systems is required.

2.2 FIXED-POINT MONITORING SYSTEMS

Despite the advantages of wireless scanning systems in monitoring networks between points, such systems have low sampling rates and therefore monitor only a sample of the entire population. Therefore, as a complementary part of a monitoring system, fixed sensors are also required to detect and count all objects (road users) and measure the traffic parameters such as counts, speeds, and gaps between objects. In the literature and practice, fixed-points monitoring systems can be divided into two groups: motorized and non-motorized (pedestrian and cyclists) systems.

2.2.1 Motorized Traffic Networks

Several technologies are commercially-available for monitoring vehicular traffic, and such systems can function precisely under various traffic flow, weather, and lighting conditions. Generally, traffic count technologies can be divided into intrusive (traditional) and non-intrusive technologies (Leduc 2008). Intrusive data collection technologies include systems that are installed on roads during which traffic interruptions and infrastructure modifications (perforation) are required. The two traditional technologies are pneumatic-road tubes and magnetic loops. In the first case, rubber-tubes are installed across the road lanes to detect vehicles by measuring changes in air pressure inside the tube. The tire of a vehicle causes changes in air pressure and a counter recorder stores the data. This system is limited to collecting data along one lane, and the counting efficiency can be affected by weather and traffic conditions. Pneumatic tubes are typically installed for short-term counting. Magnetic loops are embedded in a road in square shapes and function based on the concept of changes in the electromagnetic field near the sensors. Using this technology, traffic data including counts, speed (with two consecutive sensors), and occupancy time can be obtained.

Non-intrusive technologies are based on observations collected along a roadside without the need to make any changes to the pavement or infrastructure. Passive or active infrared detects the presence and speed of a vehicle based on the heat energy radiated from vehicles. Microwave radar detects vehicles and level-vehicle speeds based on the Doppler Effect. The measured change in the sent and received wave frequency is proportional to the object (vehicle) speed. This type of sensor is not very sensitive to weather condition changes (Gómez-del-Hoyo et al. 2015). Video image processing uses video cameras to collect images of vehicles in a traffic network, and then a post image process is performed on the recorded video to detect license plate numbers, speeds, and even to track vehicle trajectories. Applications of video processing based systems can be used for transportation facilities with homogeneous or mixed mode types (Zangenehpour et al. 2014). However, the existing systems are difficult to power and process in real-time. Thus video-based embedded systems are still limited. Moreover, the efficiency of video-based sensors decreases in bad weather or poor lighting conditions. Thermal video cameras address this issue. However, this solution is extremely costly (Fu et al. 2017).

Overall, the aforementioned technologies share similar advantages in terms of temporal coverage. Traffic volumes, speed data, vehicle gaps, and vehicle classifications can be measured over short (hour or days) and long (months or years) periods of time.

2.2.2 Non-Motorized Traffic Networks

Data collection tools are more limited in non-motorized traffic and, historically, research on non-motorized monitoring has been more limited than research on motorized monitoring. To address this gap, in recent years there has been growth in the development of non-motorized traffic monitoring solutions. The non-motorized counting solutions can be divided into pedestrian and bicycle counters (Johnstone et al. 2017, Ryus et al. 2014).

2.2.2.1 Pedestrian Counting Solutions

The most common technologies used in research and practice for the purpose of counting pedestrians are passive infrared sensors, laser scanning (Akamatsu et al. 2014), pressure pads (Ryus et al. 2014), thermal sensors 9González et al. 2016, Kristoffersen et al. 2016), and video camera sensors (Chao and Gupta 2013, Jackson et al. 2013). These counters, along with other methods currently in development, are presented and discussed in Dharmaraju et al. 2002, Johnstone et al. 2017, Markowitz et al. 2009, Ryus et al. 2014. A more expensive, but very accurate alternative to commonly-used technologies is thermal imaging cameras (González et al. 2016, Kristoffersen et al. 2016, Leykin and Hammoud 2006). Despite high accuracy, such systems do not function in real-time and are very expensive (Fu et al. 2017). Passive infrared is the most commonly used technology in practice, since it is relatively inexpensive, mobile, and battery operated. The remaining technologies are mainly used in research.

Passive infrared counting technology includes all systems that are sensitive to the radiation of infrared waves (Ozbay et al. 2010, Ryus et al. 2014). The system monitors the changes in infrared signals in the environment to detect and counts pedestrians. These sensors have a number of advantages such as relative ease to build and operate, very low power consumption, and real-time implementation, which make them very flexible and easy to install for long periods of time. However, some of the key limitations of this technology include occlusion, when installed in environments with high pedestrian volumes, and diminished performance in hot temperatures. Ideally, the device must be facing a fixed object, such as a wall, opposite the sidewalk on which it is mounted. This restricts their use at intersections, midblock crosswalks, and open spaces (Greene-Roesel et al. 2008). Additionally, an intense source of infrared signals, such as vehicle engines can trigger the sensor and cause over-counting. Cases of under-counting and over-counting have also been observed and attributed to certain temperature anomalies and weather conditions (rain or hot weather condition). Studies have reported a systematic under-counting error ranging between 0 and 25% depending on the traffic volumes and weather conditions (Greene-Roesel et al. 2008, Ryus et al. 2014).

2.2.2.2 Bicycle Counting Solutions

Automated bicycle counting systems, such as pneumatic tubes and loop detectors, similar to those used by vehicles but adapted to bicycle traffic monitoring, are widely used in practice (Johnstone et al. 2017, Ryus et al. 2014).

Inductive loop detectors (Nordback and Janson 2010) are typically used for long-term, continuous data collection, whereas pneumatic tubes (Brosnan et al. 2015, Nordback et al. 2016, Proulx et al. 2016) are used for short-term or temporary data collection. Inductive loop systems have some limitations, namely high maintenance and installation costs. The wires, installed under the pavement, can be broken due to construction or winter snow removal. This system is used solely on bike facilities, without any classification capability in mixed mode traffic networks. Pneumatic tubes are used for short-term data collection. They generally suffer from undercounting, with error rates ranging from 6% to 57%, depending on the location and configuration of deployment (Brosnan et al. 2015, Nordback et al. 2016). To monitor bike facilities more efficiently, a solution that has high accuracy, low maintenance, and installation costs and is not sensitive to varying weather and lighting conditions is necessary for both temporary and continuous data collection applications.

2.3 GENERAL SYSTEM ARCHITECTURE

In this thesis, several traffic-monitoring solutions are built and tested using the same system architecture. The two main components, hardware, and software, are developed to create systems that are highly accurate, easy to install and maintain, user-friendly, inexpensive and that able to collect and transmit real-time data to an integrated data storage and analysis platform. All these elements help make the large-scale implementation of the proposed systems feasible for any smart city initiatives. A general system architecture is divided into five elements: sensor, communication, database, analytics, and data visualization.

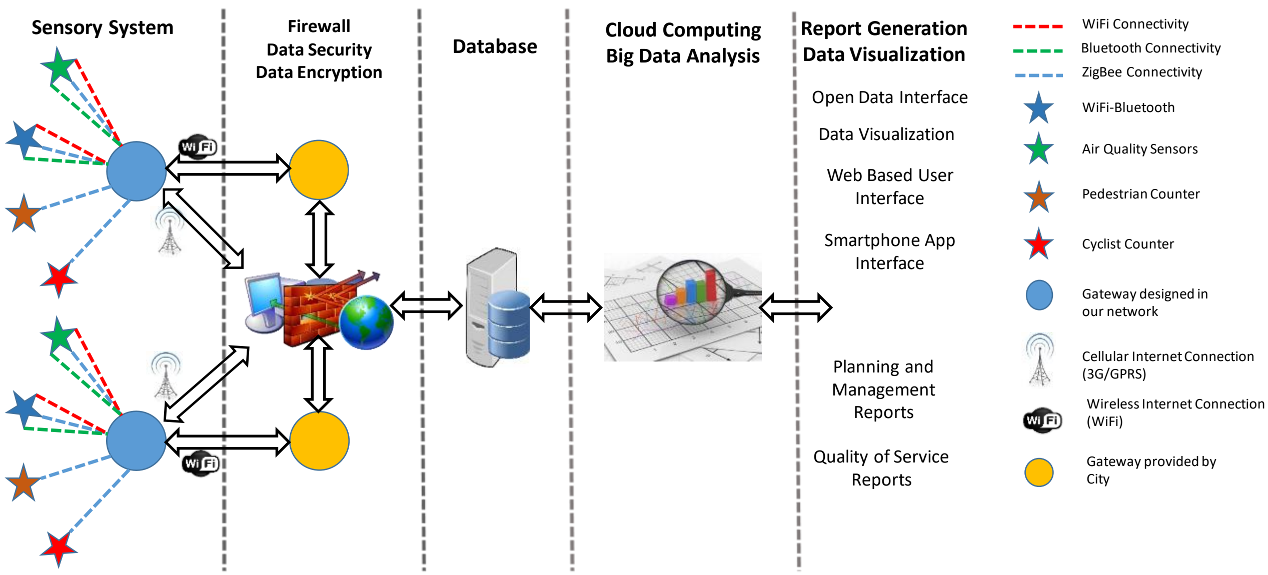

Figure 2-1. General architecture of the system

2.3.1 Sensor Layer

The sensor layer includes different types of fixed-point and between-point monitoring systems. Each sensor unit consists of hardware and software components. The software component analyzes the data collected from the sensor units. The hardware includes sensing units (Lidar, WiFi or Bluetooth modules), data telemetry, and the processing unit, which runs the software and interfaces with the other hardware components.

The sensor has five hardware components, as seen in Figure 2-2, and described below:

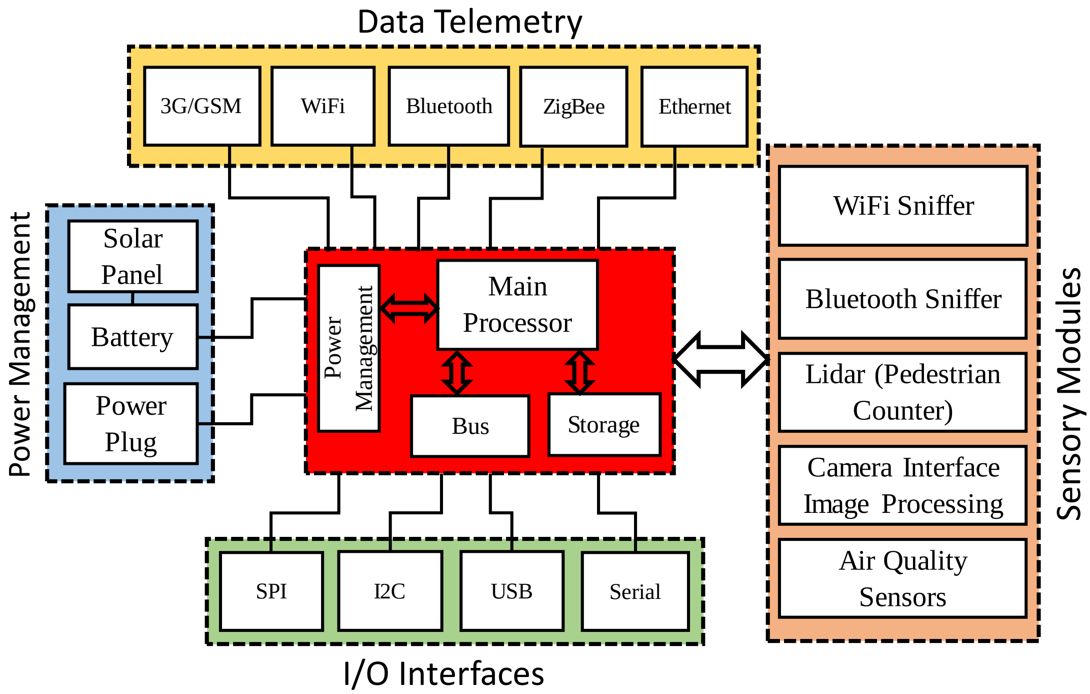

Figure 2-2. Sensor hardware components

Figure 2-2 describes the sensor hardware components

a) Main Processor: depending on the application, different types of ARM processing units are used in the sensor system. The processor handles the interface between different parts of the system hardware and runs the main data analysis algorithms. The ARM architecture helps to improve the total power consumption of the system for battery-powered applications.

b) Sensory Modules: depending on the application, different types of sensory modules are used. For wireless network scanning, WiFi and Bluetooth modules are used as sensing units. For counting applications, Lidar sensors are integrated into the system.

c) Input-Output Interfaces: different types of wired communication protocols can be used to communicate with sensory modules. The I2C protocol is used for communication with Lidar sensors. WiFi and Bluetooth modules are attached to the processor using a USB. The LoRA communication module communicates with the main processor using a serial connection. External flash memory communicates with the processor through an SPI connection.

d) Data Telemetry: depending on the application, different types of wired (Ethernet) or wireless communications protocols could be implemented to transfer data between sensors, to gateways or directly to the database. Short-range communication using Bluetooth/ZigBee protocols, mid-range, and high speed through WiFi, long-range and low power consumption using LoRA and long-range and high-speed using on GSM/LTE networks are a variety of supported communication protocols in our design.

e) Power Management Unit: manages the power sources of the system to select between power grids, battery or solar power. The power management unit is designed to reduce the internal power consumption of the system.

2.3.2 Data Security and Encryption

All the data transactions between sensors and database are encrypted to protect data security. Additionally, the Hyper Text Transfer Protocol Secure (HTTPS) which is the secure version of HTTP, is used to send data from counting sensors to the web server (running on the Amazon Cloud platform). For WiFi-Bluetooth scanners, Amazon API is used, which provides AWS-managed encryption keys to increase the security of the data.

2.3.3 Database Layer

The Amazon AWS cloud system is used to store the data. This cloud-based storage provides fast access to the data, with high security and low maintenance costs and is integrated into one location. The database is highly scalable with dynamic, pay-as-you-go pricing.

2.3.4 Cloud Computing and Data Visualization Layer

All the data transferred to the database will be accessible by the cloud computing unit. The proposed architecture uses Amazon EC2 to process the data coming from the sensors. The data analysis is done on different levels, depending on the nature of the data. The heaviest analysis is done on the cloud platform to analyze the MAC addresses reposted by each individual sensor to the database. The algorithm will read the time-stamped addresses and match them with different points on the network to extract the travel time and other traffic metrics over the network. The counting systems transfer the count data in real-time to the platform, and the analysis on those data are mainly for data visualization and integration. The fusing of all the traffic measures collected by the different sensors is also implemented on the cloud platform. The platform provides access to the raw and analyzed data though a web interface or an API with HTTP requests.

2.4 SYSTEM TESTING

The development of the monitoring system in this thesis is done through an iterative process. Once a first prototype is developed, it is tested and debugged at different stages until the final version is achieved. The summary of the steps is described below:

1. Development of the first prototype: After studying all the required features and desired performance of the system, elements of the system (processor, sensory system, etc.) are selected, and a first prototype is designed.
2. Testing:
    - Definition of the performance and feature measures: Depending on the type of the sensor, different performance measures such as counting error, speed estimation error, and detection rate, are defined. These metrics are used to evaluate if the designed prototype meets the requirements.
    - Installation and data collection: The prototype is installed in a traffic network along with a video camera system to collect the ground truth data for comparison and evaluation purposes.
    - Data processing and evaluation of system performance: The recorded video is processed along with manual ground truth data and compared to the data collected by the prototype.
    - Debugging: Issues are identified based on the validation measure. The debugging includes hardware or software bugs.

These steps are repeated until system performance is satisfactory.

2.5 REFERENCES

Abbott-Jard, M., Shah, H. and Bhaskar, A. (2013) Empirical evaluation of Bluetooth and Wifi scanning for road transport, p. 14.

Abedi, N., Bhaskar, A., Chung, E. and Miska, M. (2015) Assessment of antenna characteristic effects on pedestrian and cyclists travel-time estimation based on Bluetooth and WiFi MAC addresses. Transportation Research Part C: Emerging Technologies 60, 124-141.

Ahmed, H., EL-Darieby, M., Abdulhai, B. and Morgan, Y. (2008) Bluetooth-and Wi-Fi-based mesh network platform for traffic monitoring.

Akamatsu, S.-i., Shimaji, N. and Tomizawa, T. (2014) Development of a person counting system using a 3D laser scanner, pp. 1983-1988, IEEE.

Bacon, J., Bejan, A.I., Beresford, A.R., Evans, D., Gibbens, R.J. and Moody, K. (2011) Dependable and Historic Computing, pp. 93-117, Springer.

Bai, L., Ireson, N., Mazumdar, S. and Ciravegna, F. (2017) Lessons learned using wi-fi and Bluetooth as means to monitor public service usage, pp. 432-440, ACM.

Balan, R.K., Nguyen, K.X. and Jiang, L. (2011) Real-time trip information service for a large taxi fleet, pp. 99-112, ACM.

Brosnan, M., Petesch, M., Pieper, J., Schumacher, S. and Lindsey, G. (2015) Validation of bicycle counts from pneumatic tube counters in mixed traffic flows. Transportation Research Record: Journal of the Transportation Research Board (2527), 80-89.

Bullock, D., Haseman, R., Wasson, J. and Spitler, R. (2010) Anonymous bluetooth probes for measuring airport security screening passage time: the indianapolis pilot deployment.

Caceres, N., Wideberg, J. and Benitez, F. (2007) Deriving origin destination data from a mobile phone network. Intelligent Transport Systems, IET 1(1), 15-26.

Calabrese, F., Ferrari, L. and Blondel, V.D. (2015) Urban sensing using mobile phone network data: a survey of research. Acm computing surveys (csur) 47(2), 25.

Chao, H. and Gupta, R. (2013) Image and video based pedestrian traffic estimation, Google Patents.

Chen, M. and Chien, S. (2001) Dynamic freeway travel-time prediction with probe vehicle data: Link based versus path based. Transportation Research Record: Journal of the Transportation Research Board (1768), 157-161.

D'Andrea, E. and Marcelloni, F. (2017) Detection of traffic congestion and incidents from GPS trace analysis. Expert Systems with Applications 73, 43-56.

Dabiri, S. and Heaslip, K. (2018) Inferring transportation modes from GPS trajectories using a convolutional neural network. Transportation Research Part C: Emerging Technologies 86, 360-371.

Danalet, A., Farooq, B. and Bierlaire, M. (2013) Towards an activity-based model for pedestrian facilities.

Day, C.M., Haseman, R., Premachandra, H., Brennan, T.M., Wasson, J.S., Sturdevant, J.R. and Bullock, D.M. (2010) Evaluation of Arterial Signal Coordination. Transportation Research Record: Journal of the Transportation Research Board 2192(1), 37-49.

Dharmaraju, R., Noyce, D.A. and Lehman, J.D. (2002) An evaluation of technologies for automated detection and classification of pedestrians and bicycles, University of Massachusetts at Amherst.

Du, Y., Yue, J., Ji, Y. and Sun, L. (2017) Exploration of optimal Wi-Fi probes layout and estimation model of real-time pedestrian volume detection. International Journal of Distributed Sensor Networks 13(11), 1550147717741857.

Engelbrecht, J., Booysen, M.J., van Rooyen, G.-J. and Bruwer, F.J. (2015) Survey of smartphone-based sensing in vehicles for intelligent transportation system applications. IET Intelligent Transport Systems 9(10), 924-935.

Fu, T., Stipancic, J., Zangenehpour, S., Miranda-Moreno, L. and Saunier, N. (2017) Automatic traffic data collection under varying lighting and temperature conditions in multimodal environments: thermal versus visible spectrum video-based systems. Journal of advanced transportation 2017.

Gómez-del-Hoyo, P., Bárcena-Humanes, J.-L., Mata-Moya, D., Juara-Casero, D. and Jiménez-de-Lucas, V. (2015) Passive radars as low environmental impact solutions for smart cities traffic monitoring, pp. 1-6, IEEE.

González, A., Fang, Z., Socarras, Y., Serrat, J., Vázquez, D., Xu, J. and López, A.M. (2016) Pedestrian detection at day/night time with visible and FIR cameras: A comparison. Sensors 16(6), 820.

Greene-Roesel, R., Diogenes, M.C., Ragland, D.R. and Lindau, L.A. (2008) Effectiveness of a Commercially Available Automated Pedestrian Counting Device in Urban Environments: Comparison with Manual Counts. Safe Transportation Research & Education Center.

Haseman, R.J., Wasson, J.S. and Bullock, D.M. (2010) Real-time measurement of travel time delay in work zones and evaluation metrics using bluetooth probe tracking. Transportation Research Record: Journal of the Transportation Research Board 2169(1), 40-53.

Herrera, J.C., Work, D.B., Herring, R., Ban, X.J., Jacobson, Q. and Bayen, A.M. (2010) Evaluation of traffic data obtained via GPS-enabled mobile phones: The Mobile Century field experiment. Transportation Research Part C: Emerging Technologies 18(4), 568-583.

Hidayat, A., Terabe, S. and Yaginuma, H. (2018) WiFi Scanner Technologies for Obtaining Travel Data about Circulator Bus Passengers: Case Study in Obuse, Nagano Prefecture, Japan. Transportation Research Record, 0361198118776153.

Hu, S., Su, L., Liu, H., Wang, H. and Abdelzaher, T.F. (2015) Smartroad: Smartphone-based crowd sensing for traffic regulator detection and identification. ACM Transactions on Sensor Networks (TOSN) 11(4), 55.

Iqbal, M.S., Choudhury, C.F., Wang, P. and González, M.C. (2014) Development of origin–destination matrices using mobile phone call data. Transportation Research Part C: Emerging Technologies 40, 63-74.

Jackson, S., Miranda-Moreno, L.F., St-Aubin, P. and Saunier, N. (2013) Flexible, mobile video camera system and open source video analysis software for road safety and behavioral analysis. Transportation Research Record 2365(1), 90-98.

Johnstone, D., Nordback, K. and Lowry, M. (2017) Collecting Network-wide Bicycle and Pedestrian Data.

Kalatian, A. and Shafahi, Y. (2016) Travel mode detection exploiting cellular network Data, p. 03008, EDP Sciences.

Kristoffersen, M.S., Dueholm, J.V., Gade, R. and Moeslund, T.B. (2016) Pedestrian counting with occlusion handling using stereo thermal cameras. Sensors 16(1), 62.

Kurkcu, A. and Ozbay, K. (2017) Estimating Pedestrian Densities, Wait Times, and Flows with Wi-Fi and Bluetooth Sensors. Transportation Research Record: Journal of the Transportation Research Board (2644), 72-82.

Laharotte, P.-A., Billot, R., Come, E., Oukhellou, L., Nantes, A. and El Faouzi, N.-E. (2015) Spatiotemporal analysis of Bluetooth data: Application to a large urban network. IEEE Transactions on Intelligent Transportation Systems 16(3), 1439-1448.

Lan, Q., Gao, B., Chen, Z. and Zhu, S. (2017) Estimating Bluetooth mac scanner based pedestrian flow characteristic by taking the through pedestrian flow as a case study, p. 01007, EDP Sciences.

Leduc, G. (2008) Road traffic data: Collection methods and applications. Working Papers on Energy, Transport and Climate Change 1, 55.

Leykin, A. and Hammoud, R. (2006) Robust multi-pedestrian tracking in thermal-visible surveillance videos, pp. 136-136, IEEE.

Li, Y. and McDonald, M. (2002) Link travel time estimation using single GPS equipped probe vehicle, pp. 932-937, IEEE.

Malinovskiy, Y., Saunier, N. and Wang, Y. (2012) Pedestrian Travel Analysis Using Static Bluetooth Sensors. Transportation Research Board: Journal Of The Transpotation Research Board, 1-22.

Markowitz, F., Montufar, J. and Steindel, M. (2009) Automated Pedestrian Detection: State of the Art.

Martchouk, M., Mannering, F. and Bullock, D. (2010) Analysis of freeway travel time variability using Bluetooth detection. Journal of Transportation Engineering 137(10), 697-704.

Martin, B.D., Addona, V., Wolfson, J., Adomavicius, G. and Fan, Y. (2017) Methods for real-time prediction of the mode of travel using smartphone-based GPS and accelerometer data. Sensors 17(9), 2058.

Michau, G., Nantes, A., Bhaskar, A., Chung, E., Abry, P. and Borgnat, P. (2017) Bluetooth data in an urban context: Retrieving vehicle trajectories. IEEE Transactions on Intelligent Transportation Systems 18(9), 2377-2386.

Musa, A. and Eriksson, J. (2012) Tracking unmodified smartphones using wi-fi monitors, pp. 281-294, ACM.

Nanthawichit, C., Nakatsuji, T. and Suzuki, H. (2003) Application of probe-vehicle data for real-time traffic-state estimation and short-term travel-time prediction on a freeway. Transportation Research Record: Journal of the Transportation Research Board (1855), 49-59.

Nordback, K. and Janson, B. (2010) Automated Bicycle Counts: Lessons from Boulder, Colorado. Transportation Research Record: Journal of the Transportation Research Board (2190), 11-18.

Nordback, K., Kothuri, S., Phillips, T., Gorecki, C. and Figliozzi, M. (2016) Accuracy of bicycle counting with pneumatic tubes in Oregon. Transportation Research Record: Journal of the Transportation Research Board (2593), 8-17.

Ozbay, K., Yang, H. and Bartin, B.O. (2010) Calibration of an infrared-based automatic counting system for pedestrian traffic flow data collection.

Porter, J.D., Kim, D.S., Magaña, M.E., Poocharoen, P. and Arriaga, C.A.G. (2013) Antenna characterization for Bluetooth-based travel time data collection. Journal of Intelligent Transportation Systems 17(2), 142-151.

Proulx, F.R., Schneider, R.J. and Miranda-Moreno, L.F. (2016) Performance evaluation and correction functions for automated pedestrian and bicycle counting technologies. Journal of Transportation Engineering 142(3), 04016002.

Quayle, S.M., Koonce, P., DePencier, D. and Bullock, D.M. (2010) Arterial performance measures with media access control readers. Transportation Research Record: Journal of the Transportation Research Board 2192(1), 185-193.

Reichl, P., Oh, B., Tavakoli, S., Ravitharan, R. and Stafford, M. (2018) Using wifi technologies to count passengers in near real time in and around rail infrastructure: Rail: Smart, automated, sustainable, p. 525, Railway Technical Society of Australasia (RTSA); Technical Society of Engineers Australia.

Ryus, P., Ferguson, E., Laustsen, K.M., Prouix, F.R., Schneider, R.J., Hull, T. and Miranda-Moreno, L. (2014) Methods and technologies for pedestrian and bicycle volume data collection, Citeseer.

Saeedi, A. (2013) Utilizing wireless-based data collection units for automated vehicle movement data collection.

Schäfer, R.-P., Thiessenhusen, K.-U. and Wagner, P. (2002) A traffic information system by means of real-time floating-car data.

Schauer, L., Werner, M. and Marcus, P. (2014) Estimating crowd densities and pedestrian flows using wi-fi and bluetooth, pp. 171-177, ICST (Institute for Computer Sciences, Social-Informatics and Telecommunications Engineering).

Song, B. and Wynter, L. (2017) Real-time public transport service-level monitoring using passive WiFi: a spectral clustering approach for train timetable estimation. arXiv preprint arXiv:1703.00759.

Strauss, J., Miranda-Moreno, L., Crouse, D., Goldberg, M.S., Ross, N. and Hatzopoulou, M. (2012) Investigating the Link Between Cyclist Volumes and Pollution Levels Along Bicycle Facilities in Dense Urban Core.

Strauss, J., Miranda-Moreno, L.F. and Morency, P. (2015) Mapping cyclist activity and injury risk in a network combining smartphone GPS data and bicycle counts. Accident Analysis & Prevention 83, 132-142.

Tsubota, T., Bhaskar, A., Chung, E. and Billot, R. (2011) Arterial traffic congestion analysis using Bluetooth duration data.

Tufuor, E.O. and Rilett, L.R. (2018) Analysis of Low Cost Bluetooth-Plus-WiFi Device For Travel Time Research.

Wasson, J.S., Sturdevant, J.R. and Bullock, D.M. (2008) Real-time travel time estimates using media access control address matching. ITE Journal 78(6).

Weppner, J., Bischke, B. and Lukowicz, P. (2016) Monitoring crowd condition in public spaces by tracking mobile consumer devices with wifi interface, pp. 1363-1371, ACM.

Wieck, M. (2011) Use of bluetooth based travel time information for traffic operations.

Williams, N.E., Thomas, T.A., Dunbar, M., Eagle, N. and Dobra, A. (2015) Measures of human mobility using mobile phone records enhanced with GIS data. PloS one 10(7), e0133630.

Yoshimura, Y., Amini, A., Sobolevsky, S., Blat, J. and Ratti, C. (2017) Analysis of pedestrian behaviors through non-invasive Bluetooth monitoring. Applied geography 81, 43-51.

Zangenehpour, S., Miranda-Moreno, L.F. and Saunier, N. (2014) Automated Classification in Traffic Video at Intersections with Heavy Pedestrian and Bicycle Traffic.

Chapter 3: Development and Testing of a Real-Time WiFi-Bluetooth System for Pedestrian Network Monitoring, Classification, and Data Extrapolation

Asad Lesani[a], Luis Miranda-Moreno[a]

[a] *Department of Civil Engineering and Applied Mechanics, McGill University, Montreal, Canada*

Accepted for presentation at Transportation Research Board 95th annual meeting, Washington D.C and Published on "IEEE Transactions on Intelligent Transportation Systems". DOI: 10.1109/TITS.2018.2854895

3.1 ABSTRACT

A real-time pedestrian monitoring system provides information about traffic flow, speeds, travel times, and time spent in areas or transportation facilities of interest. This is useful in travel information systems and crowd management strategies, as well as in planning and emergencies in public spaces such as airports, parks, malls, and university campuses. While there are technologies that can obtain count data for non-motorized transportation at specific locations, most technologies cannot provide origin-destination information, trip paths, travel times, or time spent. To overcome these shortcomings, some studies have explored the use of Bluetooth sensors to capture the unique Media Access Control (MAC) addresses of mobile devices carried by pedestrians. However, this collection method may suffer from low-detection rates. As an alternative, collecting MAC data from WiFi signals has emerged. The objective of this work is three-fold: i) develop and evaluate the performance of an integrated WiFi-Bluetooth system to monitor pedestrian/cyclists activity traffic, ii) develop and validate a classification method for differentiating pedestrians from bicycles, and iii) propose a simple extrapolation method that combines counts and MAC data. Among other results, relatively high detection rates were obtained for the developed WiFi system in comparison with Bluetooth sensors. Also, the high correlation between estimated and ground

truth speeds and low classification errors are observed. Finally, the extrapolated WiFi counts and ground-truth counts were found to be highly correlated. These results demonstrate the feasibility of the proposed system and methods to estimate travel times (speeds), to classify bicycle-pedestrian WiFi signals, and to extrapolate pedestrian MAC counts.

3.2 INTRODUCTION

There has been a growing interest in the development and application of automated traffic data collection and monitoring systems, often referred to as intelligent transportation systems (ITS), in the field of transportation. There is also a burgeoning interest in technologies involved in collecting pedestrian and bicycle traffic flow data in public outdoor areas (e.g., parks, plazas, university campuses, and pedestrian streets) and indoor facilities (e.g., train terminals, airports, hospital, and stadiums). The collected data is required for various tasks during the planning, design, and operation stages of facilities. In some applications, real-time data is necessary for travel information systems, crowd management strategies, and emergencies. For example, at airports, providing real-time travel time between terminals and gates, as well as waiting times at security checkpoints, is extremely important. Monitoring both facilities and large events, such as at concerts and festivals, requires such technologies. In the case of emergency and evacuation scenarios, real-time information is also critical (Caspari et al. 2017, Longo and Cheng 2016).

For collecting counts, pedestrian sensors are commercially available and widely used in practice. These include passive & active infrared and ultrasonic counters for sidewalks, pressure & treadle mats for trails or indoor environments, etc. One can refer to (Lesani and Miranda-Moreno 2016) and (Markowitz et al. 2009) for more information. Despite their many advantages, these sensors can only provide data for a specific point in the network. In addition, when counting areas are not well defined or are very large, such as in open spaces, the performance (accuracy) of these sensors may deteriorate (Lesani et al. 2015). More importantly, point-based counting technologies are unable to identify the same individual at various points in a network to define trip routes, origins, and destinations, travel times, etc. These measures are as important as counting data in many non-motorized mobility applications. To overcome these limitations, some recent works have looked at anonymous identity-retaining tools and Media Access Control (MAC) signals. This includes the use of wireless technologies and data from Bluetooth, e.g., (Bullock et al. 2010) and (Malinovskiy et al. 2012), and WiFi access points, e.g., (Danalet et al. 2013) and (Musa and Eriksson 2012). More recently, several works have explored the use of smartphone Bluetooth and WiFi traces to collect pedestrian activity data given the high penetration rates of smartphones (Abedi et al. 2015, Ahmed et al. 2008, Bai et al. 2017, Bullock et al. 2010, Danalet et al. 2013, Du et al. 2017, Hidayat et al. 2018, Kurkcu and Ozbay 2017, Malinovskiy et al. 2012, Porter et al. 2013). In Canada, for instance, more than half of mobile phone users are smartphone users – and their share was expected to reach 60% in 2016. Most smartphones have both Bluetooth and WiFi capabilities.

Many Bluetooth-based methods and applications have been documented for vehicular traffic on highway networks. In recent years, increased development of applications based on the WiFi-Bluetooth scanning concept, to monitor pedestrian/cyclists facilities, has become apparent. Despite past efforts, some gaps can be highlighted in the literature. To our knowledge, no previous work has considered pedestrian and bicycle networks (mixed traffic on shared pedestrian bicycle spaces), in which MAC signals need to be classified by mode. In addition, the ability of WiFi counts to represent total volumes has not been studied.

To overcome these gaps in the literature, this work has three main objectives: i) to develop and test the performance of an integrated WiFi-Bluetooth system for detecting anonymous MAC addresses of devices at fixed locations in a pedestrian network mixed with bicycle traffic, ii) to propose and validate a classification algorithm for mixed pedestrian and bicycle traffic, and iii) to investigate the reliability of data extrapolation combining MAC and video data. The former objective includes comparing the performance differences of each technology.

As part of the contributions of this work, an integrated real-time system is proposed, which integrates sensors and algorithms for monitoring non-motorized transportation networks with pedestrian and bicycle traffic. Algorithms to classify and extrapolate MAC data were developed and tested on the McGill University campus. The performance of the proposed system is also quantified. The designed system works completely independently of the available infrastructure and can be easily implemented in other types of networks.

3.3 RELATED WORKS

The application and the performance of Bluetooth data collection systems for monitoring motor-vehicle traffic on highways have been researched heavily in recent years. Very few of these applications have been in pedestrian traffic. Generally, with a Bluetooth scanner, discoverable Bluetooth-enabled devices will be detectable by a sensor. Every Bluetooth device (e.g., car radio, smartphone) has a unique hardware MAC address (a 12-character hexadecimal number), which is uniquely identifiable. Bluetooth has a range of 3.3 to 33 meters, which can be upgraded to 100 meters using an external antenna (Piyare and Tazil 2011), depending on the device. It communicates power levels as users move radially closer and further from the sensor. Using multiple Bluetooth detectors throughout a network, the path and detected times of each device can be determined and used to generate origin-destination (O-D) matrices and travel times.

Several applications using Bluetooth data are documented in the literature, and various methods have been proposed to compute vehicular traffic performance measures such as travel time and O-D matrices (Friesen and McLeod 2015). Porter et al. 2013, evaluated the impact of different antennas and concluded that an antenna with a large gain and a lower sampling rate might provide more accurate travel time samples if the main focus is the collection of travel time data. However, Bluetooth technology has been used to monitor cyclists and pedestrians in very few cases. One can refer to (Hainen et al. 2013), (Jansen et al. 2014) and (Utsch and Liebig 2012). These works have employed Bluetooth sensors to measure pedestrian travel times at airport security checkpoints, to track the location of pedestrians in a laboratory, (Utsch and Liebig 2012) and to estimate the proportion of cyclists with a Bluetooth device within a city, combining Bluetooth data with inductive loop data (Jansen et al. 2014).

The advantages of Bluetooth sensors with respect to other technologies, (e.g., radio frequency identification or RFID, or plate recognition) include relatively lower costs, the ability to collect large quantities of real-time data, and the ease of installation. Given their flexibility, Bluetooth data collection devices are suitable for temporary and for permanent installation in roadway facilities of interest.

Despite the important advantages listed above, some of the limitations of Bluetooth technology have also been documented. An issue with Bluetooth detectors is that many users disable the service altogether on their devices, or otherwise keep their devices undiscoverable. This is partially due to the fact that, for many, the Bluetooth service is infrequently used. Also, leaving Bluetooth enabled reduces battery life. This can lead to low detection rates in non-motorized networks. Most of the applications involving Bluetooth technology are conducted in vehicular networks given that Bluetooth devices are mainly found in motor vehicles and very few are from smartphones. Detection rates for Bluetooth are usually reported to be between 5 and 12 percent (Malinovskiy et al. 2012).

As an alternative to Bluetooth data, some recent works have explored the use of WiFi signal devices connected to WiFi access points. These signals (MAC addresses) are used to track people traveling through a network, as one can see in (Danalet et al. 2013) and (Danalet et al. 2014). However, WiFi access point tracking requires that devices be connected to a specific wireless network and that the network encompasses the entire detection area, such as in indoor public spaces (airports, malls, university campus buildings, etc.) with available WiFi connection for users. Thus, the area under study cannot be expanded without extending the network coverage, which may be difficult. This could be an issue if the area under study is, for example, a park or a school campus. In some studies, cellular tower triangulation has been suggested as a way to track cellphones based on their cellular signal strength; however, location estimation is very coarse and therefore is only appropriate for O-D surveying (Caceres et al. 2007).

Because of the shortcomings of access point data and methods, there has been a growing interest in developing independent WiFi sniffer systems for pedestrian activity. In this case, capturing MAC addresses is not limited to the devices that are connected to a specific network. A passive WiFi scanner captures all available WiFi probe signals broadcasted by WiFi devices attempting to identify available access points. This probe signal is broadcasted independent of device connectivity to any available access points.

As part of the WiFi pedestrian-related applications, one can mention the work of (Schauer et al. 2014) in Munich Airport. This work compared various pedestrian flow techniques using both WiFi and Bluetooth scanners. The results showed that WiFi overestimated and Bluetooth underestimated flows compared to the number of boarding pass scans (ground truth). This study, however, used a small sample for validation and used only one sensor to obtain the number of detected MAC addresses at a single point. Other measures, such as O-D matrices, were not obtained since they require a network of sensors. In another work (Vu et al. 2010), the authors designed a pedestrian monitoring system which makes use of both WiFi and Bluetooth technologies. The Bluetooth data is used to assign a unique ID to each user based on a MAC address while the WiFi data is used to obtain the user's location. This data is then used to evaluate how long a person stays at one location and which location is the most popular. However, the proposed approach was not validated. In (Abedi et al. 2015), the authors empirically assessed the impact of small and large antenna gains on tracking movements of pedestrians and cyclists based on MAC address datasets. However, some issues exist in this work. Firstly, the authors considered a fixed coverage area based on the antenna gain but, in practice, the coverage area is also dependent on the type of device and network characteristics. Secondly, their proposed speed estimation approach was only validated for pedestrians (and not for cyclists). Thirdly, they classified pedestrians, runners, and cyclists only based on speed, the applicability of which is limited to large networks with large distances between sensors. In some recent works, (Kurkcu and Ozbay 2017) proposes an application to estimate the wait time in a bus terminal but the results were not validated with the ground truth data. (Du et al. 2017) proposes a method to improve the detection rate and estimation precision of pedestrian flow. (Bai et al. 2017) uses the WiFi scanning approach to count the number of pedestrians using WiFi traces at public transport stations. Other applications on transit buses have been recently published to monitor passenger demand (Hidayat et al. 2018).

Despite the work reported on WiFi/Bluetooth sensors for monitoring pedestrian activity, some gaps remain in the literature. An issue that has not been investigated is that pedestrian networks are often mixed with bicycle traffic. The classification of non-motorized users has not been investigated using mode detection algorithms. Furthermore, among available studies, no formal performance evaluation has been done on WiFi and Bluetooth detection rates based on ground truth obtained by other means. Also, the feasibility of pedestrian flow extrapolation between points has not been investigated by combining counting and MAC data.

3.4 SYSTEM OVERVIEW

The developed system is inspired by the best elements of WiFi and Bluetooth technologies, taking advantage of the portability of Bluetooth and the detection levels of WiFi. The 802.11 whitepaper

(Committee 1997) makes possible the detection of packets that are broadcast periodically by WiFi-enabled devices in a similar manner as how Bluetooth devices are detected. The WiFi device will broadcast probe signals even when the device is not being used. This probe signal will be captured by access points around the device and authenticate the connection if the device is in the list of authorized devices (based on the MAC address of the device). The designed system captures these probe signals and extracts the MAC address. The system is developed in a way that it is able to (i) track MAC addresses from WiFi traces from phones regardless of their network connection status or user settings (assuming WiFi radio is on), (ii) extract travel times and flows between two sensors per direction of travel and (iii) classify MAC addresses by mode into pedestrian or cyclist categories.

The designed WiFi packet sniffer integrates the open source packet sniffer software, AirCrack, which is used for network security penetration tests. Modifications were made to increase the detection power and the sensitivity by optimizing wireless channel selection. In the IEEE 2.4GHz WiFi protocol, the whole spectrum (from 2.4GHz to 2.5GHz) is divided into 14 channels.

A wireless connection is assigned automatically to one of these channels. A combination of the channels, 1, 6, and 11, can cover the whole spectrum with less overlap. In the packet sniffer, these channels are used to make the scanner faster and more efficient. The designed system sniffs probe signals from devices which are in managed mode (clients, also known as stations) and the devices in master mode (acting as access points). These two modes have different packet headers which our system can differentiate between by recording the client devices and excluding access points from our analysis.

The modified packet sniffer is also capable of storing the time stamp of all received packets. This information is critical for detecting the in-out time of the detected MAC address.

Capturing the MAC address of a wireless device raises the concern of protecting the privacy of its owner. This concern is addressed by encrypting all the detected MAC addresses before sending them to the servers. It is also worth noting that the MAC address is assigned by the chip manufacturer of the wireless device and does not include any personal information about the device owner; thus, no personal information can be associated.

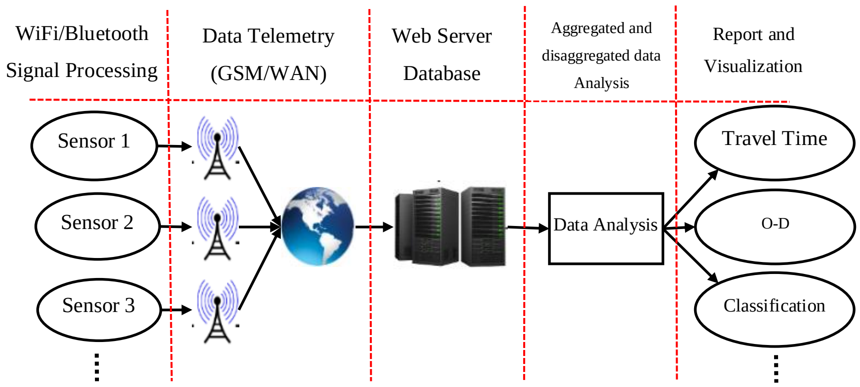

Figure 3-1. An overview of the developed system platform

Figure 3-1 shows an overview of the developed system platform. The development of the WiFi/Bluetooth sensors included the design and integration of different components. This involved the testing and selection of the best components, the design of a microprocessor, the integration of two separate modules for WiFi and Bluetooth, and a data logger. Additional details are provided as follows:

Processor: The designed system uses a 600MHz processor with a 1G RAM with a Debian Linux kernel, an open source OS. The built image of the OS kernel includes different programming languages and libraries to interface the processor with a USB 3G Modem, Bluetooth module, and wireless packet handling.

Bluetooth Module: To capture the Bluetooth MAC addresses, an upgraded high sensitivity Class I Bluetooth module has been used with an external antenna (either an omnidirectional or a directional antenna can be supported) to increase the detection zone of the sensor.

WiFi Module: This module is used to scan the 2.4GHz spectrum and capture the probe signals of WiFi devices. This module has its own antenna.

Data Logger: In order to locally record and transfer timestamped data to a web server, a unit including a Real-Time Clock module, an SD card, and a 3G Modem is used.

The final system is illustrated in Figure 3-2. It is worth mentioning that each individual sensor monitors the 2.4GHz spectrum for WiFi traffic on multiple channels. The same frequency is used to monitor Bluetooth devices. A Class I Bluetooth module is used to increase the sensitivity of the

Bluetooth scan unit and capture more Bluetooth MAC addresses from nearby devices. Moreover, packets are stored in an internal database or are transmitted via WiFi or GSM to a central database. In order to improve results, multiple sensors can be placed at a single site to increase the probability of catching packets while scanning channels. For short-term studies, the sensors can be powered by the battery while for long-term studies, sensors can be plugged into the electrical network or powered by solar panels. Secure and waterproof enclosures are used to protect the equipment against adverse weather conditions and tampering.

Figure 3-2. System hardware development and installation

The proposed WiFi detector exploits a part of the IEEE 802.11 protocol that has stations actively and frequently broadcasting the identities of their desired access points. Typically, this data is ignored by access points and other routers unless it is directed towards them specifically. Our device passively listens to all packets from all stations and records their specific MAC addresses. Such detectors can be used as a standalone way to retrieve information or can be coupled with other counting devices, such as infrared and microwave sensors, video analysis systems, and depth-based counters. Counters can detect and classify road users as they pass by, but are not well suited for identifying individual travel times, paths, and time spent in an area. The ability to single-out the identity and speed profile of most of the traffic moving through a network has two implications: (i) the paths of smartphone-carrying users can be extracted and (ii) the paths of non-smartphone-carrying users can be better estimated based on the known paths and data from other sensors.

The same criteria apply to capture the Bluetooth signals and to obtain the Bluetooth MAC addresses. However, there is one main difference: capturing a MAC address requires an active handshake between a sensor and a device, i.e. a sensor transmits probe signals to other enabled and discoverable Bluetooth devices and listens to their response.

This system is designed so that it can provide full coverage of an entire network at a relatively low cost. Also, sensors are not intrusive and can make use of existing infrastructure such as posts, wall, or barriers.

3.5 METHODOLOGY

This section outlines the four steps for data analysis: i) identification of MAC addresses between sensors, ii) estimation of travel time (speeds) between sensors and "time-seen" within a given sensor, iii) mode classification method and calibration and iv) extrapolation of MAC flow data. A procedure for implementing the methodology is then proposed.

3.5.1 Identification of MACs Between Adjacent Sensors

Consider that MAC addresses are constantly detected and reported by sensor *i*. For each detected MAC address, the algorithm searches for the same MAC in the adjacent sensors. For every detected MAC pair, the required information for data analysis is extracted. From the extracted data, time-seen and speed measures are obtained. Figure 3-3 describes parameter definitions that are used to extract these two measures based on two adjacent sensors, *i* and *j*:

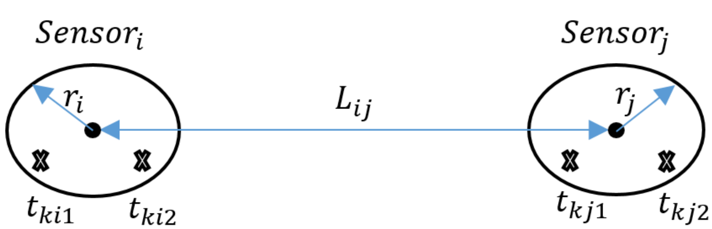

Figure 3-3. A network sample with two sensors and detection time definitions

Where, the variables L_{ij}, r_i, r_j, t_{ki1}, and t_{ki2} are defined as follows:

L_{ij}	Physical distance between sensors i and j
r_i, r_j,	Radius of the coverage area for sensors i or j
t_{ki1}	Timestamp of the first packet of data detected by sensor i from device k, also called first time-seen
t_{ki2}	Timestamp of the last packet of data detected by sensor i from device k, also called last time-seen

Then, the time-seen for a MAC address, Δt_{ki}, is defined as:

$$\Delta t_{ki} = t_{ki2} - t_{ki1} \tag{1}$$

It is worth mentioning that, for a given sensor i, t_{ki1} and t_{ki2} can be equal when it only detects a device once. That is, only one packet of data is captured by the sensor. In this case, the time-seen will be equal to zero.

To calculate the speed of an object, the location of the object at its detection time is required; however, this location cannot be determined since the device can be detected at any point within the coverage area of the sensor. The effective distance, L_{kij}^{eff}, of a detected MAC *k* between two sensors can be defined based on the two radii of coverage areas and physical distance between two sensors. In the form of an equation, L_{kij}^{eff} can be defined as:

$$L_{kij}^{eff} = L_{ij} + \alpha_i r_i + \alpha_j r_j \text{ where } \alpha \in [-1,1] \tag{2}$$

Where, α_i is a random factor $[-1,1]$ that is proportional to the location at which the MAC is detected in the coverage area. If it is detected at the beginning of the detection zone, α will be equal to +1. If it has been detected at the end of the detection zone, it will be equal to -1. The detection point is related to the location of the devices broadcasted probe signal and the detection zone is related to the type of antenna and the device antenna characteristics. Since the exact location of the detection and the exact detection zone range, α cannot be measured using information collected by the sensor, α and L_{kij}^{eff} cannot be calculated precisely. Based on the physical distance, the speed, S_{kij} of a device *k* moving between *i* and *j* can be computed as:

$$S_{kij} = \frac{L_{ij}}{t_{kj2} - t_{ki1}} \tag{3}$$

Where effective distance is kept equal to the physical distance between two sensors. This assumption can create large speed variations in cases where the physical distance between two sensors is not large enough (not significantly larger than the coverage zone of the sensor) to neglect the radius of the sensor coverage area.

In summary, the two measures available from each device traveling between two sensors are the speed of detected device k (S_{kij}) and the total time-seen in the two adjacent sensors (T_{kij}) which is equal to the sum of the time-seen of a MAC address at sensors i and j: $T_{kij} = \Delta t_{ki} + \Delta t_{kj} = (t_{ki2} - t_{ki1}) + (t_{kj2} - t_{kj2})$. Once MAC addresses have been identified between adjacent sensors, travel time or speed information is extracted. The steps to compute the travel time, detect the mode, and extrapolate the flow are described in the following subsections.

3.5.2 Travel Time and Speed Extraction

This section presents the method proposed to compute travel time and speed measures for each MAC address considering a pair of sensors:

Step 1: For any given pair of sensors, MAC addresses that were captured in both sensors are identified.

Step 2: For any MAC address k found in Step 1, the detection times are extracted from both sensors. Then for each sensor m, the data vector defined as D^m, includes all the detection times of MAC k, i.e., $D^m = \{time^m_{index}\} \;\; index \in [1,2,\ldots,\#of\ detections]$

Step 3: MAC addresses are grouped to generate a matrix showing the first time and the last time that a MAC address has been detected by sensor m. To implement a grouping algorithm, the vector D^m is first sorted based on the time. Then, all timestamped samples in D^m; are grouped as an identical group if $time^m_{index} - time^m_{index-1} < T_{th}$, where T_{th} is a threshold defining the maximum time between detection of a MAC address at a sensor that can correspond to the same trip (in our case study it has been defined as 300 seconds). In other words, if the time difference between two consecutive detections of a MAC address is bigger than 300 seconds, then it is considered a new trip for that MAC. Next, the last time-seen of a MAC address in that group is updated. Otherwise, a new group of times will be created. The output of the grouping algorithm is a matrix showing the *first time-seen* (the time of the first detected packet in a corresponding group) and the *last time-seen* (the detection time of the last sample in that group). The generated matrix is denoted as $G^m = \{(t^m_{k1}, t^m_{k2})\}$ where k indicates the index of the group. Each row of the matrix G^m shows the trip time-stamps (first time and last time seen). An example of a group matrix for a given sensor and MAC address can be as:

$$G^m = \begin{bmatrix} 11:12:32 & 11:13:54 \\ 12:44:23 & 12:45:12 \\ 16:23:12 & 16:23:14 \end{bmatrix}$$

In the given sample matrix G^m, three different trips have been detected by sensor m at different times of the day.

Step 4: Travel time and speed are computed for any given pair of sensors. Considering the pair of sensors m and n, the travel time referred to as tt^{mn} is calculated as:

$for\ i = 1{:}\,size(G^m)$
    $t_1^m = G^m(i, 1)$
    $t_2^m = G^m(i, 2)$
    $for\ j = 1{:}\,size(G^n)$
        $t_1^n = G^n(j, 1)$
        $t_2^n = G^n(j, 2)$
        $if\ t_2^m < t_1^n$: # it means that there is no overlap between detections
            $tt^{mn} = t_2^n - t_1^n$
            $s^{mn} = L^{mn}/tt^{mn}$ # $L^{mn} is\ distance\ between\ sensors$
            $if\ (s^{mn} < S_{up}^{th})\ and\ (s^{mn} > S_{down}^{th})$: # upper and lower speed limit
                $append\ s^{mn}\ to\ speed\ data$
            $break$;

The procedure calculates the travel time of trips traveling from sensor m to sensor n. The same concept can be used to get the travel time in the reverse direction by interchanging m and n in the code.

3.5.3 Mode Classification Method

This algorithm is used to classify each detected MAC address as a pedestrian or as a cyclist. For this, four different classifiers are defined in this section and evaluated later.

3.5.3.1 Classifier I: Threshold Based Classifier

This is the simplest classifier that relies only on speed thresholds. These speed thresholds are extracted from empirical speed distributions for the two types of road users. For pedestrians, a lower limit, Th_{p-low}, is established to filter out samples with very small values of speed, possibly from users who stay between sensors for long periods of time. Additionally, an upper limit, Th_{b-up}, is also defined as the cyclist speed threshold to filter out very high speed values that can be associated with motorized modes, overlap bthe etween sensors, or very short distance between sensors. In this case, a simple classifier can be defined as:

$$\begin{cases} if\ Th_{p-low} < S_k < Th_{p-up}, & Classify\ as\ pedestrian \\ if\ Th_{p-up} < S_k < Th_{b-up}, & Classify\ as\ cyclist \\ else, & Non-Classified \end{cases} \tag{4}$$

Where Th_{p-low}, Th_{p-up}, and Th_{b-up} are the predefined threshold values.

3.5.3.2 Classifier II: Statistical Speed Approach

For the second classifier, a logit model is calibrated and used to find the probability of being a pedestrian or a cyclist. The probability of belonging to a given class is defined based on a logit regression model:

$$\begin{cases} Pr(\,C_k = ped|\,S_k) = \dfrac{1}{1+e^u} \\ Pr(\,C_k = bike|\,S_k) = \dfrac{e^u}{e^u+1} \end{cases} \tag{5}$$

Where u is a liner function of the travel speed between two sensors (S_k) and $u = \beta_0 + \beta_1 S_k$, with β_0 and β_1 being the regression parameters estimated from the empirical data. The model calibration is explained later in the paper. Once the model is calibrated, the speed S_k of each detected sample k is known and the class C_k can be estimated. Once the probability of each sample is calculated, this rule is applied: if $Pr(\,C_k = ped|\,S_k)$ > 0.5, then the MAC address is classified as a pedestrian. Otherwise, it is classified as a cyclist.

3.5.3.3 Classifier III: Statistical Time-Seen Approach

Due to the slower travel speed nature of pedestrians compared to cyclists, we expect longer time-seen values at a given sensor for pedestrians and shorter values for cyclists. That is, pedestrians are expected to take more time between entering and leaving the detection zone of a given sensor. However, because the scan time interval of smartphones can be as high as 2 minutes, some samples will have very short time-seen values making it impossible to distinguish between a pedestrian and a cyclist by simply using the time-seen information.

This classifier uses the same approach as *Classifier II*, but instead of using speed data, the total time-seen T_k is used in the logit model. Again, the probability functions are defined as:

$$\begin{cases} Pr(\, C_k = ped|\, T_k) = \dfrac{1}{1+e^u} \\ Pr(\, C_k = bike|\, T_k) = \dfrac{e^u}{1+e^u} \end{cases} \tag{6}$$

And the utility function u is defined as $u = \alpha_0 + \alpha_1 T_k$ where T_k stands for total time-seen of detected MAC in both sensors. Then, if the $Pr(\, C_k = ped|\, T_k) > 0.5$, the sample is classified as a pedestrian, otherwise it is classified as a cyclist.

3.5.3.4 Classifier IV: Combined Logit Model

Here, the two previous classifiers are combined to use two sources of data, speed, and time-seen. In Classifier II, speed data is used to define the probability of belonging to each class. Empirical data shows that, in most cases (around 85% of estimated speeds), the walking speeds vary between 3km/h to 7km/h and biking speed varies between 12km/h to 16km/h. However, in some cases, the speed of a pedestrian or cyclist can vary between 7km/h to 12km/h (refereed as the mixed speed interval). These samples can belong to running pedestrians or cyclists biking at slower speeds due to high pedestrian traffic on shared paths. This could also be attributed to inaccuracy in travel time estimation due to the detection range and short distances between sensors that introduce error to the speed estimation.

To address this issue, a combination of both Classifiers II and III is used. For speed samples within mixed speed intervals, the probability of being a pedestrian and of being a cyclist are nearly equal. Therefore, using a threshold of 0.5 for the probability is not sufficient. To address this issue, probabilities for both sources of data (speed and time seen) are calculated based on classifiers II and III:

$if\ Pr(\, C_k = ped|\, S_k) > Th_p$:
    $Classify\ as\ pedestrian$
$if\ Pr(\, C_k = ped|\, S_k) < Th_b$:
    $Classify\ as\ cyclist$
$else$:
    $if\ Pr(\, C_k = ped|\, T_k) > 0.5$:

$$Classify\ as\ pedestrian$$

$$if\ Pr(\ C_k = ped|\ T_k) < 0.5:$$

$$Classify\ as\ pedestrian$$

In the next section, the calibration of each model and the values of the thresholds are discussed.

3.5.4 Flow Extrapolation

Once MAC addresses between two adjacent sensors i and j are classified by mode, a sample of the total flow of road users (pedestrians or cyclists) is obtained as the outcome. The extrapolation of the sample to the entire population is then required in order to obtain an estimate of the total volume of pedestrians or bicycles. The representativeness of the sample is thus a crucial aspect to consider. If the sample by mode is representative of the total flow of each mode, the estimation of the volumes can be relatively simple. In this paper, a simple extrapolation methodology is proposed and computed as:

$C_e^t = F_{uc} \times C_{WiFi}^t$, where the under-counting factor, F_{uc}, is defined as $F_{uc} = \frac{\sum_t C_G^t}{\sum_t C_{WiFi}^t}$ and the other variables are defined as:

C_G^t	total number of pedestrians (or bikes) counted using the camera between two sensors, i and j at time interval t
C_{WiFi}^t	total number of MACs detected between two sensors at time interval t
C_e^t	extrapolated number of pedestrians (or bikes) using MAC counts at time interval t

This simple approach can help estimate pedestrian flow between sensors assuming that the MAC sample, C_{WiFi}^t, is representative of the total flow.

3.5.5 Implementation

This section summarizes the implementation of the proposed methodology. For this, consider a MAC address k and a network of M installed WiFi-Bluetooth sensors. Also, consider the following notation:

Notation	Description
Trip	The observed trajectory of visited sensors of a given MAC address
t	The total time (in a sec) in which a MAC k moves (travels) through the sensors
n	A positive integer number showing the time window associated with the trip, $n = int\left(\frac{t}{\Delta t}\right)$, where Δt is any predefined time interval, i.e. (15-min intervals).
P_{ij}^k	Trip information captured by WiFi-Bluetooth sensor and associated with MAC address k from sensor i to sensor j where $i, j \in [0,1, \dots, M]$.
S_{ij}^k	Speed of captured trip for MAC address k from sensor i to sensor j
T_{ij}^k	Total time-seen of the captured trip for MAC address k from sensor i to sensor j
C_{ij}^k	Object class of captured trip for MAC address k from sensor i to sensor j
$\tilde{P}^k = [\, P_{ij}^k]$	Set of all captured trips associated with MAC k collected by all sensor combinations through the network.
N_b^n	A total number of objects classified as a pedestrian in time interval n.

The methodology for implementation for each given MAC address is discussed below:

Step 1: Obtain all the required information related to MAC addresses from all the sensors in a given time interval.

Step 2: For each captured trip between sensors i and j, and given MAC address k, calculate the speed and the total seen time $P_{ij}^k = (S_{ij}^k, T_{ij}^k)$.

Step 3: Classify detected object k as either a pedestrian or a cyclist and update trip information array: $P_{ij}^k = (S_{ij}^k, T_{ij}^k, C_{ij}^k)$.

Step 4: Produce the object k information matrix as a set of trips associated with MAC k, $\widetilde{P}^k = [\, P_{ij}^k]$.

Step 5: The final class of the object k (C^k) is equal to the class that has more repetition in the vector of object classes, $C^k = max(count\left(C_{ij}^k = pedestrin\right), count\left(C_{ij}^k = cyclist\right))$. This maximum repetition comes from the entire trip of the object through the network considering all sensor combinations.

Step 6: Update counts matrix for the time interval of the detected MAC address using the rule:

$$if\ C^k = pedestrian \quad then \quad N_p^n = N_p^n + 1$$

$$if\ C^k = cyclist \quad then \quad N_b^n = N_b^n + 1$$

Step 7: At the end of each time interval, pedestrian and cyclist counts for time interval n are appended to the count matrix.

Step 8: Pedestrian and cyclist counts are extrapolated based on count (volume) data.

3.6 SYSTEM EVALUATION AND DATA EXTRAPOLATION

The proposed methodology is tested within the pedestrian network of McGill University campus, located in downtown Montreal, Canada. The testing area is composed of pedestrian streets, with relatively low bicycle traffic (shared space) and practically no vehicular traffic flow. This test aims to investigate the performance of our system as well as to show the feasibility and the performance of the proposed methodology. For this, four important steps are required:

Step 1: Installing a set of sensors, including WiFi-Bluetooth sensors, video cameras, and automated counters

Step 2: Collecting and processing data over a few days, including ground truth information for model calibration

Step 3: Evaluating the performance of the designed WiFi-Bluetooth system.

Step 4: Implementing the methodology to compute speeds, O-D matrices, and volumes by mode

3.6.1 Data Collection

For the system test, three WiFi-Bluetooth devices were built, each of them with a water-proof enclosure and an internal power source (battery). The three locations chosen for sensor placement are illustrated in Figure 3-4. The location of sensors was carefully defined so that the overlap of sensing ranges between sensors do not exist. The shortest distance between sensors is around 300 m, which is greater than the detection range of a 50 m radius for each sensor. Larger distances can increase accuracy and reduce the variance in travel time and speed estimation.

In addition, a camera was installed at the Y-intersection for validation and extrapolation purposes. The camera was used to count pedestrians and cyclists, and to obtain speed samples. A wide-angle camera was selected and installed with enough height (approximately 10 meters) to cover an area of around 20 meters. This helps in allowing to consider only road users are passing between the three sensors (the path from sensor 1 to sensor 2 and, finally, to sensor 3 and vice versa). The recorded video is then used for model training, validation and extrapolation purposes.

Figure 3-4. Sensor locations at McGill University's downtown campus

As mentioned before, the McGill campus is a pedestrian network with cyclist traffic. Therefore, it is an appropriate place to test the proposed system and methods. Our data collection can be divided into three steps. A total of 90+ hours of video across 12 days, all weekdays, peak and off-peak hours were recorded. Data was collected during June, July, and October of 2015. Table 3-1 shows data collection schedules.

The video data is used for detection rates and extrapolation validation. The counts (number of pedestrians walking between sensors 1, 2, and 3 per direction) were obtained manually using video data. Then, the 15-min count data is compared with detections and extrapolated flows for validation purposes.

To calibrate the speed based classifier, a sample of 2,600 speed observations was generated using a specialized open-source software, *Traffic Intelligence* (TI), and 6 hours of recorded video on July 1st, 2015, from which trajectories, speeds, and mode type were automatically generated. This process has been documented in previous research (Zangenehpour et al. 2015), reporting 88%

accuracy in the classification algorithm. Once TI is used to classify and generate trajectories by mode, the mode misclassification errors were manually corrected by watching the entire video. Misclassified samples were fixed manually in the database. Also, we assumed that the recorded speed in a 20 m radius of the camera is the same as the rest of the path between sensors.

Table 3-1. Data collection schedules

Date	Week Day	Start	End	Total
2015-06-19	Friday	11:00	19:15	8hr, 15min
2015-06-22	Monday	13:00	21:15	8hr, 15min
2015-06-26	Friday	10:00	18:15	8hr, 15min
2015-06-30	Tuesday	10:00	17:45	7hr, 45min
2015-07-01	Wednesday	11:00	17:00	6hr, 00min
2015-07-02	Thursday	10:30	18:30	8hr, 00min
2015-07-03	Friday	10:30	18:00	7hr, 30min
2015-10-01	Thursday	11:45	17:45	6hr, 00min
2015-10-02	Friday	9:45	18:15	8hr, 30min
2015-10-07	Wednesday	9:00	17:30	8hr, 30min
2015-10-08	Thursday	9:15	18:30	9hr, 15min
2015-10-09	Friday	11:00	17:00	6hr, 00min

To calibrate the seen-time based classifier and finally validate the performance of the classifier, 200 manual trips were done on July 1st and 2nd, 2015, in different hours of the day, by research assistants registering their cellphone MAC addresses and GPS traces. Their MAC address was matched with the registered one using scanners for validation and GPS was used to obtain the travel time between points. To ensure a fair comparison between different classes, the dataset was balanced in terms of the number of samples in each class (in this case, 100 bicycle and 100 walking trips). Among 200 sample trips, 60% were used to calibrate the model, and 40% were used to evaluate classifier accuracy. These manual trips were also used for travel time (speed) estimation validation.

3.6.2 Mode Classifier Calibration

The classifier calibration process involves two steps: i) video data collection to obtain ground truth data of walking and cycling speeds from a large sample of individuals in the same network of analysis and ii) calibration of the distributions or model parameters.

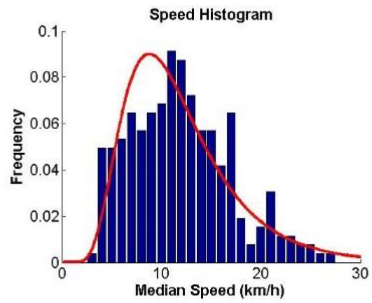

Distribution of cyclist speed

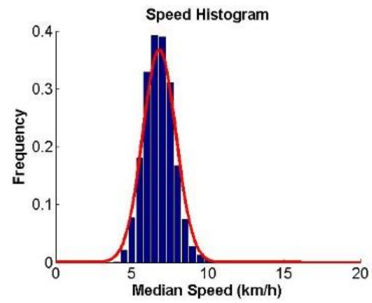

Distribution of pedestrian speed

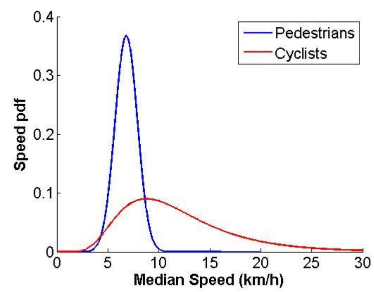

Probability function of $\boldsymbol{Pr}(\boldsymbol{S_k} | \boldsymbol{C_k})$

Figure 3-5. Speed distribution and probability functions of each object type

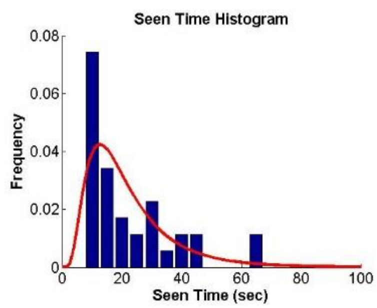

Distribution of cyclists seen time

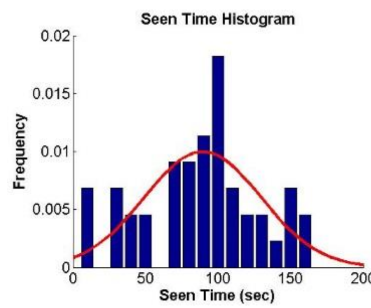

Distribution of pedestrian seen time

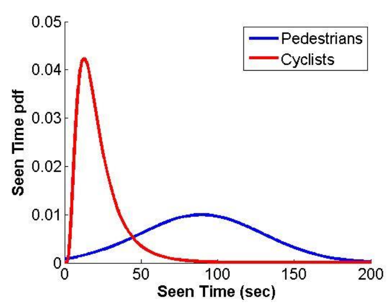

Probability function of $\boldsymbol{Pr}(\boldsymbol{T_k} | \boldsymbol{C_k})$

Figure 3-6. Seen-time distribution and probability functions of each object type

Figure 3-5 and Figure 3-6 show the speed and seen-time distribution for the samples of pedestrians and cyclists obtained from the video process. Probability distributions are then fitted for each set of data. After trying different options, the best fitted probability density functions (pdf) were found to be the Normal and Log-Normal distributions for pedestrians and cyclists, respectively.

Not surprisingly, one can see that the samples with bigger time-seen are more likely to be pedestrians. In other words, the probability of being a cyclist when the time-seen values are small (e.g., ≤ 50 seconds) is much higher than the probability of being a pedestrian.

Using the same approach, a model is fitted to the data to obtain the parameters of the utility function (α_0 and α_1) in the logit model presented in equation 6. These parameters are used in Classifier III and the binary logit model is used to predict the mode probability given the speed.

Detection rates are determined to explore the capabilities of our proposed system. The accuracy of the classification methodology is also tested here. Detection rate analysis was performed at different intervals. Network flows between campus entrances and exits were determined. Bluetooth and WiFi technologies were also tested and compared in parallel.

3.6.3 System Performance

The criteria to evaluate the performance of the system is the number of matched MAC addresses between two sensors with respect to the total volume. Here, the detection rate = N_p/V_p, where N_p is the total unique MAC addresses read in two locations, and V_p is the total traffic volume in 15-min, 30-min or 1-hr intervals. The detection rate validation was based on the volumes in 15-min intervals and a total of more than 58,000 trips detected during 12 days of data collection. To validate classification accuracy, 200 manual trips were used.

To compute detection rates, the number of MAC addresses between sensors and the total number of pedestrians in each direction from manual counting were obtained in each direction.

Table 3-2 shows a 2.5 hours sample detection rate of both the Bluetooth and WiFi technologies on October 9th, 2015. Note that the total number of pedestrians traveling from sensor 1 (main gate) to sensor 2 (Figure 3-7) was determined using video data. From these results, one can clearly see that WiFi has a much higher detection rate than Bluetooth. This result is not surprising given the low usage of Bluetooth technologies as reported in previous research (Malinovskiy et al. 2012).

Table 3-2. Sample of number of detection and detection rate for each technology

Time Period		Total Volume		WiFi				Bluetooth			
				Detected WiFi Signals		Detection WiFi Rate		Detected Bluetooth Signals		Detection Bluetooth Rate	
Start	End	Dir. 1	Dir. 2	Dir. 1	Dir. 2	DR* (Dir. 1)	DR (Dir. 2)	Dir. 1	Dir. 2	DR (Dir. 2)	DR (Dir. 2)
11:00	11:15	82	69	21	17	25.6	24.6	1	3	1.2	4.3
11:15	11:30	149	164	33	32	22.1	19.5	0	2	0.0	1.2
11:30	11:45	127	113	49	19	38.6	16.8	1	0	0.8	0.0
11:45	12:00	64	78	8	18	12.5	23.1	2	1	3.1	1.3
12:00	12:15	82	89	21	18	25.6	20.2	0	0	0.0	0.0
12:15	12:30	75	99	21	18	28.0	18.2	0	1	0.0	1.0
12:30	12:45	108	132	20	18	18.5	13.6	1	1	0.9	0.8
12:45	13:00	154	173	28	38	18.2	22.0	2	0	1.3	0.0
13:00	13:15	138	130	55	30	39.9	23.1	1	0	0.7	0.0
13:15	13:30	70	87	22	15	31.4	17.2	0	2	0.0	2.3

DR = Detection rate

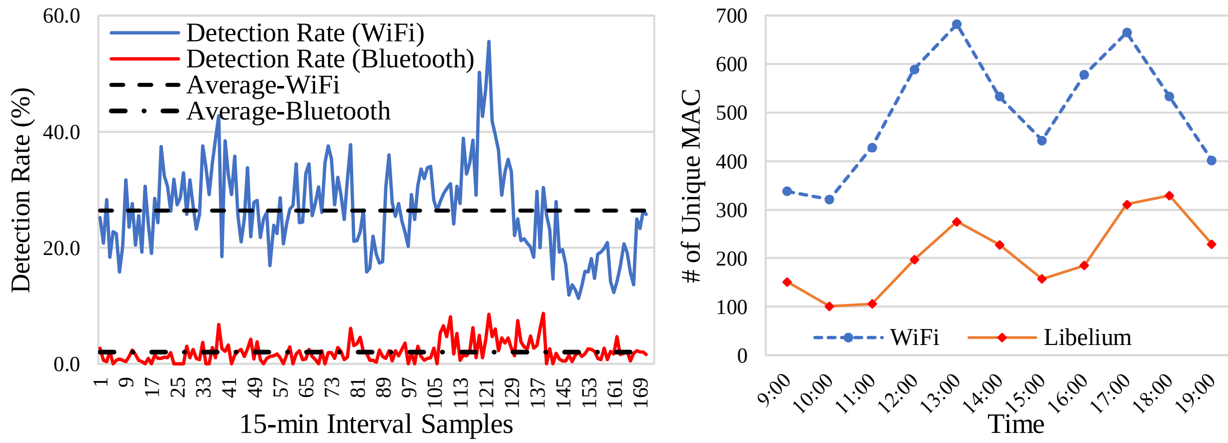

Figure 3-7. a) Detection rate comparison, b) proposed System WiFi vs. Libelium WiFi

Figure 3-7.a presents the detection rates measured in 15-min time intervals. Note that only 170 intervals (from the first 6 days out of 12) were used to make this figure clear. Again, the detection rate of WiFi was significantly higher than Bluetooth, with average detection rates of 27% and 2%, respectively. As a complementary assessment of our systems, a commercial sensor was installed in parallel with one of our sensors. Figure 3-7.b compares our developed system with a Meshlium sensor, a Bluetooth-WiFi sensor designed by Libelium (*www.libelium.com*). To compare the two systems fairly, we used the same antenna and installed both sensors at the same location. The better performance of our proposed WiFi detector in comparison with Libelium sensor comes from better channel hopping technic we used to detect the WiFi packets. The 2.4GHz WiFi frequency band is divided into 14 different channels covering 2.412GHz to 2.484GHz (https://en.wikipedia.org/wiki/List_of_WLAN_channels) . Each channel has overlap with the previous and next three channels. In our scanning algorithm, we are just scanning the three main channels, 1, 6 and 11 which are covering the whole WiFi frequency band. This implementation helped us to speedup scanning algorithm which directly affects the detection rate of the sensor.

Table 3-3 shows some statistics on detection rates of both WiFi and Bluetooth technologies. Due to different patterns in the number of trips captured by a given sensor for different flow rates, we divided the pedestrian-bike flow into different categories and calculated statistical parameters for each category separately. Based on the results, we can see a decrease in the average detection rate with an increase in volumes. This drop may be due to the short amount of time available for the system to process WiFi probe signals in high-volume conditions. This could potentially be solved by the use of a redundant system (e.g., two WiFi modules could be implemented in the same sensor). Also, higher variations in the detection rates are expected with high pedestrian flows. This concept can be seen in Table 3-3 where the standard deviation of the detection rate samples increases when the pedestrian flow increases.

Table 3-3. Some statistics on detection rates (15-min intervals)

Ped. Flow	# of Samples	WiFi				Bluetooth			
		Average	Std.	Min	Max	Average	Std.	Min	Max
<80	9	28.22	5.26	18.42	35.82	3.42	3.02	0.00	8.70
80-120	22	30.09	5.92	20.99	42.70	2.35	1.97	0.00	6.74
120-160	59	27.23	7.01	14.17	55.56	2.17	1.99	0.00	8.50
160-200	31	25.89	8.79	12.28	47.34	2.10	1.41	0.00	5.20
200-240	19	26.04	8.62	15.76	50.22	1.28	1.09	0.00	4.93
>240	29	22.13	8.86	11.27	38.85	1.43	1.16	0.26	6.23
Dataset	169	26.40	7.75	11.27	55.56	2.02	1.80	0.00	8.70

3.6.4 Travel Time Validation

In addition to the detection rate, the accuracy of travel times obtained from the sensors was validated using ground truth data. For this, estimated travel times and, then, speeds were computed based on timestamped detected MAC addresses between sensors 1 and 3 and were compared with "ground truth" travel times (speed) obtained from 200 manual trips.

In large networks, there might be more than one route between two different nodes or sensor locations. Therefore, route choice behavior and travel time filtering should be considered as part of future work. This potential problem can be solved by adding a route choice model or by increasing the sensor density. In the current application, sensors were strategically located to avoid this issue. Alternative routes between sensors existed but had longer travel times because of significantly longer distances. In addition, the camera was installed with a complete view of the only existing path between sensors on campus. Therefore, we can easily count the users taking the connecting path between sensors and remove the rest. For instance, there are other paths from sensor 1 to sensor 3 through off-campus streets; however, these routes are associated with long travel times which is based on the average walking speed of pedestrians and the length of alternative paths (420 seconds compared to 200 seconds). These detected travel time samples were then removed (outliers) using an upper threshold.

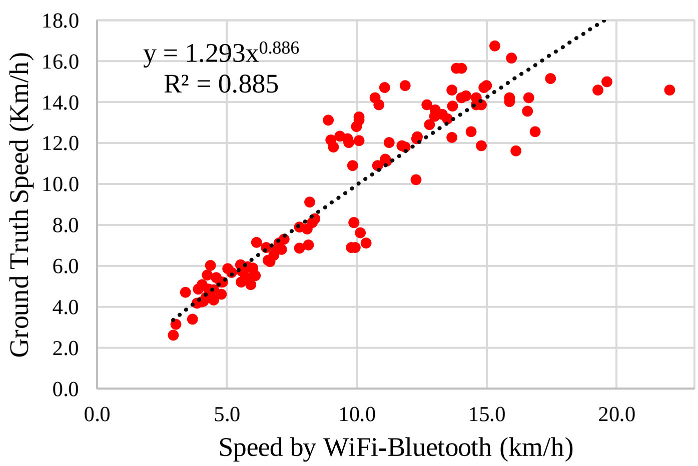

Figure 3-8. Ground truth speed data vs. speed estimated by the sensor

Figure 3-8 shows the plotted speed values estimated using WiFi sensors versus ground truth speeds. Again, it needs to be mentioned that the ground truth speeds are calculated based on manual trips the volunteers have done carrying their phone and registering their GPS location. One can see that the estimated speeds are highly correlated to the ground truth data with an R-squared value equal to 0.88. As depicted in the plot, the real and estimated speed data are very close to each other demonstrating accuracy of the proposed system in speed or travel time estimation. An average error of about 11.5% was observed.

As mentioned earlier, since the exact location of the last detection cannot be measured, the physical distance between sensors is used as the effective distance. Therefore, the larger the distance between sensors relative to the detection area of each sensor, the greater the accuracy of speed estimation. The antenna used in this study is a 2dBi omnidirectional antenna. Our estimated coverage range with this antenna is about 50 m (that is similar to the range used in (Abedi et al. 2015)). In this study, the effect of the range on the variance of the speed estimation was investigated. As described in Table 3, the variance of the hourly speed estimation is equal to 0.16 for short distance between sensors (about a 300 m distance between sensor 1 and 2) and 0.01 for longer distance between sensors (about 600 m between sensor 1 and 3). This addresses the challenge of selecting the proper antenna, which depends on the distance between sensors. For an antenna with lower gain, the detection rates will be lower, but the speed estimation accuracy will increase. However, for pedestrian networks, where the speed of the users are low (around 5 km/h), the selected antenna meets these requirements. As a simple example, assume that the radius of each sensor's detection area is about 50 m and that the physical distance between sensors is 300 m.

Then for a sample of travel time equal to 180 seconds, the speed value can be calculated as: $S_{ij} = \frac{d_{ij} \pm r_i \pm r_j}{t_{ij}} = \frac{300 \pm 50 \pm 50}{180}$ which leads to a maximum of 8 km/h and a minimum of 4 km/h, indicating very high speed estimation variance. Instead, if the distance between sensors were 600 m and travel time were 360 seconds, the values would be 7 km/h and 5 km/h, respectively, which shows less speed estimation variance.

Table 3-4 shows the hourly average estimated pedestrian speed and the variance between two pairs of sensors for about 9 hours of data. In this test, the distance between sensor 1 and 2 was small (about 150 m). We expected a larger variance for average travel time measured between sensors 1 and 2 in comparison with the average travel time between sensors 1 and 3 (which were 350 m apart). The variance of the average speed between sensors 1 and 2 was 10 times more than the variance of the average speed between sensor 1 and sensor 3. Based on these results, it is recommended that the distance between sensors be as large as possible to increase the accuracy of travel time measurements.

Table 3-4. Hourly average pedestrian speed between sensors

Start	End	From Roddick to Intersection (km/h)	From Roddick to Milton (km/h)	Average (km/h)
11:00	12:00	5.2	4.8	5.0
12:00	13:00	5.8	4.7	5.4
13:00	14:00	5.3	4.8	5.2
14:00	15:00	5.3	5.0	5.1
15:00	16:00	5.5	4.7	5.1
16:00	17:00	5.4	4.9	5.1
17:00	18:00	5.0	4.7	4.9
18:00	19:00	5.3	4.7	5.1
19:00	20:00	6.4	4.9	5.6
Variance $(km/h)^2$		**0.16**	**0.01**	**0.04**

3.6.5 Calibration and Validation of the Mode Classifiers

Here, the implementation of the mode classification method is presented, and the evaluation of the alternative classifiers is discussed. As defined in the methodology section, four different classifiers are proposed and calibrated using the sample of video speeds classified by mode and summarized in Figure 3-5 and Figure 3-6. Using the estimated speed observations and 200 time-seen observations, the parameters of the logistic models are determined. As mentioned before, 60 percent of data was selected randomly and was used to calibrate the model, and the rest was used as a test dataset to evaluate the performance of each classifier. The estimated parameters for the speed-based model are $\beta_0 = -8.9$ and $\beta_1 = 0.91$. For the time-seen model, the parameters are $\alpha_0 = -2.63$ and $\alpha_1 = -0.06$. From this, the probability of being a pedestrian or a cyclist can be computed given the speeds or time-seen and the corresponding parameters.

To evaluate the accuracy of the classifier, the dataset which includes 200 manual samples of bicycle and pedestrian trips with known speed and the mode is used. To evaluate the performance, the classification error is used as a measure. This is defined as the total number of misclassified samples (MSCL) divided by the total number of samples in that class. The same measure is used over the entire dataset as a global measure of performance as well as for each mode.

Table 3-5. Performance measure of each developed classifier

Mode	# of Samples	Classifier I		Classifier II		Classifier III		Classifier IV	
		MSCL	% Error	MSCL	% Error	MSCL	% Error	MSCL	% Error
Ped.	40	9	22.5	5	12.5	8	20.0	1	2.5
Bike	40	3	7.5	6	15.0	5	12.5	2	5.0
Total	80	12	15.0	11	13.7	13	16.2	3	3.7

MSCL: Number of misclassified (by developed classifier) samples in that class of users

The results are reported in Table 3-5, from which one can clearly observe that Classifier IV has the best performance, globally and when separating classes. The error percentage is around 4%. This clearly shows the advantage of fusing the two pieces of information (speed and time-seen data), which significantly improves the classification accuracy. Classifier I is relatively simple (based on a simple threshold on speed), it works very well for classifying bike users, but it performs poorly for classifying pedestrians with an error of around 22%. This leads to an average error of 15% on the entire dataset.

3.6.6 Extrapolation

This section explores the accuracy of the simple extrapolation method briefly described in the methodology section. For this application, only the WiFi system outcomes are considered based on the fact that detection rates were greater than 20% in 4 out of 5 cases (in contrast with the very low Bluetooth rates).

To investigate the correlation between estimated WiFi counts and observed counts using video, a regression model using a second-degree polynomial function is fitted to the data with two variables, total WiFi counts and total ground truth video counts. The dataset including 12 days of 15-min interval manual counts with their corresponding number of detected trips using WiFi scanner are used for extrapolation. To further evaluate the performance of the proposed method, the dataset is divided into two groups; a training dataset, including seven days of data used for model calibration and a testing dataset to evaluate the model accuracy.

Figure 3-9.a shows the outcome between ground-truth total volume and WiFi counts using 15-min intervals for training dataset. Different type of models was tested to fit on data and the second-degree polynomial function had the best R-squared value. From this, a high R-squared value of 0.70 indicates a high correlation between the WiFi counts and the ground truth counts collected using video data. Using the training dataset, the correction factor was estimated to be 3.38 and was applied to the test dataset to evaluate the accuracy of the model. Figure 3-9.b shows the result of extrapolation using two days of test dataset. According to the plot values, the extrapolated values are very close to the ground truth 15-min pedestrian flow and the hourly pattern of the flow is tracked well by the extrapolated data. Statistical analysis on estimation errors on test dataset shows 17.1 and 14.41 for average and median estimation error respectively, demonstrating the potential of our developed platform for estimating the flow on pedestrian networks. These numbers can perhaps be improved by using more complex estimation methods.

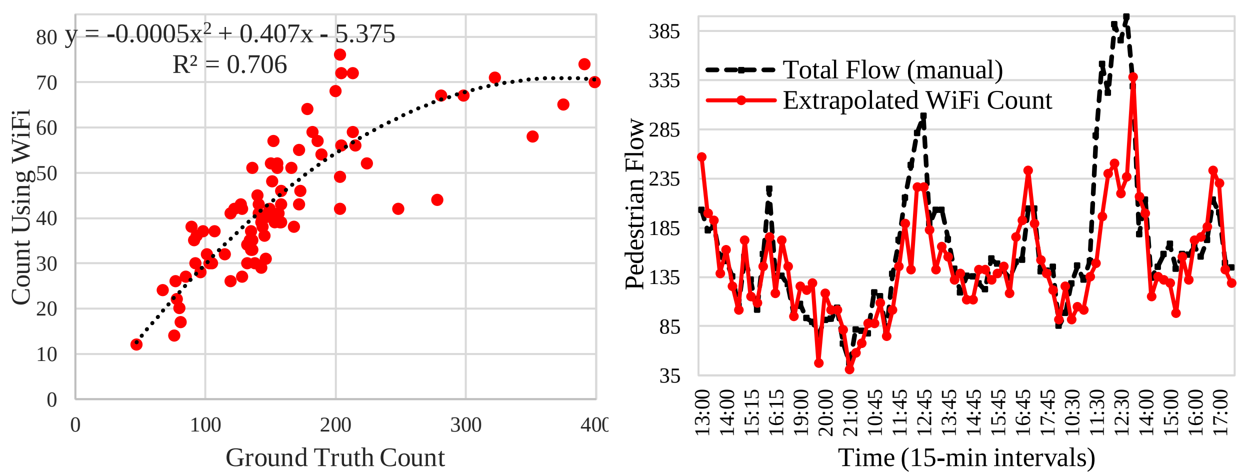

Figure 3-9. a) correlation and between WiFi count and ground truth data, b) ground truth data vs. extrapolated counts

3.6.7 Some Limitations and Future Work

It should be noted that a limited set of observations was obtained at higher or lower speeds and counts (Figure 3-8 and Figure 3-9). This is because very few or no observations were obtained at these extreme conditions. Outside of this range, the system needs more validation.

The system was tested only in a small network. Additional tests in different environments and network sizes can be carried out to validate the performance of the system and the methods in other conditions. The system could be integrated with other designed automated pedestrian counting systems such as ultrasonic or LIDAR technology. A sensor-based counting system could be connected to the main processor through a wire or Bluetooth and data could be transferred to a server through the Internet. The system will be integrated to obtain data for extrapolation in a few locations in a network of sensors. The classification of pedestrians, cyclists, and vehicles is another topic that can be investigated. The MAC address could be classified based on historical data. Received Signal Strength Indication (RSSI) can be explored as an additional source of information which might be useful for classification purposes. The daily and long-term travel patterns of MAC addresses could also be investigated to learn more about the short and long-term periodicity of visits and time spent on public spaces.

3.7 CONCLUSIONS

This research developed and evaluated the performance of a Bluetooth-WiFi sniffer to detect anonymous MAC addresses of devices in pedestrian-bicycle networks. A comparative analysis was reported between these two technologies. Also, as part of the contributions, mode classification and extrapolation methods were proposed and evaluated using ground truth data. Our system was designed to work in real time so that all captured MAC addresses can be transferred to a web server at a time frame predefined by the user. The system can operate with a battery for a few days or with a solar panel for a longer period of time. Key system parameters associated with its performance can be controlled and adjusted by the user. The proposed system and analytical methods were evaluated using video counts and GPS data as ground truth. About 90 hours of video data were recorded for this purpose. In addition, GPS traces and pre-defined MAC addresses were used to compare travel time estimated using a WiFi-Bluetooth system with ground truth data.

Among other outcomes, promising results were obtained with the WiFi detection rates being higher than those typically reported in past studies using only Bluetooth technologies. In the network case study, an average detection rate of 26% for the WiFi system (with detection rates up to 50%) was observed. In comparison, the average detection rate for Bluetooth technology was as low as 2%. In fact, Bluetooth technologies alone are unfeasible in pedestrian networks given the low detection rates. Therefore, WiFi protocol can then be seen as a better alternative to Bluetooth in pedestrian networks mixed with bicycle traffic.

The accuracy of estimated travel times or speeds was also investigated using ground truth data collected through manual trips and then compared with estimated speeds using MAC address captured by sensors. The preliminary results show a high correlation between estimated speed and ground truth speed data with an R-squared value of 0.88. In addition, an average estimation error of about 11.5%, with a standard deviation equal to 9%, was obtained using the developed system.

For mode classification, four classifiers were calibrated and tested ranging from simple classifiers based on speed threshold values to more complex classifiers using fused-statistical logit models. The average error percentages using logit models with speed and time-seen (separate models) as variables were about 14% and 16% respectively. However, when using a combined model with speed and time-seen duration (Classifier IV), the method showed much better results with an average classification error percentage of 3.7%.

Furthermore, the extrapolation of WiFi MAC counts was tested using video data for pedestrian flow. A simple extrapolation method was used to estimate pedestrian flows from WiFi counts by assigning a correction factor to the number of WiFi counts in each 15-min intervals. An R-squared value of 0.70 was obtained when correlating WiFi counts and total pedestrian volumes. The extrapolated results show an average estimation error of 17.1%. This provides some evidence concerning the potential of using extrapolated WiFi counts as a surrogate of total volumes.

3.8 ACKNOWLEDGMENT

We acknowledge the important contribution of the research assistants Taras Romancyshyn, Philip Morse, and Nawfal Kammah in data processing. Funding for this project was provided in part by the Natural Science and Engineering Research Council and Canada Foundation for Innovation.

3.9 REFERENCES

Abedi, N., Bhaskar, A., Chung, E. and Miska, M. (2015) Assessment of antenna characteristic effects on pedestrian and cyclists travel-time estimation based on Bluetooth and WiFi MAC addresses. Transportation Research Part C: Emerging Technologies 60, 124-141.

Ahmed, H., EL-Darieby, M., Abdulhai, B. and Morgan, Y. (2008) Bluetooth-and Wi-Fi-based mesh network platform for traffic monitoring.

Bai, L., Ireson, N., Mazumdar, S. and Ciravegna, F. (2017) Lessons learned using wi-fi and Bluetooth as means to monitor public service usage, pp. 432-440, ACM.

Bullock, D., Haseman, R., Wasson, J. and Spitler, R. (2010) Anonymous bluetooth probes for measuring airport security screening passage time: the indianapolis pilot deployment.

Caceres, N., Wideberg, J. and Benitez, F. (2007) Deriving origin destination data from a mobile phone network. Intelligent Transport Systems, IET 1(1), 15-26.

Caspari, A., Levine, B., Hanft, J., Planner, P.T., Planning, R.N. and Reddy, A. (2017) Real-Time Estimation of Platform Crowding for New York City Subway: 1 Case Study at Wall St 2/3 Station in Financial District 2. situations 60, 61.

Committee, I.C.S.L.M.S. (1997) Wireless LAN medium access control (MAC) and physical layer (PHY) specifications, IEEE Std.

Danalet, A., Farooq, B. and Bierlaire, M. (2013) Towards an activity-based model for pedestrian facilities.

Danalet, A., Farooq, B. and Bierlaire, M. (2014) A Bayesian approach to detect pedestrian destination-sequences from WiFi signatures. Transportation Research Part C: Emerging Technologies 44(0), 146-170.

Du, Y., Yue, J., Ji, Y. and Sun, L. (2017) Exploration of optimal Wi-Fi probes layout and estimation model of real-time pedestrian volume detection. International Journal of Distributed Sensor Networks 13(11), 1550147717741857.

Friesen, M.R. and McLeod, R.D. (2015) Bluetooth in intelligent transportation systems: a survey. International Journal of Intelligent Transportation Systems Research 13(3), 143-153.

Hainen, A.M., Remias, S.M. and Bullock, D.M. (2013) Collection and analysis of multi-modal airport land side probe data from Bluetooth enabled mobile devices, pp. 1304-1309, Institute of Electrical and Electronics Engineers Inc., The Hague, Netherlands.

Hidayat, A., Terabe, S. and Yaginuma, H. (2018) WiFi Scanner Technologies for Obtaining Travel Data about Circulator Bus Passengers: Case Study in Obuse, Nagano Prefecture, Japan. Transportation Research Record, 0361198118776153.

Jansen, S., Hoting, D., Runge, J., Brinkhoff, T., Nicklas, D. and Sauer, J. (2014) 9 Million Bicycles? Extending Induction Loops with Bluetooth Sensing, pp. 113-116, IEEE Computer Society, Los Alamitos, CA, USA.

Kurkcu, A. and Ozbay, K. (2017) Estimating Pedestrian Densities, Wait Times, and Flows with Wi-Fi and Bluetooth Sensors. Transportation Research Record: Journal of the Transportation Research Board (2644), 72-82.

Lesani, A. and Miranda-Moreno, L.F. (2016) Development and Testing of a Real-Time WiFi-Bluetooth System for Pedestrian Network Monitoring and Data Extrapolation.

Lesani, A., Miranda-Moreno, L.F., Fu, T. and Romancyshyn, T. (2015) Development and Testing of an Ultrasonic-Based Pedestrian Counting System.

Longo, S. and Cheng, B. (2016) Real-Time Privacy Preserving Crowd Estimation Based on Sensor Data, pp. 95-102, IEEE.

Malinovskiy, Y., Saunier, N. and Wang, Y. (2012) Pedestrian Travel Analysis Using Static Bluetooth Sensors. Transportation Research Board: Journal Of The Transpotation Research Board, 1-22.

Markowitz, F., Montufar, J. and Steindel, M. (2009) Automated Pedestrian Detection: State of the Art.

Musa, A. and Eriksson, J. (2012) Tracking unmodified smartphones using wi-fi monitors, pp. 281-294, ACM.

Piyare, R. and Tazil, M. (2011) Bluetooth based home automation system using cell phone, pp. 192-195, IEEE.

Porter, J.D., Kim, D.S., Magaña, M.E., Poocharoen, P. and Arriaga, C.A.G. (2013) Antenna characterization for Bluetooth-based travel time data collection. Journal of Intelligent Transportation Systems 17(2), 142-151.

Schauer, L., Werner, M. and Marcus, P. (2014) Estimating crowd densities and pedestrian flows using wi-fi and bluetooth, pp. 171-177, ICST (Institute for Computer Sciences, Social-Informatics and Telecommunications Engineering).

Utsch, P. and Liebig, T. (2012) Monitoring Microscopic Pedestrian Mobility Using Bluetooth, pp. 173-177, IEEE Computer Society, Los Alamitos, CA, USA.

Vu, L., Nahrstedt, K., Retika, S. and Gupta, I. (2010) Joint bluetooth/wifi scanning framework for characterizing and leveraging people movement in university campus, pp. 257-265, Association for Computing Machinery, Bodrum, Turkey.

Zangenehpour, S., Miranda-Moreno, L.F. and Saunier, N. (2015) Automated classification based on video data at intersections with heavy pedestrian and bicycle traffic: Methodology and application. Transportation Research Part C: Emerging Technologies 56, 161-176.

Link Between Chapter 3 and Chapter 4

In Chapter 3, an embedded WiFi-Bluetooth scanning system has been developed and tested for collecting real-time MAC data in non-motorized environments. A framework for classification of MAC signals (in pedestrians and bicycles) has been presented along with a simple way to extrapolate signals into pedestrian counts. For this purpose, MAC addresses are matched between sensors installed in different locations, then based on the time stamp of the detections, travel times (average speeds) of the users are estimated. The information is then used to build a framework to classify the detected signals and extrapolate the total flow based on the WiFi traces.

In the next Chapter (Chapter 4), the same scanning system is evaluated in an arterial context. As seen in Chapter 3, Bluetooth scanners perform poorly for non-motorized environments. However, Bluetooth technology has been used intensively in motor-vehicle traffic networks. The findings show that most of the Bluetooth MACs detected by our device belong to the motorized users. It proves that there is a potential in using our proposed embedded system in a multimodal network, which the Bluetooth scanning system provides accurate insights about the vehicular activity. These insights can be used to develop mode classifiers based on WiFi data (which covers all user modes). The following chapter evaluates the performance of using Bluetooth and WiFi data in vehicular networks and compares the results with ground truth data. It also builds the base for our future work on using embedded WiFi-Bluetooth system in the multi-modal traffic network.

Chapter 4: Arterial Traffic Monitoring Using an Integrated WiFi-Bluetooth System

Asad Lesani[a], Taras Romancyshyn[a], Luis Miranda-Moreno[a]

[a] *Department of Civil Engineering and Applied Mechanics, McGill University, Montreal, Canada*

Accepted for presentation at Transportation Research Board 95th annual meeting, Washington D.C.

4.1 ABSTRACT

There are a number of sensory systems available in the market to monitor traffic networks. However, these types of technologies cannot provide detailed data of user trip pattern (O-D matrices) and speed over the network. To achieve this, the system should be able to collect anonymous data pertaining to the vehicles in the network. In recent studies, Bluetooth (BT) technology has been widely used as a motor-vehicle traffic monitoring system using captured unique Media Access Control (MAC) address of Bluetooth devices. However, little is known about the performance of WiFi technology regarding detection rates and travel time estimation in comparison with Bluetooth technology. Hence, in this paper, we developed and tested an integrated Bluetooth-WiFi system to investigate the performance of each technology. To increase the detection rates, a high sensitivity class I Bluetooth module is integrated into the system. The performance of the two systems is then evaluated against ground truth data obtained from manual video processing at 5 min and 15 min intervals. At each individual (specific) sensor, the results indicated a higher detection rate of WiFi in comparison with the Bluetooth technology on a single sensor or when a network of sensors are implemented (more than two sensors). However, Bluetooth detection rates are higher when just two sensors are considered due to the fact that the WiFi probe signals are sent randomly in one or two minute intervals and that the arrival to the detection zone of each sensor might not lie in the interval when the device is sensing the probe signal.

In addition, the speed estimation errors decreased from 8.6% (Bluetooth only) to 5.8% (Bluetooth-WiFi). Although the usage of Bluetooth in recent years has dropped, there is merit in having both technologies integrated into the same system, particularly in urban traffic networks.

4.2 INTRODUCTION

In the transportation field, there has been a growing interest in the development of traffic monitoring systems, often referred to as intelligent transportation systems (ITS) technologies, to estimate reliable and efficient traffic measures, such as travel times, operating speeds and volumes in arterials or highways. The ability to measure travel times, route choices, volumes, and congestion levels are all very important tools for practitioners and researchers alike looking to plan and improve infrastructure.

Among the popular technologies for monitoring and collecting real-time or short-interval counts and directions, one can mention traditional loop detectors, and video cameras (Datondji et al. 2016, Robert 2009, Katsuki and Tatsubori 2018, Sochor et al. 2017, Wang et al. 2018) used also for traffic surveillance. More recently, other traffic sensors such as acoustic, ultrasonic, radar, and video-based detection sensors have become popular. Depending on the sensor, traffic volume, speeds and in a few cases, time gaps can be obtained at different levels of temporal aggregation. Some technologies can provide vehicle level speeds per lane with a high level of precision in highway conditions. Computer vision algorithms can capture microscopic traffic parameters by grouping features and detecting group velocities from the previously captured elevated video, though these metrics are extracted in post-processing (Sochor et al. 2017). Most of these detectors are not disruptive to traffic because they are installed out-of-lane and often use existing roadside infrastructure. However, these traffic sensors are often very expensive and difficult to install and power in fixed locations. Also, the need for real-time traffic and travel time information is becoming increasingly important in urban areas for which large sets of devices are needed. In this regard, the use of these sensors for collecting data is insufficient because of their limited coverage and high costs of both, installation and maintenance.

While all the sensors previously mentioned can accurately detect and count their respective modes of transportation, they lack the ability to provide travel times and O-D matrices. For this, individual vehicles need to be tracked as they move outside of each individual sensor's range and through the network. This issue led us to look at anonymous identity-retaining tools. In this area, smartphones have become the device of choice for many people buying new phones all over the world. In Canada, more than half of mobile phone users use smartphones, and the penetration rate is expected to reach 60% in 2016. Almost every phone available today has Bluetooth functionality, and most smartphones have both Bluetooth and WiFi. These wireless communication protocols (IEEE 802.11 for WiFi, formally IEEE 802.15.1 for Bluetooth) offer convenient ways for users to connect peripherals or to the Internet, and for devices to be detected by appropriate hardware.

In order to overcome the high cost and limitations of traditional data collection methods, simpler approaches have emerged using wireless technologies, such as Bluetooth (Lan et al. 2017, Yoshimura et al. 2017, Ahmed et al. 2008, Bullock et al. 2010, Malinovskiy et al. 2012, Martchouk et al. 2010, Porter et al. 2013, Saeedi 2013, Tsubota et al. 2011) WiFi access points (Hidayat et al. 2018, Reichl et al. 2018, Weppner et al. 2016, Ahmed et al. 2008, Danalet et al. 2013, Musa and Eriksson 2012), and cellular tower data (Caceres et al. 2007). In this context, Bluetooth surveillance has been researched heavily in recent years. In broad terms, a Bluetooth-enabled device that is discoverable can be detected by another Bluetooth radio, which in this case would be the detector. Every Bluetooth device has a unique hardware Media Access Control (MAC) address (a 12-character hexadecimal number), which is uniquely identifiable. A Bluetooth device has a range of anywhere from 3.3 meters to 33 meters (depending on the device and version of Bluetooth) and communicates power levels as users move radially closer and further from the sensor.

Using multiple detectors throughout a network, the path and rough speed of each device can be determined and used to generate OD surveys, travel times, and congestion levels (Hidayat et al. 2018, Tufuor and Rilett 2018, Barcelo et al. 2010, Blogg et al. 2010, Carpenter et al. 2012, Laharotte et al. 2014, Martchouk et al. 2010, Saeedi 2013, Tsubota et al. 2011, Wasson et al. 2008). Several applications in which Bluetooth devices have been used to compute travel time measures and other traffic performance measures have been reported recently. Among the first works, one can refer to Wasson et al. 2008, which conducted a study to estimate travel times in freeways and arterials in the greater Indianapolis area. In another study, Kurkcu and Ozbay 2017 explored their use for computing congestion measures to evaluate the impact of highway work zones using as a case study a rural interstate in Indiana. Among the studies in urban environments, Quayle et al. 2010, measured segment travel time, average running speed, and origin-destination in arterials in Portland, Oregon. Yu et al. 2014 evaluated an incident detection algorithm which makes use of Bluetooth data on an arterial road in Tigard, Oregon. In a different application, Day et al. 2010, evaluated signal coordination by combining travel time measurements with detector event data. Szuch and McDaniel 2011, estimated travel time reliability along goods movement corridors used heavily by trucks in Calgary. Other studies have compared alternative methods, such as floating car versus Bluetooth data collection (Haghani et al. 2010). In most recent studies Salanova Grau et al. 2017, uses Bluetooth data to generate origin-destination and flow estimation over time. Lewandowski et al. 2018 proposes a method, which utilizes mobile devices (smartphones) and Bluetooth beacons, to detect passing vehicles and recognize their classes.

The advantages of Bluetooth methods over conventional technologies have been highlighted in several documents including relatively lower costs (hardware and software are inexpensive), ability to collect large quantities of data over time, and ease of installation. Given their flexibility, Bluetooth data collection devices are suitable for temporary or permanent installation in roadway facilities of interest. These sensors can be used to measure travel times in highways and arterials (Hidayat et al. 2018, Tufuor and Rilett 2018, Malinovskiy et al. 2012, Martchouk et al. 2010, Saeedi 2013).

Despite the important advantages listed above, a number of limitations have also been documented. The issue with Bluetooth detectors is that many users disable the service altogether on their devices, or otherwise keep their devices undiscoverable. This is partially due to the fact that for many people, the Bluetooth service is not frequently used. Also, leaving Bluetooth enabled can have a negative effect on battery life. This, along with detection error, leads to low detection rates. Detection rates for Bluetooth are usually reported between 5% and 12% (Malinovskiy et al. 2012, Porter et al. 2013). For instance, Wieck 2011, investigated the technology on an arterial corridor with 6 intersections and found a matching rate that varied from 3% to 11.4%. While the small sampling rate can be statistically adequate given the fleet size, higher detection rates between sensors are always preferred to increase system reliability. Despite recent developments, Bluetooth-based systems can still have difficulties monitoring traffic in arterials or facilities with a high traffic mix, in particular for corridors with high volumes of pedestrians and bikes. WiFi access point tracking requires that devices be connected to a specific wireless network and that the network encompasses the entire detection area. Cellular tower triangulation is very coarse so it is only appropriate for origin-destination surveying (Bonnel et al. 2018, Bonnel et al. 2017, Caceres et al. 2007).

To overcome the issues with Bluetooth and increase its accuracy rate, some researchers have begun considering WiFi detection as an alternative (Hidayat et al. 2018, Tufuor and Rilett 2018, Danalet et al. 2013, Musa and Eriksson 2012). WiFi is another common wireless service, but it has a much higher use-rate than Bluetooth because, while enabled, it allows users to connect to known networks when in range to save on cellular data usage (if applicable). WiFi has been used in existing networks to track devices that are connected to a specific network (Danalet et al. 2013). This is particularly useful for networks with a large wireless coverage area and many nodes, such as a university campus. Devices must be connected to the given wireless network and must be within the coverage area. The area studied thus cannot be expanded without extending the network coverage, which can be difficult as it means expanding the area supporting access to the Internet to its users. This could be an issue if the area under study is, for example, a highway, a neighborhood, or anything other than a campus. Because of the mentioned shortcomings of using access point data to monitor traffic networks using WiFi protocol in recent years, a growing interest in developing independent WiFi sniffer systems can be seen. In these systems, capturing MAC addresses is not limited to the devices that are connected to a specific network.

In the literature, few studies have compared the performance of Bluetooth and WiFi scanners in providing usable and representative travel data. In regards to road traffic, Abbott-Jard et al. 2013, compared the performance of the two technologies with data collected along a major arterial and freight route in Brisbane, Australia. The results indicated that 1191 matching MAC-ID were able to be identified from the data produced by the Bluetooth scanners compared to 149 from the data produced by the WiFi scanners. In addition, the percentage of usable data from the Bluetooth and WiFi scanners were 81% and 19% respectively. The authors mentioned that WiFi technology may have been affected by interference with other WiFi signals in the area.

This work proposes and evaluates the performance of a system to detect anonymous MAC addresses of devices at short distances at temporal or fixed locations. Proposed herein is a technique for capturing signals from WiFi-enabled mobile devices for the purpose of measuring travel times, speeds, and user activity over a network. This document also discusses the potential advantages of the WiFi data collection system as an alternative or complement to Bluetooth technology for monitoring devices throughout a network.

Our system is inspired by the best elements of both WiFi and Bluetooth, taking advantage of the portability of Bluetooth and the detection levels of WiFi. After reviewing the 802.11 whitepaper (Committee 1997), it became clear that it was possible to detect packets that are broadcast periodically by WiFi-enabled devices in a similar manner to the way Bluetooth devices are detected. The system we set out to create is able to: i) track MAC addresses from WiFi traces from phones regardless of their network connection status or user settings (assuming WiFi radio is on) and ii) extract travel times and flow rates per direction.

4.3 SENSOR SYSTEM OVERVIEW

In this section, the developed system is introduced. First, we take a look at the hardware design and elements and, then, software development and data analysis methodology is explained.

4.3.1 Hardware Components

The first step in developing the system was designing the different components of the WiFi/Bluetooth sensor. These tasks required a number of steps, including the selection and testing of the best components, the design of a microprocessor, integration of a Bluetooth and WiFi modules and data logger. Additional details are provided as follows:

1. ***Processor**:* The designed system uses a 600MHz processor with 64M RAM with OpenWRT, an open source Linux based OS. The built image of the OS kernel includes different programming languages and libraries to interface the processor with a USB 3G Modem, Bluetooth module, and a wireless packet handling.
2. ***Bluetooth Module**:* To capture the Bluetooth MAC addresses, a serial Bluetooth module is used in our system. The Bluetooth module is a “class I” Bluetooth device (higher sensitivity in comparison with class II Bluetooth devices used in smartphones) with an external antenna.

3. ***WiFi Module***: This module is used to scan the 2.4GHz spectrum and capture probe signal of WiFi devices.
4. ***Data Logger****:* In order to record locally and transfer timestamped data to a web server, a unit including Real Time Clock module, SD card and 3G Modem is used.

The final system is illustrated in the following pictures:

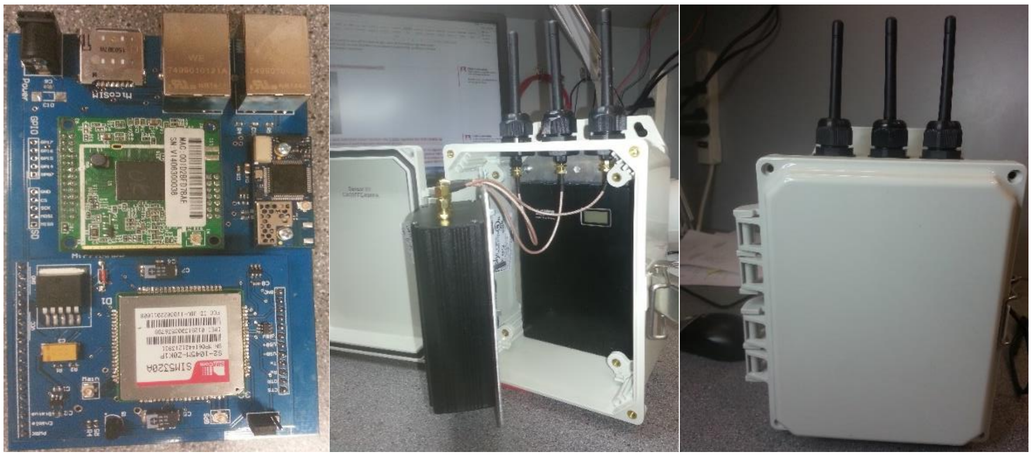

Figure 4-1. System hardware development

It is worth mentioning that each individual sensor monitors the 2.4 GHz spectrum for WiFi traffic on multiple channels. The same frequency is used to monitor Bluetooth devices. A class I Bluetooth module is used in our system to increase the sensitivity of the Bluetooth scan unit and capture more Bluetooth MAC addresses from nearby devices. Moreover, packets are stored in an internal database or transmitted via WiFi or GSM to a central database. In order to improve results, multiple sensors can be placed at a single site to increase the probability of catching packets while scanning channels. For short-term studies, the sensors can be powered by the battery while for long-term studies, they can be plugged into the municipal electrical system or be powered by solar panels. The secure, waterproof housing is used to protect the equipment against adverse weather and tampering.

The proposed WiFi detector exploits a part of the IEEE 802.11 protocol that has stations actively and frequently broadcasting the identities of their desired access points. Typically, this data is ignored by access points and other routers, unless is it directed toward them specifically. Our device passively listens to all packets from all stations and records their specific MAC addresses. Such detectors can be used as a standalone way to retrieve information or can be coupled with other counting devices, such as infrared and microwave sensors, video analysis systems, and depth-based counters. These other counters do a good job of catching and classifying all traffic as they pass by, but are not well suited for identifying individual paths. The ability to single out the identity and speed profile of most of the traffic moving through a network has two implications: (i) the paths of smartphone-carrying users can be extracted, and (ii) the paths of non-smartphone-carrying users can be better estimated based on the known paths and data from other sensors.

The same criteria are used to capture the Bluetooth signals and get the MAC addresses of Bluetooth devices, but with some differences. In regards to Bluetooth technology, capturing a MAC address requires active handshaking between a sensor and a device, i.e., a sensor transmits probe signals to other enabled and discoverable Bluetooth devices and listens to their response.

Among the advantages of the developed system with respect to the existing one, is that the full coverage of the entire facility with a set (cluster) of devices is relatively low cost. Devices are not intrusive and make use of infrastructure that already exists (such as posts and barriers). Additionally, the designed system is also completely compatible with a developed pedestrian counting system based on ultrasonic technology. The pedestrian counting system is connected to the WiFi-Bluetooth system through a wire or Bluetooth communication protocol to transfer data to the main processor which then relays the data to a server.

4.3.2 Data Collection and Analytics

The process of extracting travel speed data from pairs of Bluetooth sensors involved numerous steps. These steps are presented conceptually in Figure 4-2.

4.3.2.1 Deleting non-matching MAC addresses

The first step involved deleting MAC addresses that did not appear in both datasets obtained from each sensor. This step was done first in order to avoid uselessly computing the results determined using the subsequent steps for MAC addresses in one sensor which could not be matched to identical MAC addresses in another sensor and, therefore, could not produce a travel time result.

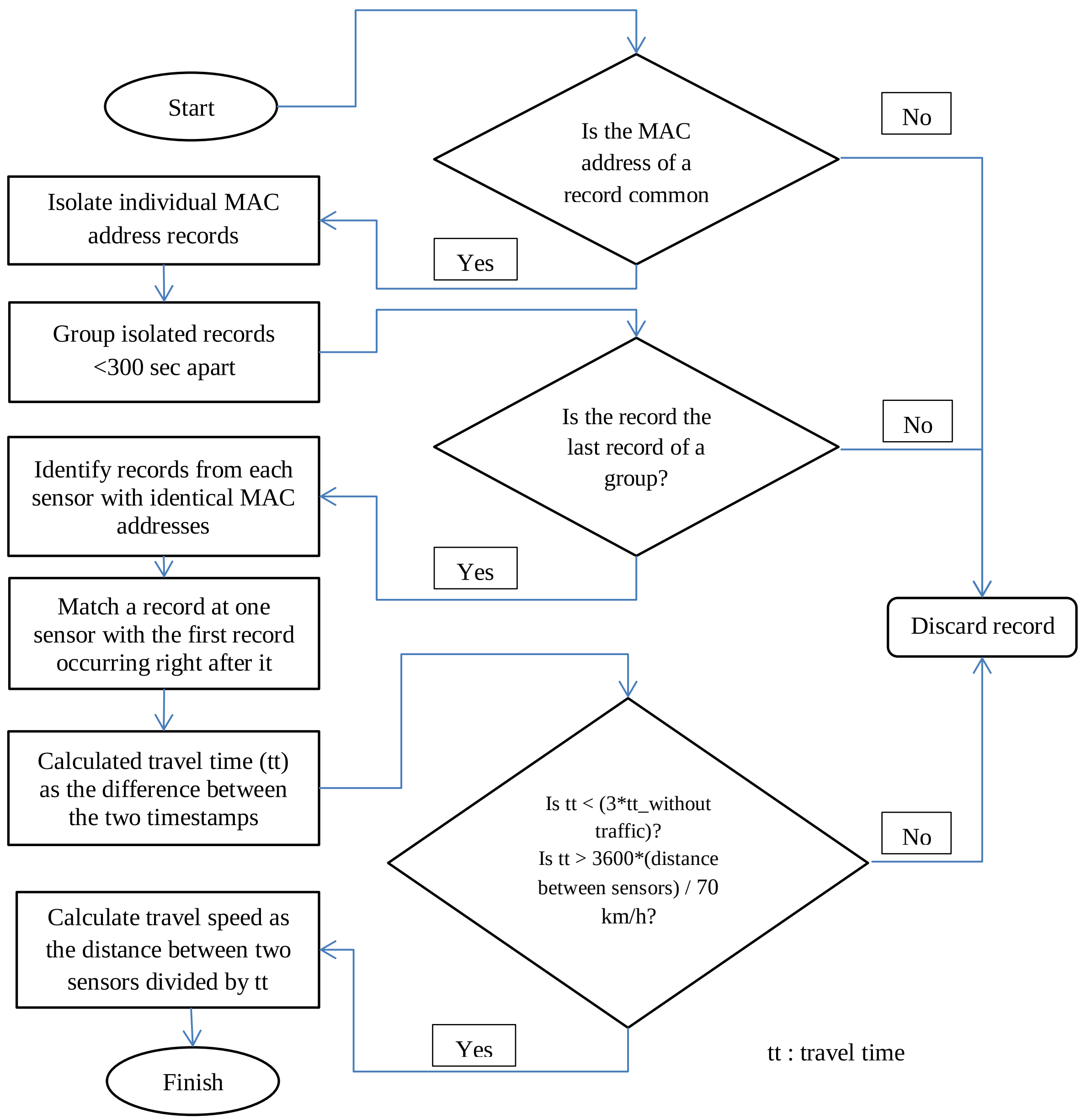

Figure 4-2. Determining travel speeds for one direction between two sensors

4.3.2.2 Grouping MAC addresses

When a vehicle travels within the detection area of a sensor, it can be detected multiple times. It is therefore important to group those records in order to identify the timestamps associated with the vehicle passing the sensor. A threshold named *time limits* is used to define group sizes. For example, if a time limit of 30 seconds is chosen, two records with the same MAC address with timestamps 25 seconds apart would be grouped together. In this paper, a 300 second time limit was chosen to group identical MAC addresses.

4.3.2.3 Selecting a representative timestamp for each MAC address

It is important to note that a sensor typically records multiple readings of each unique MAC address as it passes through its field of detection. This presents a challenge because it is difficult to clearly define at what time the vehicle passes a particular sensor. In this paper, the last recorded time was chosen arbitrarily to identify the representative timestamp for a MAC address.

4.3.2.4 Matching identical MAC addresses and computing directional travel time

In order to compute directional travel times, for each MAC address detected at one sensor, identical MAC addresses that appeared in the second sensor were isolated. After numerically sorting the list of identical MAC addresses from sensor two, the MAC address from sensor one was paired with the identical MAC address in sensor two which had the first timestamp larger than the timestamp at sensor one.

4.3.2.5 Obtaining travel speeds

After obtaining the raw travel times, the values were subject to basic filtering. An upper limit was set based on three times, the travel time without traffic between the two sensors as estimated from Google Maps. A lower limit was set based on the travel speed obtained from traveling 70 km/h on the road segment. This was calculated based on the distance between the two sensors as estimated from Google Maps. Any travel times above or below these values were deleted from the dataset. After doing so, the travel speeds were calculated based on the estimated distance between the two sensors.

4.4 SYSTEM EVALUATION AND TEST

4.4.1 Testing Definition and Performance Measures

The test was implemented along one of the main urban corridors of Montreal, Avenue du Parc. The study segment featured bi-directional traffic and was about 1550 m in length. It had three lanes in each direction and crossed five signalized intersections. It is also worth mentioning that one lane in each direction performs as an exclusive bus-taxi lane and they are active either during the morning (southbound) and evening (northbound) peak periods. The site selection was based on the availability of appropriate utility poles along the roadway to be used to install the sensors. Six sensors were installed in different locations to cover the whole arterial. Figure 4-3.a shows the location of the devices for the serial test, in which multiple sensors were located along the corridor, with only one sensor per location. Figure 4-3.b shows a site installation view. Data were collected for two days for which a total of 18 hours of data was used for detection rate validation and about 8 hours was used for travel time and speed validation.

a) Device locations along Avenue du Parc b) Sensor installation

Figure 4-3. Test on Avenue du Parc.

For validation purposes, two video cameras were installed at the same locations of the Sensor 1 and 5 to calculate the ground truth travel times between them as well as flow rates. The travel time was calculated by matching identical vehicles seen in the two videos. For processing the video data and extracting the travel times we played the videos for both cameras at the same time with a small time delay between them. Then, for a sample of vehicles seen in upstream camera, we attempted to match them with similar vehicles seen in the downstream camera based on their color and body type. We collected 25 travel time samples for each 15 min intervals. Additionally, flow rates were obtained manually using the two cameras.

The site was first chosen along the arterial based on coverage area and distance from neighboring sensors. Sensors were installed in lockable, weatherproof enclosures with internal battery packs. The aim was to collect data for a few hours every day in order to test different configurations and locations. As mentioned before, permanent installations or collection campaigns that required data for several days would require using a solar-powered battery or plugging into the municipal electrical network. For the test, six water-proof enclosed devices were deployed. Details on the testing site and results are provided in the following subsections.

It is important to mention that the criteria to evaluate the performance of the system were i) the number of detections per locations, ii) the number of matched MACs between two sensors with respect to the total volume (detection rate = Total unique MACs read in two locations / Total traffic volume (in one or both directions) in 15 min, 30 min or 1 hr intervals), and iii) travel time (speed) measurements. Detection rate criteria can be used for extrapolation and origin-destination studies as well as for arterial and highways travel speed/time estimation and prediction applications.

4.4.2 Detection Rate Analysis

Regarding the first analysis conducted, the number of paired MACs between sensors was compared with the manually counted traffic flow. For detection rate validation, data coming from the closest camera to Sensor 6 was used. Because of the turning movements at intersections, we made sure that the extracted trips from MAC pairs also pass the location of the camera in order to compare the data with the ground truth data of traffic flow. To do so, the sensor combinations were limited in a way that at least one of the sensors (Sensor 5 or 6) were in the sensor combination.

Table 4-1 shows three hours of ground truth traffic flow and traffic flow estimated by Bluetooth and WiFi technologies. As it can clearly be observed, the detection rates of the WiFi were much higher than those of the Bluetooth in most of the intervals.

Complementary to the table, Figure 4-4 shows the detection rate values for all the samples. The dashed lines show the average value of the detection rate for each technology. Test results indicate that the average detection rate was 27.2% for WiFi and 16.2% for Bluetooth. It should be noted that the detection rate of the Bluetooth technology in our system was slightly more than those reported in previous studies (between 10% to 15%). The high detection rate of WiFi can be helpful in the construction of origin-destination matrices and the extrapolation of the total flow based on the number of total trips.

Table 4-1. Three-hour sample of flow and detection rates

Time		Total Traffic Flow	Captured by WiFi	Detection Rate by WiFi (%)	Captured by Bluetooth	Detection Rate by Bluetooth (%)
11:45	12:00	224	30	13.4	41	18.3
12:00	12:15	184	33	17.9	34	18.5
12:15	12:30	177	74	41.8	18	10.2
12:30	12:45	188	37	19.7	30	16.0
12:45	13:00	203	59	29.1	36	17.7
13:00	13:15	194	41	21.1	35	18.0
13:15	13:30	184	39	21.2	31	16.8
13:30	13:45	194	34	17.5	25	12.9
13:45	14:00	210	38	18.1	28	13.3
14:00	14:15	185	41	22.2	26	14.1
14:15	14:30	187	50	26.7	18	9.6
14:30	14:45	184	41	22.3	34	18.5
14:45	15:00	206	42	20.4	32	15.5
Two days samples Average		199.8	54.37	27.2	35.4	16.2

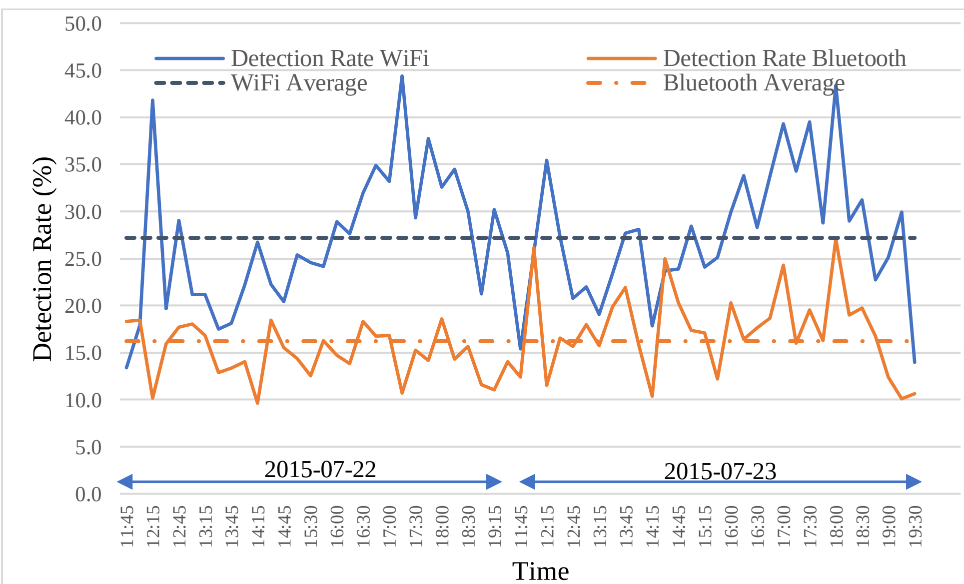

Figure 4-4. trips detection rate by Bluetooth and WiFi technologies

4.4.3 Origin-Destination Study

Since the MAC is a unique address set by the manufacturer of the device, by capturing it and keeping it in the database, a user can be detected at different locations and times. Having samples of a users' activity in the network at different spatial points plus information about the past trips of the same user, one can conduct quality origin-destination studies. Table 4-2 shows a sample of detected activity of users in the arterial captured using our system. Although there were samples recorded throughout the day for the same user, there were many samples in which a user was detected by just two sensors. Nonetheless, adding these types of trips to the database and comparing them with a user's previous trip(s) can give us a clue about the user activity pattern.

Table 4-2. A sample of user time stamped detected activity

F8:F1:B6:F-:--:--		90:27:E4:C-:--:--		00:37:6D:2-:--:--	
6	9:21:37	2	14:35:37	3	10:22:35
6	9:21:54	2	14:36:14	3	10:23:35
6	9:22:11	6	14:38:38	5	10:24:32
4	9:23:58	6	14:38:42	6	10:25:32
4	9:24:15	5	16:23:33	5	10:26:53
1	9:26:31	5	16:23:35	5	13:28:21
1	9:26:37	4	16:24:03	2	13:29:17
1	16:30:05	2	16:25:44	2	13:29:35
2	17:55:13	1	16:26:19	1	13:30:04
4	17:57:35			1	13:30:32
4	17:58:42			1	13:31:38
5	17:58:43				
6	17:59:29				

4.4.4 Travel Time Analysis

Travel time estimation is one of the most important functions of the developed system. In this paper, the travel time of a part of the arterial with a length of 1000 meter was calculated using two installed cameras and the average speeds of the ground truth were compared with the estimated values using our developed WiF-Bluetooth technologies. Again, there were 6 deployed sensors in the whole arterial that were used to get MAC data. In travel time estimation, there is an inherent error related to the effective distance concept. When travel time is calculated, it is important to know if the MAC address was detected when the device entered or left the detection area of the sensor or somewhere between them. The detection point will change the effective distance between sensors. If we assume that the detection radius of the sensor i is r_i and the distance and travel time between two sensors are d_{ij} and t_{ij}, then the average speed between two sensors would be $S_{ij} = \frac{d_{ij} \pm r_i \pm r_j}{t_{ij}}$. The numerator in that equation is referred to as the effective distance. In practice, it is not possible to find the exact coverage area of each sensor and the exact location of the detected MAC address in the coverage area. Therefore, it is not possible to find the exact effective distance between two sensors. As an example, assume that the distance between two sensors is about 1.5 km and the detection range of the sensor is about 100 m (it can be changed based on the type of the WiFi or Bluetooth device). If a car with a wireless device has an average speed of 30 km/h then the travel time between the two sensors would be 180 seconds. So based on the travel time, the estimated speed using the sensor would be something between 26 km/h and 34 km/h. So, we expect an error ±13% in our estimation. To reduce this error, the sensors should be installed in locations with reasonable distances between them.

The results of speed estimation using Bluetooth, WiFi, and combinations of both sensors are depicted in Figure 4-5. In each plot, straight horizontal lines show the average speeds of ground truth data and data collected by each sensor type. As depicted in the figure, the developed system shows promise in estimating the average speed at each time interval. The average errors of 8.67 %, 11.19 %, and 5.82 % were obtained for the Bluetooth, WiFi and mixed system respectively. Therefore, integrating WiFi with Bluetooth can increase the accuracy of the system in travel time estimation. For the travel time test, only non-adjacent pairs of sensors were considered to avoid overlapping issues.

Table 4-3 presents some statistics on the estimation error.

Table 4-3. Some statistics on the estimation error with the two technologies

	Average	Median	Variance	Maximum	Minimum
Bluetooth	8.67	5.89	65.7	25.38	0.16
WiFi	11.19	10.8	70.4	28.3	0.6
Mixed	5.82	4.94	24.2	15.5	0.09

Based on the values on the table, the Bluetooth system performance was better than the WiFi system. Based on the results, WiFi technology usually underestimated the travel speed while on the other hand; Bluetooth technology typically overestimated the average speed. The mixed system seems to have balanced out the errors and got more accurate speed estimation results. Also, based on the results we can see that the mixed system can reduce the variance of the estimation error by about 64%.

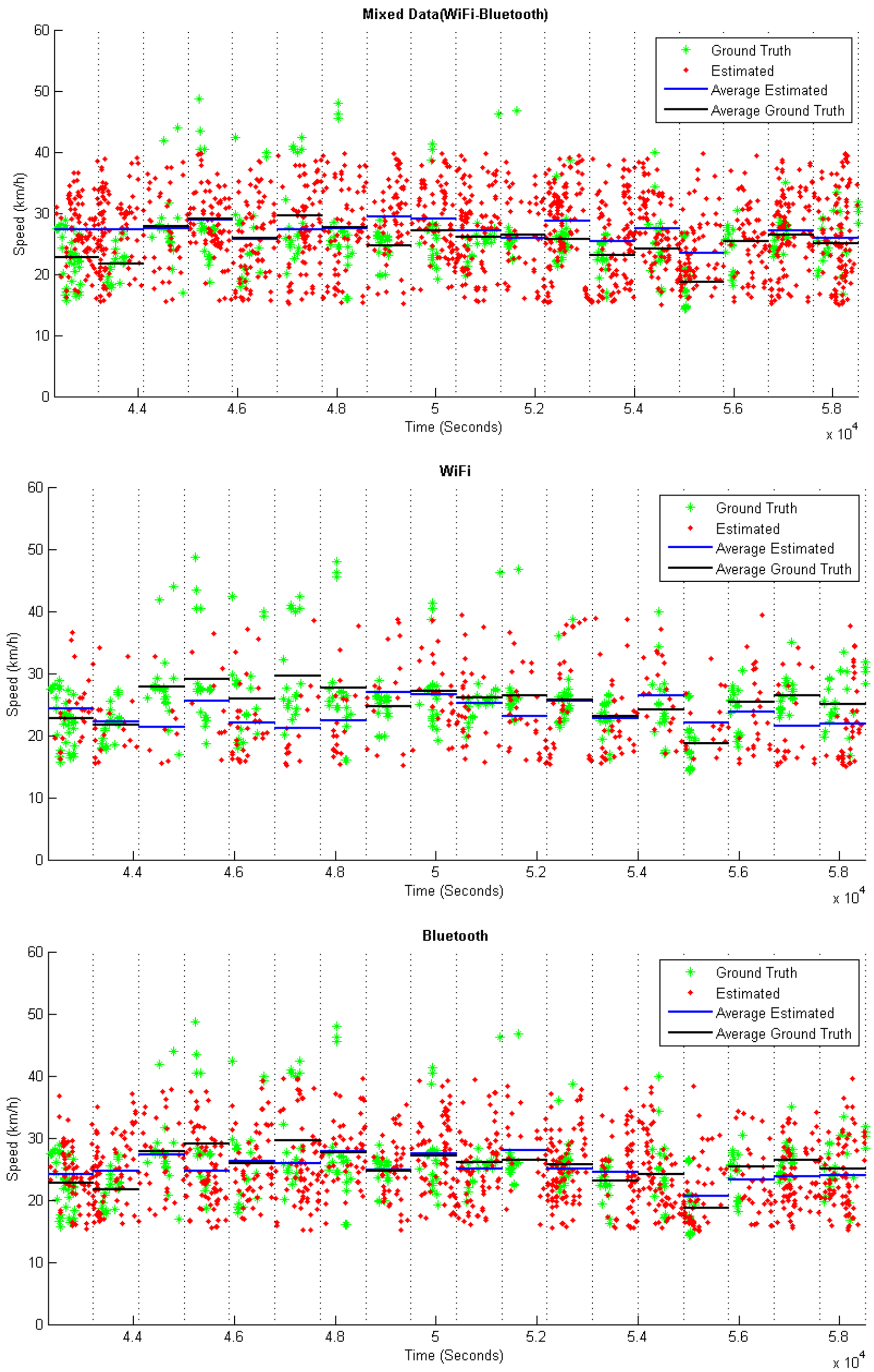

Figure 4-5. Speed, a) mixed in top, b) WiFi in the middle, c) Bluetooth in bottom

Also, the number of travel time samples for Bluetooth was much higher than the WiFi samples. The reason is that a Bluetooth device is easier to be captured when it is active and discoverable. So, we see more than one sample for each unique MAC address when we consider all the sensor combinations. On the other hand, for WiFi, when it is on, the MAC would be detected just in the scan interval. This scan interval depends on the device type. For example, the scan interval on average is two minutes for a Samsung Galaxy III. This means that even if the WiFi is ON we will not capture it at every sensor in an arterial and that the number of samples for a unique WiFi MAC will be less than the number of samples for a unique Bluetooth MAC. However, if just two sensors are considered, then the number of unique MACs for WiFi was much bigger than Bluetooth (detection rate).

4.5 PRELIMINARY CONCLUSIONS AND WORK IN PROGRESS

This research developed and evaluated the performance of a Bluetooth-WiFi system to detect anonymous MAC addresses of devices at short distances at mobile or fixed locations. The sensors are able to capture signals from WiFi-enabled mobile devices and, enabled and discoverable, Bluetooth devices for the purpose of measuring travel times (speeds) and generating origin-destination matrices. The system was tested in an arterial, and both technologies are compared with ground truth travel times obtained through manual video processing. Existing literature has mainly concentrated on applications of Bluetooth systems for travel time estimation in highways.

The designed system works in real-time and provides a rich MAC database from both Bluetooth and WiFi signals. Results show higher detection rates for WiFi compared to those reported with Bluetooth when a single sensor is considered or a network of sensors is implemented (more than two sensors). However, if just two sensors are considered, the detection rate of Bluetooth technology is higher than that of a WiFi system. This conclusion comes from the fact that when the Bluetooth is in discoverable mode, it will be detected most of the time, but for WiFi technology, the device is detected whenever it is sending probe signals, which happens randomly in one to two-minute intervals. Depending on the application, the integrated system can increase the accuracy of travel metrics compared to using only Bluetooth. For instance, testing the WiFi-Bluetooth system in an arterial for two days, with about 20 hours of video data for manual validation, indicates that the average detection rate was 27.2% for WiFi and 16.2% for Bluetooth.

Additionally, our system's performance was evaluated in terms of travel time estimation. A platform including six sensors with ten different combinations gave an average of 43 and 27 travel time samples in 15-min intervals for the Bluetooth and the WiFi system respectively. However, these numbers dropped to 17 and 23 samples for Bluetooth and WiFi respectively after removing duplicates and just keeping one sample for each MAC. The initial results show an average speed estimation error of around 8.6 %, 11.1 %, and 5.8 % for Bluetooth, WiFi, and the mixed system respectively.

In summary, the advantages and constraints of both technologies can be summarized as such:

- For WiFi: (+) Higher detection rates than Bluetooth technologies, (+) works well in low-speed networks (e.g., downtown areas), (+) O-D matrices can be richer than Bluetooth technologies because of the higher penetration rate, (-) road user classification is required and can be more complex than Bluetooth since it includes transit users, cyclists, and pedestrians with smartphone devices. (-) Travel times for vehicles are less accurate than Bluetooth.
- For Bluetooth: (+) It works better than WiFi at high speeds (e.g., urban highways), (+) travel times are more accurate for cars (when considering only one technology type). Bluetooth data comes mainly from cars. (-) It has lower detection rates: 10%-15%. The detection rates of MACs for smartphones represents only 1-3%, which is very low.

Several research works are still in progress. Software optimization is already underway to ensure that we are not missing any data and are only collecting relevant data. This will include packet truncation, optimized channel scanning, and device lookup tables for classifying both the manufacturer and type of device (laptop, smartphone, vehicle, etc.). Classification of pedestrian, bikes, and vehicles is another work that should be investigated. A mode classification algorithm will be part of future work. In addition to travel-time (speed) model as a classifier, an idea to explore will be the use of historical data, e.g., one can consider all detected MAC addresses over time and check the speeds of each MAC address in different times/days; then classify it based on its historical data.

Developing a noise filtering methodology would be also part of future work. In travel time data, a lot of noise coming from samples stopping in between sensor can be seen. This part is essential for delay estimation applications at intersections.

4.6 REFERENCES

Abbott-Jard, M., Shah, H. and Bhaskar, A. (2013) Empirical evaluation of Bluetooth and Wifi scanning for road transport, p. 14.

Ahmed, H., EL-Darieby, M., Abdulhai, B. and Morgan, Y. (2008) Bluetooth-and Wi-Fi-based mesh network platform for traffic monitoring.

Barcelo, J., Montero, L., Marques, L. and Carmona, C. (2010) Travel time forecasting and dynamic origin-destination estimation for freeways based on bluetooth traffic monitoring. Transportation Research Record (2175), 19-27.

Blogg, M., Semler, C., Hingorani, M. and Troutbeck, R. (2010) Travel time and origin-destination data collection using Bluetooth MAC address readers, Planning and Transport Research Centre (PATREC), Canberra, ACT, Australia.

Bonnel, P., Fekih, M. and Smoreda, Z. (2018) Origin-Destination estimation using mobile network probe data. Transportation Research Procedia 32, 69-81.

Bonnel, P., Hombourger, E., Olteanu-Raimond, A.-M. and Smoreda, Z. (2017) Potential and limitations of mobile phone passive data to build origin-destination matrices. REVUE D ECONOMIE REGIONALE ET URBAINE (4), 647-671.

Bullock, D., Haseman, R., Wasson, J. and Spitler, R. (2010) Anonymous bluetooth probes for measuring airport security screening passage time: the indianapolis pilot deployment.

Caceres, N., Wideberg, J. and Benitez, F. (2007) Deriving origin destination data from a mobile phone network. Intelligent Transport Systems, IET 1(1), 15-26.

Carpenter, C., Fowler, M. and Adler, T. (2012) Generating route-specific origin-destination tables using bluetooth technology. Transportation Research Record (2308), 96-102.

Committee, I.C.S.L.M.S. (1997) Wireless LAN medium access control (MAC) and physical layer (PHY) specifications, IEEE Std.

Danalet, A., Farooq, B. and Bierlaire, M. (2013) Towards an activity-based model for pedestrian facilities.

Day, C.M., Haseman, R., Premachandra, H., Brennan, T.M., Wasson, J.S., Sturdevant, J.R. and Bullock, D.M. (2010) Evaluation of Arterial Signal Coordination. Transportation Research Record: Journal of the Transportation Research Board 2192(1), 37-49.

Haghani, A., Hamedi, M., Sadabadi, K.F., Young, S. and Tarnoff, P. (2010) Data collection of freeway travel time ground truth with Bluetooth sensors. Transportation Research Record (2160), 60-68.

Haseman, R.J., Wasson, J.S. and Bullock, D.M. (2010) Real-time measurement of travel time delay in work zones and evaluation metrics using bluetooth probe tracking. Transportation Research Record: Journal of the Transportation Research Board 2169(1), 40-53.

Katsuki, T. and Tatsubori, M. (2018) System and method for automated road identification in distant traffic camera images, Google Patents.

Laharotte, P.-A., Billot, R., Come, E., Oukhellou, L., Nantes, A. and El Faouzi, N.-E. (2014) Spatiotemporal Analysis of Bluetooth Data: Application to a Large Urban Network.

Malinovskiy, Y., Saunier, N. and Wang, Y. (2012) Pedestrian Travel Analysis Using Static Bluetooth Sensors. Transportation Research Board: Journal Of The Transpotation Research Board, 1-22.

Martchouk, M., Mannering, F. and Bullock, D. (2010) Analysis of freeway travel time variability using Bluetooth detection. Journal of Transportation Engineering 137(10), 697-704.

Musa, A. and Eriksson, J. (2012) Tracking unmodified smartphones using wi-fi monitors, pp. 281-294, ACM.

Porter, J.D., Kim, D.S., Magaña, M.E., Poocharoen, P. and Arriaga, C.A.G. (2013) Antenna characterization for Bluetooth-based travel time data collection. Journal of Intelligent Transportation Systems 17(2), 142-151.

Quayle, S.M., Koonce, P., DePencier, D. and Bullock, D.M. (2010) Arterial performance measures with media access control readers. Transportation Research Record: Journal of the Transportation Research Board 2192(1), 185-193.

Saeedi, A. (2013) Utilizing wireless-based data collection units for automated vehicle movement data collection.

Salanova Grau, J.M., Stamos, I., Mitsakis, E., Margaritis, D., Tzenos, P. and Aifadopoulou, G. (2017) Estimation of traffic flow from Bluetooth detections.

Sochor, J., Juránek, R. and Herout, A. (2017) Traffic surveillance camera calibration by 3d model bounding box alignment for accurate vehicle speed measurement. Computer Vision and Image Understanding 161, 87-98.

Szuch, C. and McDaniel, Z. (2011) Measuring goods movement travel time and reliability: Proposed methodology, p. Golder Associates, Transportation Association of Canada (TAC), Edmonton, AB, Canada.

Tsubota, T., Bhaskar, A., Chung, E. and Billot, R. (2011) Arterial traffic congestion analysis using Bluetooth duration data.

Wang, H., Mazari, M., Pourhomayoun, M., Smith, J., Owens, H. and Chernicoff, W. (2018) An End-to-End Traffic Vision and Counting System Using Computer Vision and Machine Learning: The Challenges in Real-Time Processing. SIGNAL 2018 Editors, 13.

Wasson, J.S., Sturdevant, J.R. and Bullock, D.M. (2008) Real-time travel time estimates using media access control address matching. ITE Journal 78(6).

Wieck, M. (2011) Use of bluetooth based travel time information for traffic operations.

Yu, W., Park, S., Kim, D.S. and Ko, S.-S. (2014) Arterial Road Incident Detection Based on Time-Moving Average Method in Bluetooth-Based Wireless Vehicle Reidentification System. Journal of Transportation Engineering.

Link Between Chapter 3, 4 and Chapter 5

In Chapters 3 and 4, a WiFi-Bluetooth scanning system has been developed and used to monitor traffic network in either vehicular or mixed-mode pedestrian-cyclist networks. A basic flow extrapolation mechanism has been introduced and applied to the detected WiFi traces to estimate the pedestrian flow. However, calibrating extrapolation functions requires ground truth data of pedestrian/cyclists flow. The models also need to be updated over time using manual or automated counts. In chapter 5, a novel automated pedestrian/cyclists counting system based on Lidar technology is developed and tested. The system can work in different traffic lighting and weather conditions in real-time, and the count data can be accessible either locally or through a cloud-based platform. In our platform, the count data can be used to dynamically update the extrapolation functions for future developments. The system can also be used for other applications such as monitoring the level of service, and applications such as advanced warning systems and adaptive traffic light controls.

Chapter 5: Development and Testing of a Laser-Based Automated Pedestrian/Cyclist Counting System

Asad Lesani[a], Anthony Andreoli[a], Luis Miranda-Moreno[a]

[a] *Department of Civil Engineering and Applied Mechanics, McGill University, Montreal, Canada*

Accepted for presentation at Transportation Research Board 95th annual meeting, Washington D.C, Patent application submitted with Disclosure Number D2018-0070, To be submitted to "Transportation Research Part C: Emerging Technologies".

5.1 ABSTRACT

This research introduces the design elements of a pedestrian and cyclist counter, based on Laser Technology, Light Detection and Ranging (Lidar). The proposed counting system is designed for collecting data on various facilities such as sidewalks and cycle tracks. The system is built with two single beam Lidar sensors, which measure the distance to objects with a high sample rate. The system can detect, count and identify the direction of non-motorized road users in real time. To achieve this, a unique pattern recognition-based algorithm reads the distance values, extracts the defined features, measures direction and counts the number of pedestrians or cyclists in real-time. Due to the narrow laser beam, the developed sensor performs in situations where cyclists or pedestrians travel in parallel over the detection area. The system is designed to address occlusion, which is a source of undercounting for traditional, side-mounted counting systems.

To evaluate the performance (accuracy) of the proposed system, manual video-based counting was performed under different traffic conditions. The video counts were defined as the ground truth. Two levels of data aggregation are used for validation: firstly, at the disaggregated data level using one-by-one matching of the sensor distance patterns and the ground truth counts, and secondly, using aggregated 15-min interval counts. The results indicate that in 80% of the 15-min automated counting samples, the counting error was between 0-5% and 0-2% for pedestrians and cyclists, respectively. The Lidar system was compared to an existing infrared-based pedestrian counter and

an inductive loop cyclist counter. The proposed system performed significantly better than existing systems. On bicycle facilities, an average directional count error of 0.7% was achieved using the proposed system compared to an average of 4.7% using the inductive loop detector. Furthermore, the proposed system addresses occlusion; it achieved a count error of 2.2% in cases involving two or three cyclists passing in front of the sensor in parallel. For pedestrians, the disaggregate and aggregate counting errors are less than 3.5% and 3.0%, respectively. The proposed system is simple to install (it does not require pavement cutting as with inductive loop detectors), which reduces the installation and maintenance cost. The system allows the user to set the coverage area of the sensor, which addresses a fundamental challenge for infrared counters that require the presence of a blocking barrier on one side of study space. This advantage makes the proposed system more versatile for site selection and installation. However, the system has a higher power consumption with respect to existing technologies.

5.2 INTRODUCTION

The promotion of non-motorized transportation, walking, and biking, is one of the main goals of municipal governments and organizations across the world. In many cities, policies and projects to accommodate non-motorized modes have gained momentum in the last decade. With this, the planning, implementation, and operation of pedestrian and bike facilities have created a need for non-motorized monitoring systems. Consequently, traffic monitoring technologies and methods for automatically collecting such data have been developing at a greater pace. Pedestrian and cyclist counting data can be gathered short-term (for a few hours or a few days) at a set of locations or, long-term, to obtain traffic patterns and long-term changes in the traffic flow. The data obtained from these systems can then be used to evaluate the impact of new infrastructure (before-after studies), to generate extrapolation (expansion) factors, to estimate average annual daily volumes, to determine exposure measures for road safety studies, or to evaluate the impact of policies Johnstone et al. 2017, Kristoffersen et al. 2016, Lu et al. 2018, Miranda-Moreno and Lahti 2013, Ryus et al. 2014, Strauss et al. 2012.

Traditionally, pedestrian and cyclists count data collection methods used by cities and municipalities relied heavily on manual counting procedures, particularly for short-term counts. In manual counting, individuals count the number of pedestrians or cyclists using a facility, either directly at the site or from video recordings of the area, typically for a few hours. This method is costly; it requires a great deal of time and resources. In addition, the temporal coverage is very limited; only a few hours of counts are obtained at each site. Short-term manual counts can be very sensitive to temporal factors (time of the day, the day of the week, and season) and weather conditions. In order to standardize short-term counts that are taken at different periods of time, and in varying weather conditions, adjustments factors have been developed based on permanent (long-term) counting stations from which continuous count data is obtained.

Given the importance of non-motorized traffic monitoring, data collection over short and long periods of time is becoming a more common practice in many cities around the world. Given a large number of locations in a network where data is needed, automatic data collection methods and systems are essential. In response, there is an increased investment in the development of large-scale automated pedestrian (and bicycle) counting programs in North America. Today, many cities are either improving or launching such programs, with budgets that range in the hundreds of thousands of dollars per year. These cities and metropolitan areas include Vancouver, Ottawa, Montreal, San Francisco, Portland, San Diego, and others.

For automatic data collection, several technologies have been developed in recent years; some of which are available for commercialization, including passive infrared, radar, and computer vision-based counters. The advantages and drawbacks of these technologies have been documented in the literature Greene-Roesel et al. 2008a, Lindsey et al. 2013, Proulx et al. 2016, Ryus et al. 2014. While advances in computer vision processing have allowed for the collection of pedestrian flows in open spaces including sidewalks and intersections, very few video technologies are capable of automatically collecting data continuously and in real time. Video-based monitoring could be expensive in the long-term when infrastructure (video cameras and computers) is not available as an embedded system. Standard video sensors perform poorly in low-light conditions and severe weather. Thermal video sensors address this problem; however, they are an expensive solution. Despite recent technology developments, there still exists a need to develop low-cost and flexible data collection systems that can be easily installed to provide short- and long-term data in real-time and to integrate such data into a platform for analysis and data fusion.

The main objective of this research is to develop and evaluate the performance of a monitoring system that automatically detects and counts pedestrians or bicycles based on the emission of laser beams. This paper describes the system elements and algorithm developed for the detection and counting of pedestrians and bicycles on non-motorized facilities, such as sidewalks and cycle tracks. The performance of the sensor was evaluated and compared to two of the most commonly used commercially available types of sensors: an infrared sensor for pedestrians and an inductive loop detector for bicycles. The limitations and advantages of the system are discussed along with plans for future work.

5.3 LITERATURE REVIEW

Several monitoring technologies for automatic pedestrian and cyclist data collection, in indoor and outdoor environments, are commercially available. Typically, collection devices are used to detect and count the number of pedestrians/cyclists passing through doors, indoor corridors in terminals or buildings, park trails, sidewalks, cycle tracks, intersection crosswalks, mid-block crossings, etc. Ryus et al. 2014.

In order to benefit from the advantages offered by automated data collection, transportation agencies are installing various commercially-available counting systems, as has been done in the past for motor vehicle traffic monitoring. Counting technologies are presented and discussed in the works by Markowitz et al. 2009a and Dharmaraju et al. 2002. The most popular types of automated pedestrian detection devices and techniques include passive and active infrared technology, piezoelectric pads, laser scanners, as well as video-image processing. Some of the mentioned technologies can be used in mixed mode networks. For bicycle counting, inductive loop detectors Nordback and Janson 2010 and pneumatic tubes Brosnan et al. 2015 are the most common commercial systems.

Passive infrared counting technologies identify and count pedestrians based on a temperature differential. This category of sensors has several advantages such as relative ease to build and operate, very low power consumption, real-time implementation, acceptable accuracy and operation in wet and foggy weather. However, the technology also suffers from significant limitations including occlusion, when installed in environments with high pedestrian volumes and density; poor performance under extreme temperatures; and the requirement for the device to be facing a fixed object, such as a wall. This last limitation restricts their use at intersections, midblock crosswalks, and open spaces Greene-Roesel et al. 2008b. Additionally, an intense source of infrared signals, such as vehicle engines, can cause over-counting. This limitation places restrictions on the types of sites that are suitable for counting. Cases of under-counting and over-counting have also been observed and attributed to certain temperature anomalies and weather conditions (rain). Studies have reported a systematic under-counting error as high as 25%, depending on the traffic volumes and weather conditions Greene-Roesel et al. 2008b. In this study, an infrared sensor, manufactured by Eco-Counter, is tested at a location without the presence of the wall. In outdoor environments, the errors can be larger, as discussed in Lindsey et al. 2013, Markowitz et al. 2009b.

With recent progress in image processing algorithms and computing technologies, the use of computer vision processing has been proposed as a technique for counting and classifying pedestrians and cyclists in mixed mode networks Ismail et al. 2009. The main benefit of using computer vision processing is that it can obtain counts, speeds, and trajectories of multiple mode types. The drawbacks of video-based systems are their high installation and maintenance costs and limitations regarding camera placement, light and weather conditions. Existing video-based techniques perform poorly at night or in adverse weather. A more expensive, but highly accurate, the alternative is the use of thermal imaging cameras Leykin and Hammoud 2006. It should also be noted that video-based systems in transportation are still overwhelmingly reliant on post-processing rather than real-time processing of data. This reliance makes large-scale data collection costly and cumbersome, as videos must be regularly collected from installed cameras.

Infrared sensors are the most commonly-used sensor for counting in outdoor environments. Alternative technologies such as radio wave, laser pulse, and thermal sensors are less common than infrared counters. Radio wave sensors work based on the variation of the wave frequency of the received and sent signal (i.e., Doppler Effect). The variation of the frequency has a linear relationship with the speed of the object. A laser pulse system functions based on scanning the detection area and producing a three-dimensional image of the object. Based on the video processing algorithm, the speeds and flows can be calculated. However, laser pulse systems have some significant limitations including high computational requirements and acquisition costs.

Thermal sensors can be mounted above entryways to count people entering and exiting key locations. A recent study Ozbay et al. 2010 tested a thermal sensor on trails and compared the results with that of an infrared sensor. The authors reported mean percentage errors ranging from -15% to 1% for the thermal sensor, which was considerably lower than the errors for the infrared sensor, which ranged between -28% and 0%.

Little research has explored the use of devices emitting ultrasonic waves to detect and count pedestrians in urban environments. While ultrasonic sensors have been used in the field of intelligent transportation systems Krammer and Schweinzer 2006, Leibe et al. 2005, these systems have been neglected when it comes to automated pedestrian detection and counting. In Lesani et al. 2015, the authors designed an ultrasonic-based pedestrian counter and tested it, against an infrared-based pedestrian counter, at sidewalk locations. The results were promising in terms of accuracy, real-time performance, and cost. However, there are some issues with using low-cost ultrasonic technology such as low sample rates (less than 1 sample per 20 milliseconds), the divergence of ultrasonic waves by distance (beam with a 15-degree angle), and low effective range (four meters). This research is an effort towards the development of a low-cost counting system that provides a high level of accuracy in demanding conditions such as high flow, open spaces, and multi-modal detection.

In the following sections, hardware and software implementation is described. The algorithms used to obtain pedestrian/cyclist counts from the raw distance measure extracted from the Lidar range finder is described as part of the software design section.

5.4 HARDWARE DESIGN

The hardware design consists of two parts, the processor and the sensor. In the designed hardware, a low power ARM micro-controller is used as a processing unit. Two Lidar (Light Detection and Ranging) sensors are used to measure the distance between the sensors and moving objects: pedestrians, bicycles, or another road user. The sensor data is transferred to the microcontroller through the I^2C protocol. The Lidar sensor has a range of 40 meters and a 500Hz sampling rate. As a result of narrow laser beams (0.3 degrees) and insensitivity to varying light and weather conditions, the sensor provides an output with low noise, which results in a robust and accurate range finding system. To extract the direction of the road users, the measurements of two Lidar range finder sensors are obtained at the same time. Based on the time difference between detections, the direction is extracted. Figure 5-1 shows the snapshot of the sensor box prototype with a description of the elements. A built-in camera is used for manual counting and validation.

The spacing between the sensors is important for detecting the object direction and is calibrated based on the maximum expected speed of the object and the sample rate of the sensor. Considering an upper limit for cyclist speed as 10m/s and a 20cm spacing between sensors, the travel time between two sensors is calculated as 20ms. Considering an average sample rate of 2ms, a minimum of 10 distance samples are read for the same object passing from sensor one to two, or vice versa. With this spacing, it is ensured that the system has a sufficient number of samples to detect the direction of the object occurately.

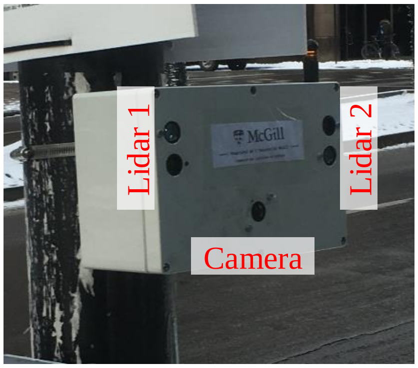

Figure 5-1. The sensor with element description

In addition to the sensory system, a real-time clock module (RTC) has been added to the controller to allow for time-stamped counting. To transfer real-time counts to the server, a GSM modem is integrated into the system. In the first prototype, a Raspberry Pi module was used to read measurements from the Lidar sensor and store time-stamped range values in a text file for offline processing, and for development of the data analysis algorithms. Then, to reduce the system power consumption, the data-analysis codes have been transferred to an ARM microcontroller, from Texas Instruments, for real-time applications.

Once the system components are built, they are embedded in a solid waterproof enclosure. Figure 5-2 provides a picture of the system hardware (left) and the sensor with the enclosure installed at one of the testing sites (right). In the prototype design, all the measurement samples are recorded and saved on the local processor storage for post-processing.

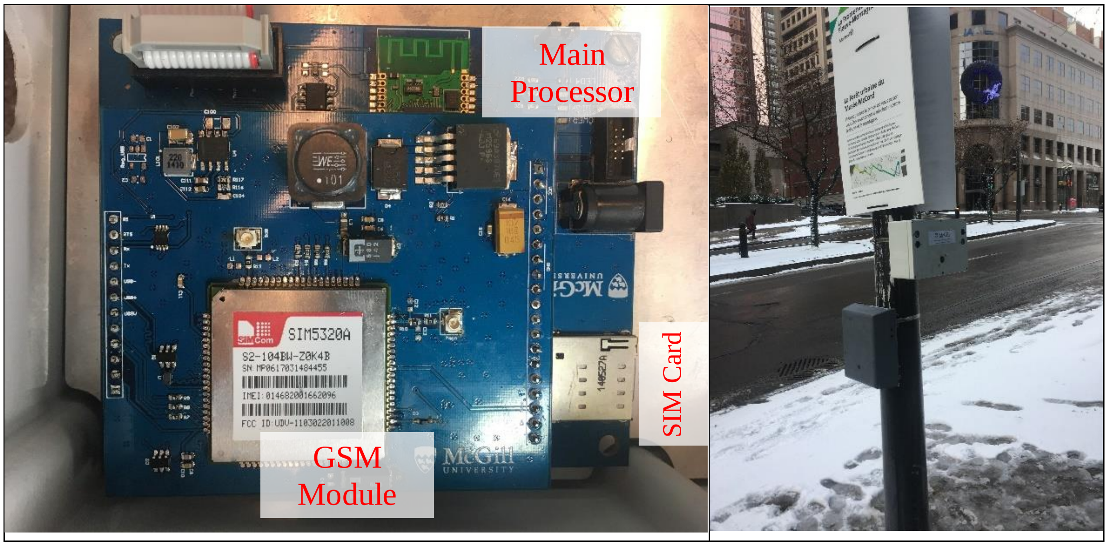

Figure 5-2. System hardware and installation

5.5 SOFTWARE DESIGN

In this section, the methodology used to analyze raw distance measurements is described. The algorithm is divided into two parts, the main loop which gets the raw data and prepares arrays of information, and, the second part which processes the data and generates time-stamped object counts with direction. The same algorithm is used for both pedestrian and cyclist counting, but with different threshold values for the two applications.

5.5.1 Definitions and Main Routine:

This section includes the definition of the different variables and notations used in the algorithms:

d_i : Distance value measured by Lidar *i*
t_i : Timestamp of the measurement by Lidar *i*
TH_{dist} : Threshold defining the area for counting purposes. Any objects with distance values exceeding the threshold will be ignored.
d_1 , d_2 : Distance value read by sensor 1 and 2 at the current sample
d_{0i} , t_{0i} : Distance and time stamp by sensor *i* at the previous sample

The remaining parameters are defined as they are used.

Once the user defines the counting zone of interest, the algorithm reads distance values from the two Lidar sensors. On average a new distance value (d_i) is available to be read every four milliseconds. Then, the values of the distances are compared with a distance threshold (TH_{dist}).

The threshold is used to filter out the objects that travel outside of the user-defined counting zone. Relax Time (RT) is then introduced for real-time implementation. Once there are no longer any objects in the coverage area, a timer begins. New objects are not counted until the timer reaches the RT value. In this system, the RT is set to 500ms. a larger RT might append too many objects to be processed in real-time, whereas, a shorter RT might cause overcounting. Every time a new object is detected within the counting zone, the timer is reset to zero. The RT helps to avoid dividing an object into two separate objects, and it enables the processing of a group of closely-spaced objects, at the same time, which is necessary for handling parallel objects.

The next step is to cluster distance data into *packets*, *skips,* and *groups.* Once the RT is over, the distance values stored in the *dist* array construct a *packet* of data. Each packet is then clustered into subgroups called *skips*. A *skip* is defined as any jump (change) in measurement time stamps (in comparison with the previous measurement) that is bigger than a temporal threshold, *THtime* (50ms). It means that if the differences between time stamps of two consecutive measurements are bigger that *time,* a new *skip* is created. The *skip* data could belong to a person, a part of a body (hand, backpack or body) or even two people walking/biking close to each other or in parallel. To address all of these possibilities, the *skip* data is clustered into subgroups based on a distance threshold, called the *Tightness Threshold, or THtight.* If the difference between two consecutive measurements in each skip is bigger than *THtight*, a new *group* will be generated.

Figure 5-3 shows a few seconds of distance data measured by one of the Lidar sensors plotted and a visual description of the terms. The green dot plot shows the raw distance data. Any drops in distance values indicate the presence of an object between the sensors and in counting zone. The green arrows show the start and end of each *packet* of data. As defined previously, a *packet* ends if, for at least 500ms (the RT), the distance values are bigger than *THdist*. The orange arrows show the start and end of the *skip* data. It can be seen that the first *packet* includes one *skip,* while the second *packet* includes three *skips.* Each *skip* then will be clustered based on the distance threshold into different *groups*.

As mentioned previously, the proposed system uses two Lidar sensors to get the direction of the moving object. Typically, the same pattern of the data is seen on the second sensor data, with a delay. The time stamp of each *group* data is assigned to an object and is used to detect the direction of the moving objects.

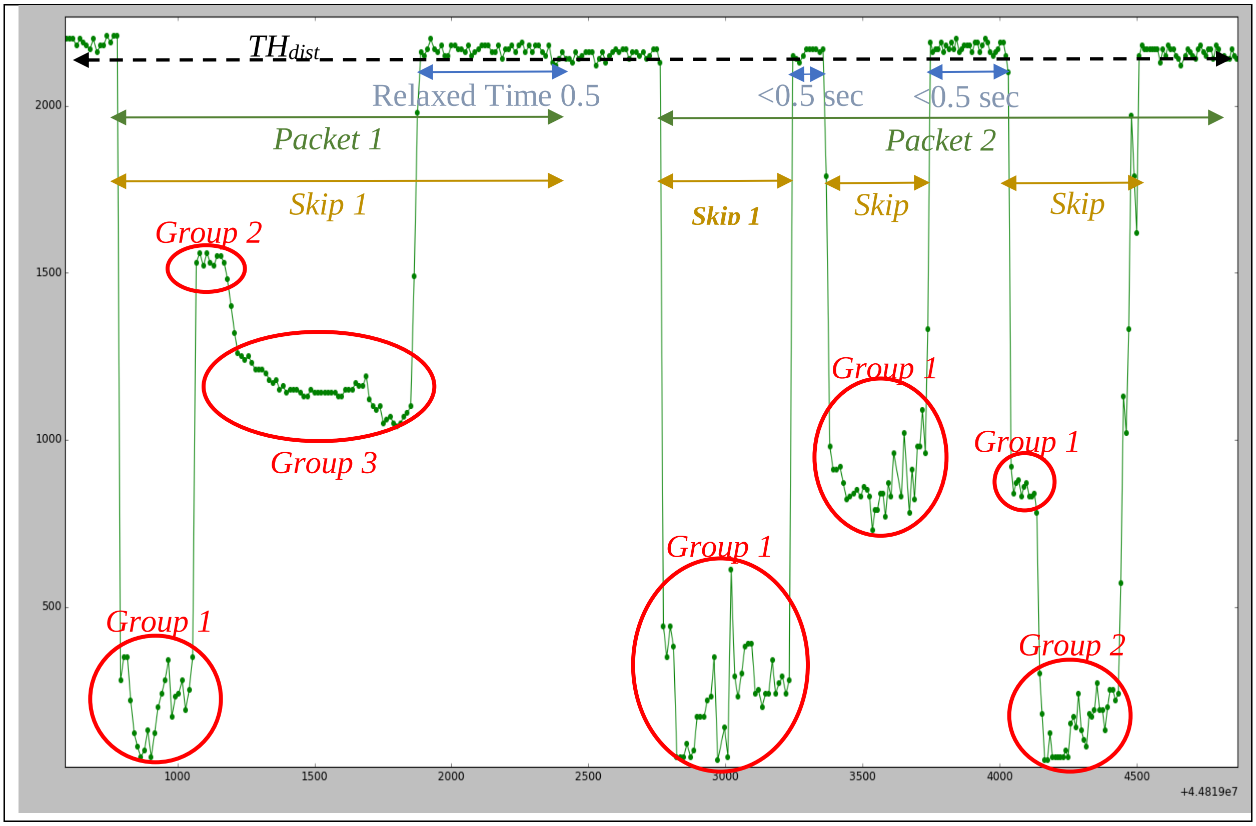

Figure 5-3. A sample plot of distance data with term definitions

Due to real-time implementation on a micro-controller, which has limited available memory, it is not feasible to store all the raw distance data. Therefore, at each time interval, the last and current distance values and their corresponding timestamps are used to construct *skip* and *group* data. For each *group* data, the following statistics are stored for the future processing: the average of the distances within that *group* (*dist_ave*), the time stamp of the first sample, t_s, and the time stamp of the last sample, t_e. At the end of the *RT*, these parameters are used to count the number of objects (pedestrian or cyclists) and their direction of travel. Figure 5-4 presents the flow chart of the real-time implementation of the algorithm:

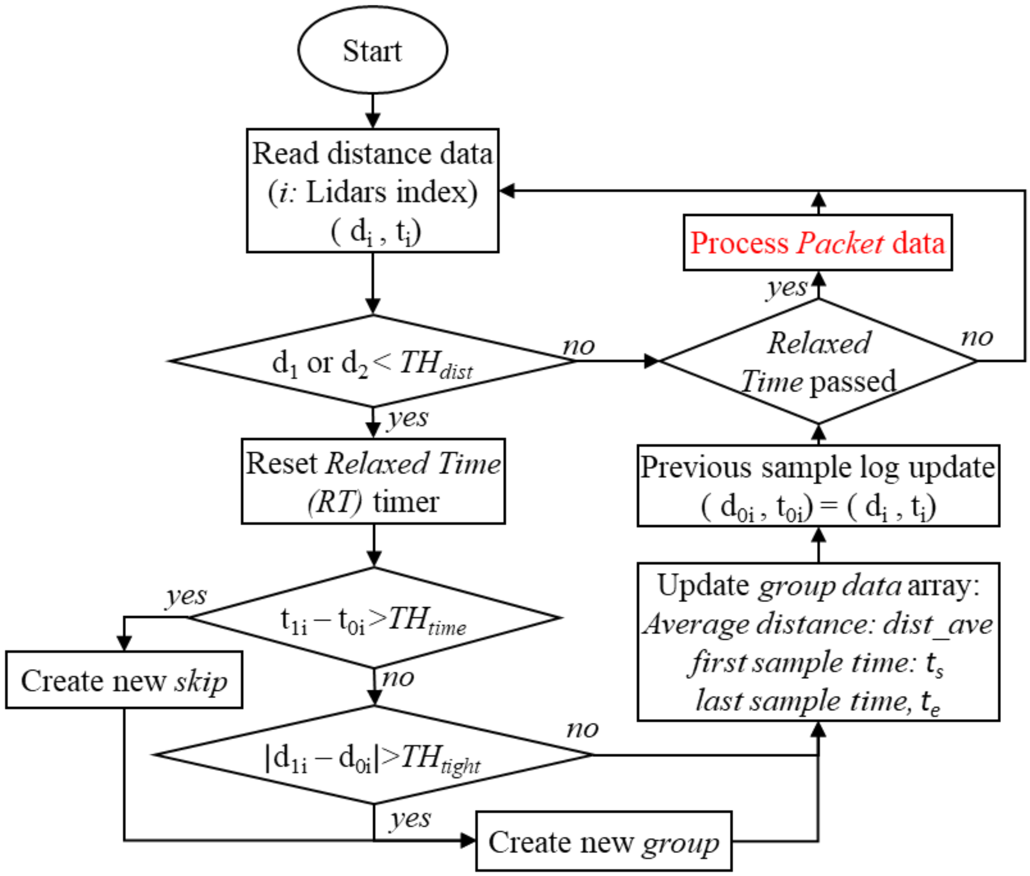

Figure 5-4. Flow chart of real-time implementation of the algorithm

The *Process Packet Data* Routine in the flowchart includes the decision-making section which outputs the time-stamped detected objects with their direction. The routine includes clustering on time and distance values and some conditions on the duration of each *group* data within the detected *packet*. This routine is described in the following subsection.

Once the corresponding *group data* for each object has been detected, then the direction of the object is estimated based on the time stamp of the first sample of the group data associated with that object in two Lidar sensors, $t_{s\text{-}lidar1}$ and $t_{s\text{-}lidar2}$:

- ✓ if $t_{s\text{-lidar1}}$ is bigger than $t_{s\text{-lidar2}}$ then the direction is from Lidar 2 to Lidar 1
- ✓ if $t_{s\text{-lidar1}}$ is less than $t_{s\text{-lidar2}}$ then the direction is from Lidar 1 to Lidar 2

5.5.2 Counting and Direction Detection Routine

In this subsection, the counting and direction detection routine (*Process Packet Data Routine*) is described. As described previously, the input of this routine is an array of some statistics on all individual *group* data within each *packet* of data and for each Lidar sensor. This routine is called at the end of *RT* interval. Figure 5-5 describes decision-making graphically.

The plots show the raw distance data of five cyclists: one individual cyclist, and two groups of two parallel cyclists. The green points represent the raw distance values collected by one sensor. Figure 5-5-a shows the data of each *group* and *skip,* generated by the main loop (described in the flowchart). As can be seen, the five cyclists create distance values that are grouped into seven different *groups.*

The decision-making algorithm includes four steps which are described below.

A) Clustering on time (ClusterT), clustering on *groups,* first and last sample timestamps (t_s, t_e): The *group* data is clustered based on the difference between the time stamp of the last sample in *group i* (t_{si}) and the time stamp of the first sample of the next *group, i+1.* A threshold is used in this process. This level of clustering helps to connect the gaps between the different parts of one object (for example the gap between the hands and body of the cyclists) and prevent any overcounting. Additionally, the process helps to distinguish two object walking/biking back to back in close proximity.

    - ✓ If $t_{s(i+1)} - t_{ei} > TH_{ClusterTime}$: New Cluster
    - ✓ Else: Same Cluster

   Figure 5-5-b shows how this level of clustering works. $TH_{ClusterTime}$ is equal to 150ms. Based on this threshold, *group1* and *group2* are combined to build the first cluster (*clusterT1).* Since the time gap between *group2* and *group3* is larger than the threshold, *group3* creates a new cluster. This procedure is repeated for all *groups.*

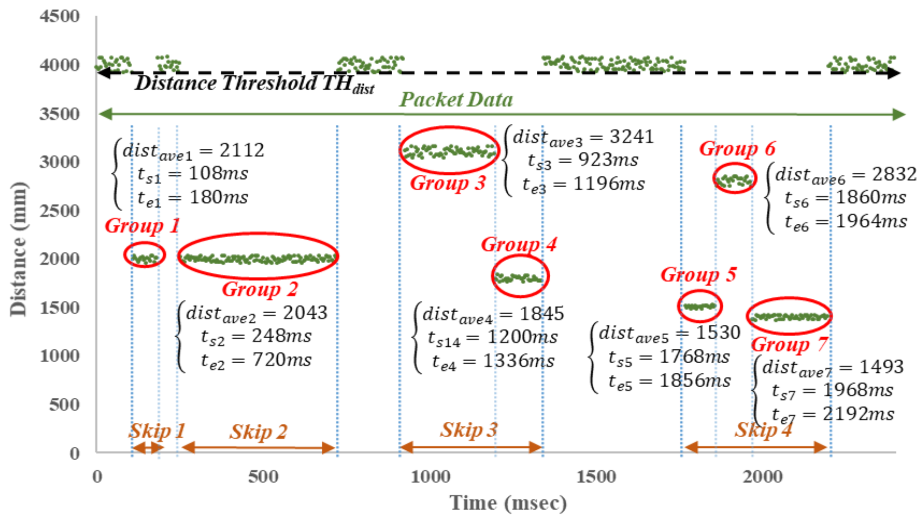

a - Visual interpretation of the skip and group data

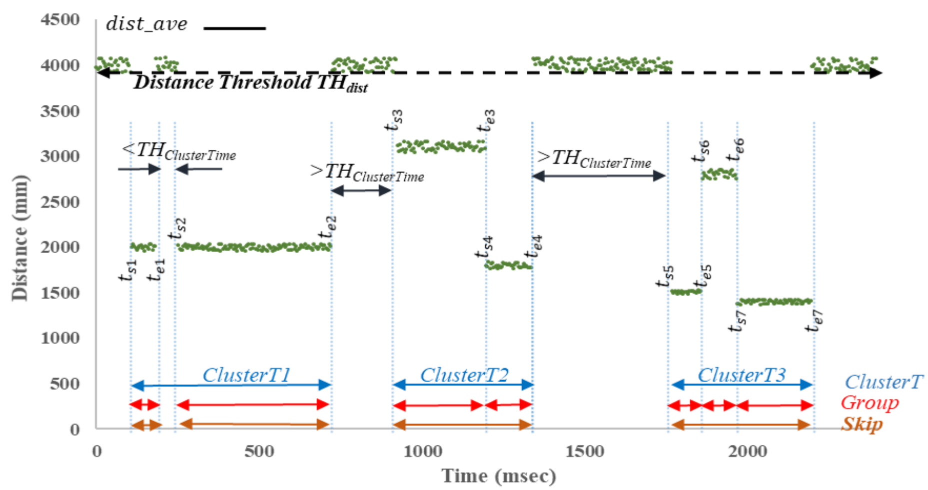

b - Visual interpretation of the first clustering step

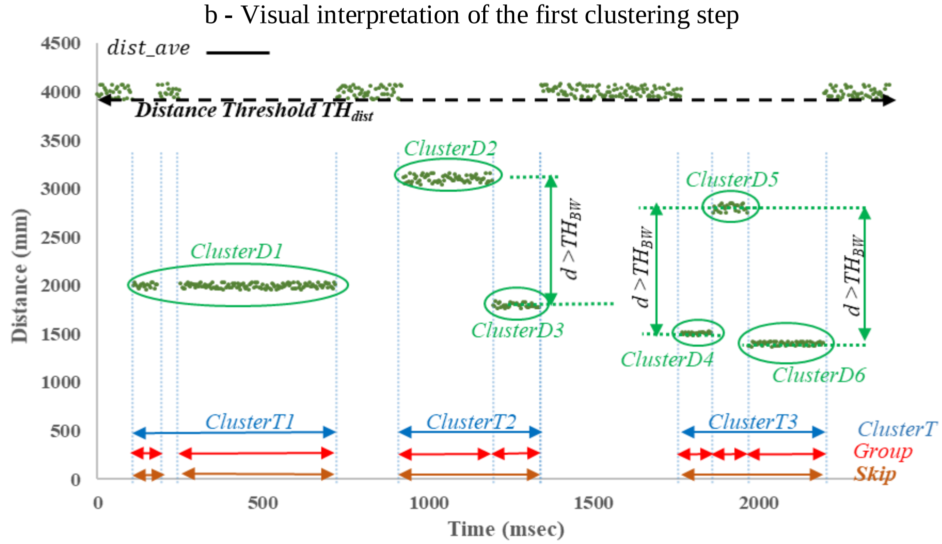

c - Visual interpretation of the second clustering step

Figure 5-5. Visual description of the decision making steps

B) Clustering on groups average distances, *dist_ave* (ClusterD)*:* Each cluster created in the previous step is clustered based the average distance values of the *groups* existing in that cluster, using a threshold, TH_{BW}. This threshold helps to detect the parallel objects, walking/biking side by side, and at the same time helps to reduce over-counting of different parts of an individual object (such as two hands for a single person).

- ✓ If $\left|dist_{ave,i} - dist_{ave,i+1}\right| > TH_{BW}$: New Cluster
- ✓ Else: Same Cluster

Figure 5-5-c shows how this clustering step works. ClusterT2, created in the previous step, will be divided into two clusters ClusterD1 and ClusterD2. ClusterT3, is then clustered into three new clusters, ClusterD1, ClusterD2, and ClusterD3.

C) In the third step, the average distance value of all pairs of *groups* existing in the same ClusterT, are compared. If the difference between their average distance values is below the threshold, TH_{BW}, then the time gap between those *groups* are calculated. If the gap is less than $TH_{ClusterTime}$, then two *groups* are combined as one object. This situation, though rare, occurs when the hands of the closer object to the sensor are detected, followed by the body of the second object, followed by the body of the closer object. As an example, ClusterD4 and ClusterD6 are combined because the difference between their average distance values is 37mm which is less than the threshold of 700mm, TH_{BW}, assigned for cyclists and the time gap between them (112ms) is less than THClusterTime, which is 150ms.

D) For each new cluster, the duration of the cluster is checked with another threshold called $_{duration}$, to ensure that small objects are not counted. The pedestrian and cyclist counting algorithms differ only in the threshold values. The values of the thresholds defined in the algorithm have been calibrated based on more than 300 hours of datasets collected on different facilities with different traffic and network conditions. Each object on the recorded video was manually compared with the raw data during the algorithm development to determine the best threshold values. Table 5-1 defines the value of the parameters used in the algorithm.

Table 5-1. Values of the Thresholds

Parameter	Value		Description
	Pedestrian	Cyclists	
THdist	-	-	Defined by the user (the interested counting range)
RT	1 sec	1 sec	Relaxed Time, the time before processing the *packet* of data
THtime	50msec	50msec	Time distance gap between samples to build *skips*
THtight	100mm	100mm	Distance gap between samples to build *groups*
TH_{BW}	350mm	700mm	Threshold on distance gap between two objects
$TH_{ClusterTime}$	300msec	150msec	Threshold on time gap between two objects
$TH_{duration}$	80msec	30msec	Threshold on minimum duration of a pedestrian/cyclists passing in front of sensor (to remove noises)

5.6 SYSTEM EVALUATION

This section presents the approach that was used to evaluate the performance of the developed Lidar-based counting system.

5.6.1 Site selection and installation

First, various locations with pedestrian and bicycle traffic were carefully selected. Two different pedestrian sidewalks and four exclusive bicycle paths (cycle tracks) in Montreal were selected to evaluate the performance of the developed system. The sites were chosen the test for alternative site characteristics, pedestrian traffic conditions, and peak patterns. For each site, several hours of data (covering both peak and off-peak hours) were collected. Additionally, video recording was used to manually count the objects; to be used as ground truth data.

Figure 5-6 shows photos of the selected sites. Selected sites have different site characteristics and flow patterns to evaluate system performance under varying conditions.

Site 1: Maisonneuve (West) – cycle track

Site 2: Maisonneuve (East) - cycle track

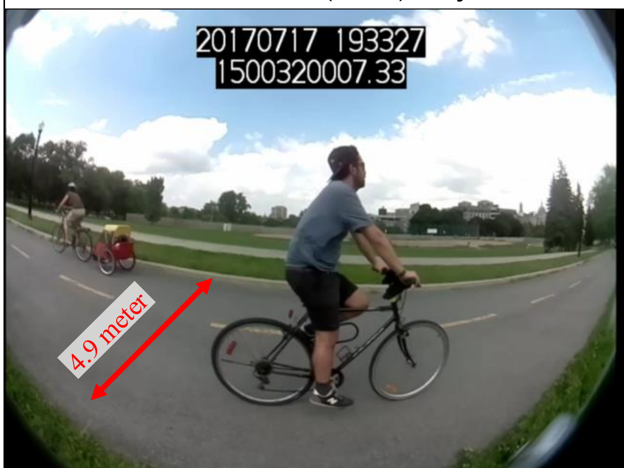

Site 3: Du Parc – cycle track

Site 4: University – cycle track

Site 5: Saint Catherine –sidewalk

Site 6: McGill College –sidewalk

Figure 5-6. Photos of selected bicycle and pedestrian facilities

Site 1 and 2, de Maisonneuve: These two sites represent locations with the highest flow of all bike paths in Montreal. These sites have a flow of approximately 600 cyclists/hour, which can be challenging for counting technology. At these sites, peak hour occurs in both directions at the same time, leading to many parallel cyclists (two or three) traveling in the field of view of the sensor. These two sites have been selected to show the performance of the system in challenging, high-flow situations.

Site 3, Avenue du Parc: This site has been selected to challenge the performance of the system in high and low speeds. Due to the high road grade, northbound cyclists travel as slow as 6km/h and southbound as high as 35km/h. This site is located on a bike path that forms the backbone of the Montreal network, connecting the north part of the city to downtown. Typically, morning and evening directional peak hours represent cyclists traveling to work and home respectively.

Site 4, University street: This bike path is used by McGill University students traveling to and from school as well as by commuters. There are directional peak hours in the morning and evening and relatively high cyclist flows.

Site 5, Saint-Catherine street: This site was chosen due to the high volume of morning and mid-afternoon users. The sidewalk along this street is heavily populated with users: people heading to work, grabbing lunch, general shoppers, and students. The sidewalk is approximately four meters wide and represents an ideal study site for testing against conventional sidewalk dimensions, heavy-use, and densely packed groups.

Site 6, McGill College street: The second site was located very close to the main entrance of McGill University. This site was selected to evaluate the performance of the system on wide sidewalks (approximately eight meters) with high pedestrian flows. As in site 2, the proximity of the study area to the signal-controlled intersection results in large groups of pedestrians with very little distance between them. This site was chosen to compare the performance of the Lidar-based system with infrared technology.

The sensors were installed on existing infrastructure, such as posts. A built-in camera is used to acquire ground truth counts from manual counting. The camera has been installed in the sensor enclosure between the Lidar sensors to have the same field of view as the proposed counter system.

This helps match the time-stamped detection with the recorded video for algorithm development and testing purposes. In order to test our developed system against existing technologies, an infrared pedestrian counting system (pyro-box counter) for sidewalks and inductive loop detectors for cyclist facilities were installed in parallel. These technologies were furnished by Eco-Counter (http://www.eco-compteur.com).

5.6.2 Performance measures

Two outcomes are used for validation: i) disaggregated counts representing each individual pedestrian or bicycle and its direction and ii) aggregated counts representing pedestrians or bicycles counted in 15-min intervals.

For the disaggregated counts, each row of the data shows the time stamp of the counted pedestrian or cyclist and their direction. Therefore, an error can occur at the detection level, when detecting (or not detecting) the road user, as well as in the direction measure. Table 5-2 shows a sample of the generated validation data at the disaggregated level. Each row of data represents one object in the video. The first column shows the time associated with each pedestrian or cyclist from video data and the second column shows the direction of the object. The "sensor count" column is 1 if the captured object has been captured by the sensor as well, otherwise, it is set to 0. "Direction Error" is 1 if the detected direction from the sensor is different from the ground truth direction of the object (second column). If the system over-counts, the 5th and/or 6th column will be filled depending on the direction of the object. This table is used in both algorithm development (to visually check all the distance patterns and compare with ground truth data to define the thresholds) and performance evaluation. Once the disaggregated data has been generated, the 15-min intervals will be generated based on the detection time.

Table 5-2. A sample of the disaggregated level of data validation

Time of Day	Ground truth Direction	Sensor count	Sensor direction	Detection error	Direction error	Overcount direction 1-2	Overcount direction 2-1
14:47:26	2-1	1			0	-	-
14:47:29	2-1	1			0	-	-
14:47:34	1-2	1		1	0	-	-
14:47:39	1-2	0					

After the ground truth and sensor, counts are obtained from the collected video, both the detection and direction errors are computed and reported for the disaggregated counts based on the outputs from Table 5-2.

In a similar way, aggregated counts for every 15-min interval were computed. The error and deviation between the sensor and ground truth counts are computed using the Absolute Percentage Deviation (AAPD):

$$error_i = \frac{A_i - G_i}{G_i} \tag{1}$$

$$AAPD = \frac{1}{n}\sum_{i=1}^{n}\left|\frac{A_i - G_i}{G_i}\right| \tag{2}$$

where A_i is the automated count for time i (15min in this case), and G_i is the manual count for time i.

5.6.3 Results

Generating ground truth disaggregated-count data for validation can be time-consuming and difficult in high pedestrian flow conditions and when pedestrians are found in groups. For this reason, disaggregated ground-truth data was only generated for the first site (Saint-Catherine). For the second site, disaggregated pedestrian counts were only obtained for 15-min intervals. On the other hand, for bicycle facilities, all the validations have been done at both levels, disaggregated and aggregate.

5.6.3.1 Cyclists Counting Evaluation

This section presents the results of the validation of the proposed system for counting cyclists at the four sites described previously. For each site, directional counts and errors are presented at the aggregate and disaggregate level. For all sites, except site 2 (Maisonneuve-East), the count data coming from the inductive loop detectors is also presented to compare with our developed technology and ground truth. The counting time period at each site was selected to cover both off-peak and peak hours. Table 5-3 shows some key statistics of each site: duration of data collection, total count by each technology, detection, and direction count errors (for disaggregated and aggregated levels).

Table 5-3. Statistic on data collection, total counts and error at disaggregated level

Measures and errors		Site 1: Maisonneuve (West)	Site 2: Maisonneuve (East)	Site 3: Parc	Site 4: University
Total Duration		05:30:36 hrs	03:43:40 hrs	04:22:23 hrs	04:01:02 hrs
Total ground truth counts		1913	2688	1216	1326
Sensor Total Counts		1912	2683	1215	1326
Sensor Direction Error (counts)		8	14	3	6
Sensor Over Counts		7	3	1	1
Detection Error (%)		0.05	0.19	0.08	0.00
Direction Error (%)		0.42	0.52	0.25	0.45
Lidar vs ground truth AAPD (%)	Direction 1-2	0.6	0.4	0.1	0.1
	Direction 2-1	0.9	0.4	2.0	1.5
Loop vs ground truth AAPD (%)	Direction 1-2	4.9	-	3.4	2.5
	Direction 2-1	6.2	-	4.3	6.5
Total Parallel bikes		97	200	120	78
Total Missed Bikes		4	4	3	0
Direction Error		1	7	1	2

From the results (reported in Table 3), the following points can be highlighted:

- At the disaggregate level, when comparing the ground truth with the sensor counts, the detection error ranges from 0.0% to 0.19% at the four sites. The direction error is also very small across sites, ranging from 0.25 to 0.52%.
- At the aggregate (15min) level, the AAPD for Lidar vs. ground truth ranges from 0.1 to 2% across sites. Regarding the comparison between loop detectors and ground truth, the AAPD ranges between 4.3% and 6.5%; the magnitudes of these errors is significantly larger than the errors obtained with the developed system.
- Additionally, a test was done in situations with the potential for occlusion; resulting from bikes traveling in parallel in the detection area. The total number of cyclists that passed the sensor field of view in parallel was recorded on video and compared with the developed system to determine the performance of the system in both counting and direction detection. The recorded data showed a total of 495 cyclists biking in groups of at least two cyclists (in the detection area of the sensor). Among them, 11 were missed, corresponding to a 2.2% error.

Additionally, 11 cyclists had an incorrect detected direction, corresponding to a 2.2% error. High bicycle flow conditions typically imply that multiple cyclists will pass the sensor at the same time and in parallel. This situation is a challenge for all counting technologies that are side-mounted. This evaluation of the system performance demonstrated that the proposed system addresses this high-flow case with high accuracy.

Aggregated counts were also analyzed for accuracy. Figure 5-7 shows the distributions of the counts over time using 15-min intervals and the three outcomes: ground truth, Lidar and inductive loop sensors in each direction. The count data tracks the ground-truth daily traffic pattern, showing high accuracy in directional counting, even during peak hours (high cyclist flows). The plots show higher accuracy of count data coming from Lidar technology in comparison with inductive loop detector data.

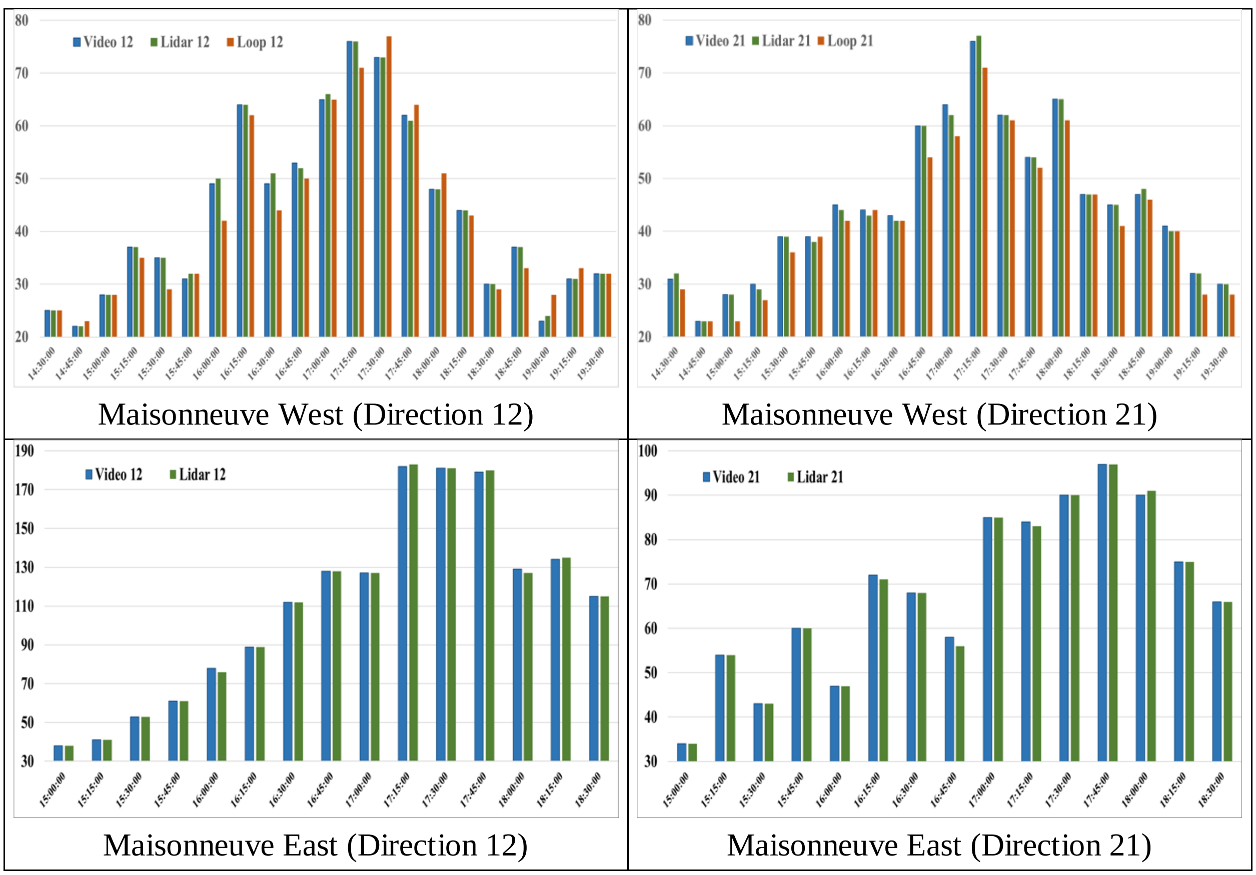

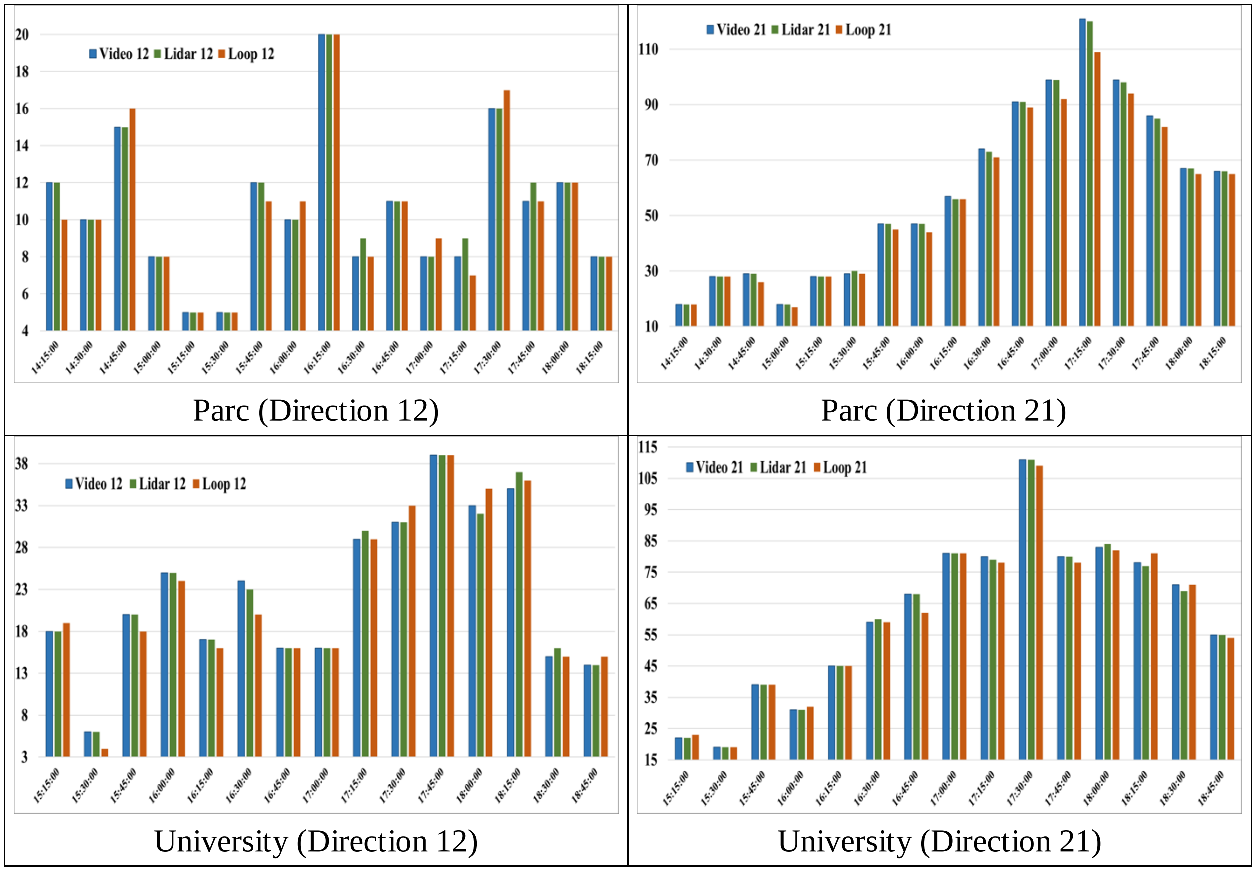

Figure 5-7. Bicycle 15-min interval counts (ground truth, Lidar and loop detector)

5.6.3.2 Pedestrian Counting Evaluation

The development and testing of the pedestrian counting algorithm were done after the completion of the bicycle counting system. The pedestrian system was tested at two pedestrian sidewalk locations, described previously: Saint-Catherine and McGill College. Data was collected during both morning and afternoon flow peaks. As in the bicycle test, video data was recorded to generate ground-truth counts. An infrared sensor was also installed at both sites following the manufacturers' instructions and the recommended settings to compare the developed system with a commercially-available infrared system.

In a similar manner, counts were obtained at the disaggregated and aggregate (15-minute) levels. The results for each site are summarized in Table 5-4:

Table 5-4. 15-minute aggregate pedestrian test results

Measure		Saint Catherine	McGill College
Total Duration		04:15:00	06:15:00
Total counts		3996	3623
Sensor Direction Error (counts)		139	95
Sensor Over Counts		15	3
Sensor Total Counts		124	92
Detection Error (%)		-2.72	-2.45
Direction Error (%)		3.47	2.54
Lidar vs ground truth AAPD (%)	Direction 1-2	2.12	2.63
	Direction 2-1	2.88	1.41
Infrared vs ground truth AAPD (%)	Direction 1-2	-	65.9
	Direction 2-1	-	21.1

From this table, a few observations can be made:

E) In the disaggregated data error analysis, the detection errors are less than 3%. Direction errors are slightly larger but still low (3.5% and 2.5% respectively at the two sites). Note that the magnitude of these errors are lower than those reported in the literature for similar environments in Montreal Miranda-Moreno and Lahti 2013.

F) The aggregated data (15-minute intervals) has a low error as well; the AAPD does not exceed 3% at the two sites when comparing Lidar with the ground truth counts. The errors are much lower than the infrared sensor, which reports large errors (21% and 65% for site 2).

G) Undercounting is more frequent than the overcounting. This is due to an occlusion in dense groups. As with other technologies that are side-mounted, the proposed Lidar system undercounts in situations where pedestrians are densely packed, causing occlusion in the data received. The direction detection error is attributed to undercounting; incorrect direction detection rarely occurs due to the sensor falsely predicting the direction of the object. The overcounting is attributed to a number of possible situations: a pedestrian raises a hand simulating a second pedestrian, a pedestrian carrying a back-pack, the sensor not being set up at optimal height, and finally, a pedestrian making drastic movements with-respect-to the sensor beam.

At the Saint Catherine site, the infrared sensor showed more than a 200% overcount because of the existing store glass window. For this reason, the infrared data was not used for comparison purposes. The is one of the challenges of using infrared-based counting systems. The infrared sensor, a commercial product, performs unpredictably, and with poor results. As can be seen by the red bar in the plots of Figure 5-8, the infrared sensor is known to undercount and overcount without any deterministic pattern.

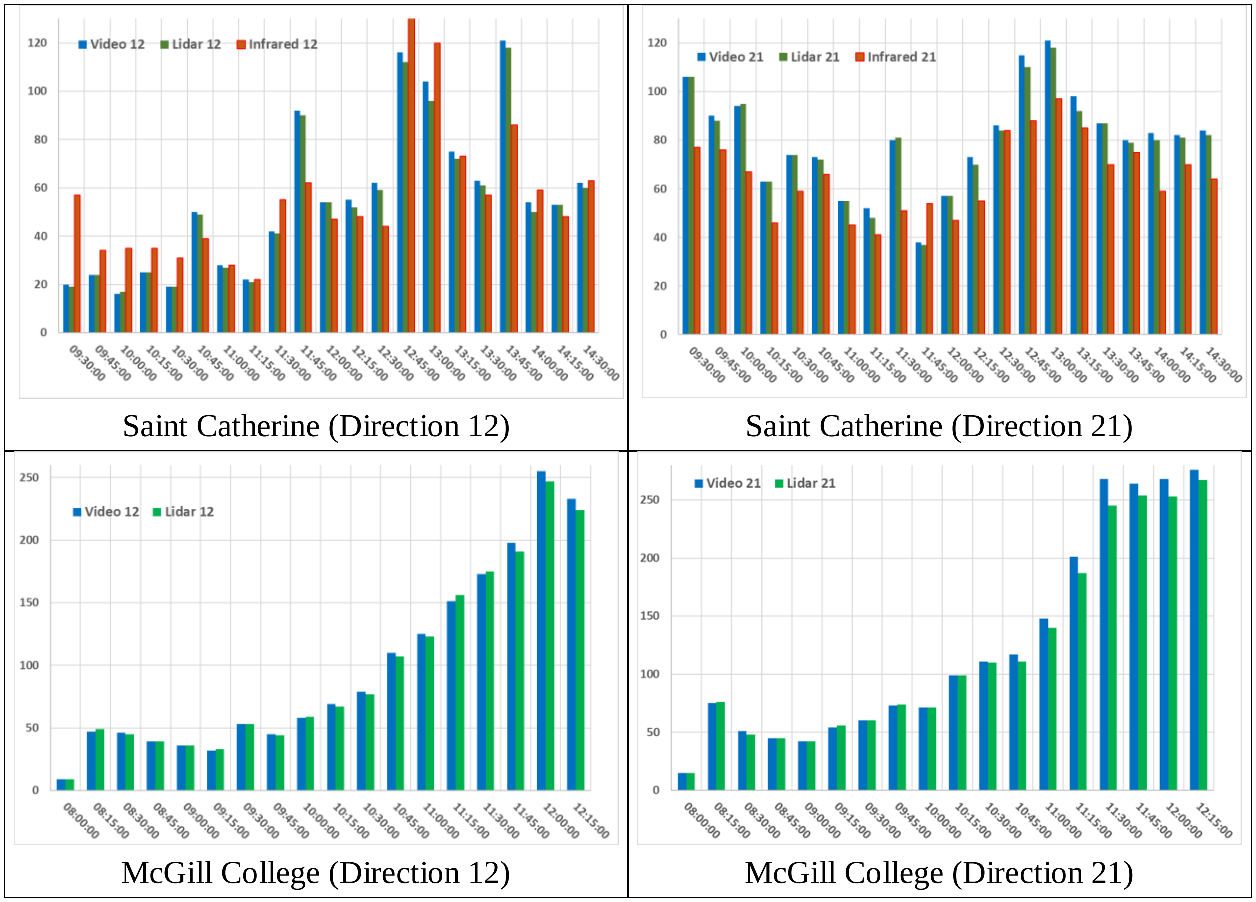

Figure 5-8. The 15-min interval counts (ground truth, Lidar and loop detector)

Figure 5-8 also demonstrates the ability of the Lidar to closely follow the ground-truth pedestrian patterns over time. Figure 5-9 shows the linear correlation between the manual count and the automatic count using the proposed system. Highly correlated results (more than a 0.99 R^2 value) are evidence that the proposed system can provide reliable and accurate counts, and can be used in sidewalks with higher volume where the counts are extrapolated using correction factors.

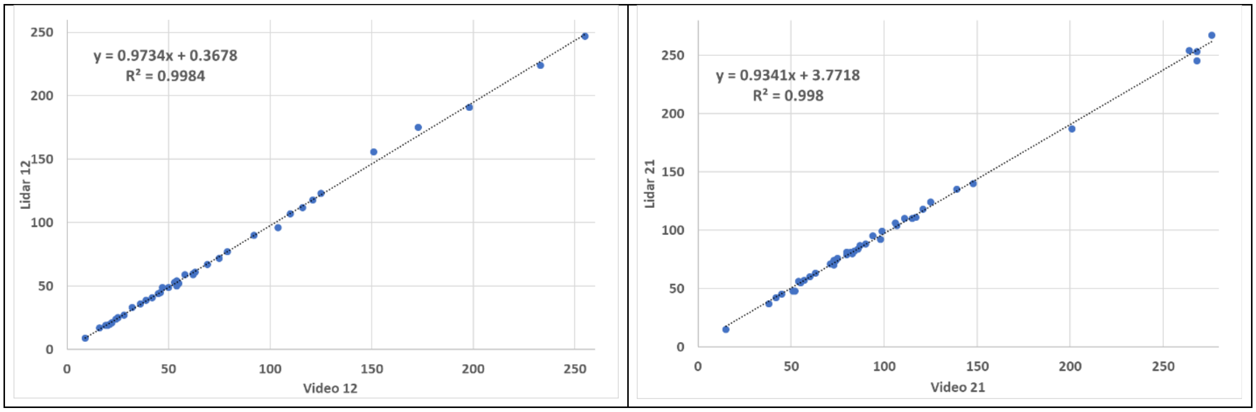

Figure 5-9. The correlation plots between ground truth and Lidar count data (15min intervals)

5.7 CONCLUSIONS AND FUTURE WORK

This paper outlines the development and evaluation of an original automated counting system for bicycle and pedestrian facilities based on Lidar technology. The system components, hardware, and software are described along with the testing protocol. Six different sites were selected for testing the accuracy of the proposed counting system and its functionality in different challenging situations including high volume traffic, occlusion, stop-and-go pedestrian flow conditions, and wide sidewalks. Video data was collected to obtain manual counts, defined as the “ground truth”. Sites and counting periods were selected to observe a large variability in the magnitude of counts. Two level-of-accuracy validations were considered using different data aggregation: i) disaggregated level, in which each captured object was visually matched with the output of the sensor (one-for-one). This validation shows all overcounting, undercounting and direction detection errors, and ii) aggregated level, in which LIDAR counts are aggregated in periods of 15-minute intervals and compared with different technologies and ground truth.

The initial findings show the potential of this counting system with promising results for different traffic conditions (low to relatively high volumes) in peak and off-peak hours on both pedestrian and bicycle facilities. The results, for different traffic conditions and network topology, show that in 80% of 15-min automated counting samples the error was between 0-5% and 0-2% for pedestrian and cyclists counting respectively.

For the bicycle facility validation, disaggregate errors of less than 0.5% were observed across testing sites (both detection and direction errors). For the aggregate counts (15-min intervals), an average directional count error of around 0.7% was obtained when comparing the proposed system with ground truth counts. The aggregate-count error from loop detectors vs ground truth was of 4.7% on average. The results clearly show the performance of the proposed system in comparison with current systems. A low, 2.2% count error, in cases that a group of two or three cyclists are traveling in parallel, along with the path, in front of the sensor, address the concern of occlusion for side-mounted counting systems.

For the pedestrian facility validation, disaggregate detection and direction errors were below 3.5% at all testing sites. When using aggregate counts, the errors of the proposed Lidar system with respect to the ground truth were of the same order of magnitude (less than 3%). On the other hand, infrared sensor errors were many time higher than those obtained from the proposed system; aggregate errors of more than 60% at one of the sites. The performance of the Lidar counter is high for pedestrian monitoring.

H) It is important to highlight that, in addition to improved accuracy over other pedestrian and cyclist monitoring technologies, the proposed system presents other advantages:

I) Installation: in the case of bicycle facilities, installation does not require traffic flow disruption due to pavement cutting. The traditional loop detector system required pavement perforation, increasing installation and maintenance cost.

J) Flexible Use: the proposed system can be installed as a mobile or fixed sensor for either pedestrian and bicycle counting. Therefore, the proposed system is an alternative to pneumatic tubes (for mobile bicycle counting), inductive loops (for permanent bicycle counting), or infrared sensors for pedestrian counting.

K) The setting of the Counting Area: the proposed system allows users to set the coverage counting area, which addresses a key challenge associated with infrared counters that require the presence of a wall or blocking barrier on one side of study space. This advantage enables its use on open space facilities, such as bike paths and trails.

L) Occlusion: the proposed system handles the issue of occlusion associated with all side-mounted counting systems. The results show that the system is accurate on high-flow pedestrian and bicycle facilities.

M) High Temperatures: Lidar technology is not sensitive to temperature, whereas infrared-based sensor accuracy is significantly affected by hot-sunny conditions.

Although the proposed system has a strong performance for counting pedestrians and cyclists at different facility types, some limitations should be highlighted. The principal limitation of the proposed Lidar sensor, with respect to other sensors, is the high energy consumption. Infrared or loop detector sensors can function for several years on a single set of batteries, while the Lidar system will consume the same amount of energy in a few days. The power consumption limits the device to be a short-term counting system in the absence of external power. In order to operate as a permanent counting system, our proposed system could be integrated with a low-power passive infrared that would trigger the Lidar sensors once movement is detected. Another solution would be to provide external power by integrating a solar panel into the system or by hardwiring the system to the city electric network. Additionally, the performance of the proposed system under bad weather conditions requires further testing. The Lidar system can also underperform in very high-volumes or in traffic conditions with a high-frequency of pedestrians walking in groups. The error rate associated with occlusion under these conditions could increase significantly.

5.8 REFERENCES

Brosnan, M., Petesch, M., Pieper, J., Schumacher, S. and Lindsey, G. (2015) Validation of bicycle counts from pneumatic tube counters in mixed traffic flows. Transportation Research Record: Journal of the Transportation Research Board (2527), 80-89.

Dharmaraju, R., Noyce, D.A. and Lehman, J.D. (2002) An evaluation of technologies for automated detection and classification of pedestrians and bicycles, University of Massachusetts at Amherst.

Greene-Roesel, R., Diogenes, M.C., Ragland, D.R. and Lindau, L.A. (2008a) Effectiveness of a commercially available automated pedestrian counting device in urban environments: Comparison with manual counts.

Greene-Roesel, R., Diogenes, M.C., Ragland, D.R. and Lindau, L.A. (2008b) Effectiveness of a Commercially Available Automated Pedestrian Counting Device in Urban Environments: Comparison with Manual Counts. Safe Transportation Research & Education Center.

Ismail, K., Sayed, T. and Saunier, N. (2009) Automated collection of pedestrian data using computer vision techniques.

Johnstone, D., Nordback, K. and Lowry, M. (2017) Collecting Network-wide Bicycle and Pedestrian Data.

Krammer, P. and Schweinzer, H. (2006) Localization of object edges in arbitrary spatial positions based on ultrasonic data. Sensors Journal, IEEE 6(1), 203-210.

Kristoffersen, M.S., Dueholm, J.V., Gade, R. and Moeslund, T.B. (2016) Pedestrian counting with occlusion handling using stereo thermal cameras. Sensors 16(1), 62.

Leibe, B., Seemann, E. and Schiele, B. (2005) Pedestrian detection in crowded scenes, pp. 878-885, IEEE.

Lesani, A., Miranda-Moreno, L.F., Fu, T. and Romancyshyn, T. (2015) Development and Testing of an Ultrasonic-Based Pedestrian Counting System.

Leykin, A. and Hammoud, R. (2006) Robust multi-pedestrian tracking in thermal-visible surveillance videos, pp. 136-136, IEEE.

Lindsey, G., Hankey, S., Wang, X. and Chen, J. (2013) The Minnesota bicycle and pedestrian counting initiative: methodologies for non-motorized traffic monitoring.

Lu, T., Mondschein, A., Buehler, R. and Hankey, S. (2018) Adding temporal information to direct-demand models: Hourly estimation of bicycle and pedestrian traffic in Blacksburg, VA. Transportation Research Part D: Transport and Environment 63, 244-260.

Markowitz, F., Montufar, J. and Steindel, M. (2009a) Automated Pedestrian Detection: State of the Art.

Markowitz, F., Montufar, J. and Steindel, M. (2009b) Automated Pedestrian Detection: State of the Art.

Miranda-Moreno, L.F. and Lahti, A.C. (2013) Temporal trends and the effect of weather on pedestrian volumes: A case study of Montreal, Canada. Transportation Research Part D: Transport and Environment 22, 54-59.

Nordback, K. and Janson, B. (2010) Automated Bicycle Counts: Lessons from Boulder, Colorado. Transportation Research Record: Journal of the Transportation Research Board (2190), 11-18.

Ozbay, K., Yang, H. and Bartin, B.O. (2010) Calibration of an infrared-based automatic counting system for pedestrian traffic flow data collection.

Proulx, F.R., Schneider, R.J. and Miranda-Moreno, L.F. (2016) Performance evaluation and correction functions for automated pedestrian and bicycle counting technologies. Journal of Transportation Engineering 142(3), 04016002.

Ryus, P., Ferguson, E., Laustsen, K.M., Prouix, F.R., Schneider, R.J., Hull, T. and Miranda-Moreno, L. (2014) Methods and technologies for pedestrian and bicycle volume data collection, Citeseer.

Strauss, J., Miranda-Moreno, L., Crouse, D., Goldberg, M.S., Ross, N. and Hatzopoulou, M. (2012) Investigating the Link Between Cyclist Volumes and Pollution Levels Along Bicycle Facilities in Dense Urban Core.

Link Between Chapter 5 and Chapter 6

Chapter 5 presents a new technology for counting pedestrians and cyclists using single beam Lidar technology. As discussed in the previous chapter, the sensor should be mounted from the side of the pedestrian/cyclist facility and, to get the best performance, the installation height should be around 1.5 m from the ground. As all technologies installed from the side, the performance of the system can drop because of the occlusion problem when a group of people is walking tightly/closely together. Despite the use of a narrow laser beam in our solution, which can detect any small gap between the objects, the performance of the system in wide sidewalks may be affected.

There is also a need for classifying the objects in counts in mixed mode traffic network. To address these issues, Chapter 6 proposes a new counting system based on 2D Lidar technology which is mounted from the top. Using this proposed solution, the sensor counts the objects and detect their direction in real-time, which can be used in congested and high volume pedestrian/cyclist facilities. Our proposed solution also has the potential to detect the class of the objects based on their shape.

Chapter 6: Development and Evaluation of a 2D Lidar based Real-Time Pedestrian Counting System for High-Volume Conditions

Asad Lesani[a], Ehsan Nateghinia[a], Luis Miranda-Moreno[a]

[a] *Department of Civil Engineering and Applied Mechanics, McGill University, Montreal, Canada*

Accepted for presentation at Transportation Research Board 96th annual meeting, Washington D.C and to be submitted for publication "Transportation Research Part C: Emerging Technologies".

6.1 ABSTRACT

Automated monitoring of pedestrians on non-motorized facilities with high pedestrian flows is extremely challenging. Several automated sensor solutions are commercially available that have been evaluated in the literature including traditional point-based sensors, such as inductive loop detectors for bicycles and infrared sensors for pedestrians. More recently, image-based systems based on video or thermal video cameras have been developed. Despite the various options, some key limitations of existing solutions exist, in particular, the lack of low-cost solutions using embedded systems capable of performing in real-time under high volume (flow) conditions. This work aims at developing and evaluating the performance of a novel, real-time counting system, developed for environments with extremely high pedestrian flows. The proposed system is based on a Laser Technology Light Detection and Ranging (Lidar). The system uses as an input the distance measurements from a two-dimensional Lidar sensor with a set of distinct laser channels and an angular resolution of three degrees between each channel. The developed system processes those measurements using a clustering algorithm to detect, count, and identify the direction of travel of each pedestrian. The system's performance is evaluated by comparing its directional counting results with manual counts (ground truth) using disaggregate and aggregate (15-minutes intervals) counts at two different monitoring locations. The results demonstrate that the system

accurately counts more than 97% of the pedestrians at the disaggregate level, with a false direction detection rate of 1.1%. The over-count error is 0.7% and the under-count errors are 1.3% and 2.7% for the two selected sites. At the aggregate level (15-minutes intervals), the average absolute percentage deviations (AAPDs) are 1.6% and 4.3% while the weighted AAPDs are 1.5% and 3.5% for the first and second sites, respectively. The accuracy of the proposed system is higher than the traditional technologies used for the same purpose.

6.2 INTRODUCTION

Active transportation, such as walking and cycling, has gained momentum in recent years in many North American cities. For instance, cycling ridership and network size have risen sharply in the last decade (Pucher et al. 2011, Ussery et al. 2018). The increase of bicycle and pedestrian activity has created more complex traffic conditions on the traditional road network and on non-motorized transportation facilities. To evaluate the needs of active modes, such as new infrastructure, and the impacts of policies and investments, cities have been looking for efficient and innovative ways to collect data for non-motorized traffic (Pucher and Buehler 2017). Similar to vehicular traffic, non-motorized counting can be collected using permanent and short-term monitoring systems. The few technologies have emerged for short-term, and long-term counting of active users have many well-documented limitations (FHWA 2016, NCHRP). Firstly, traditional bicycle counting systems, such as loop detectors, are associated with high installation and maintenance costs and require pavement cutting which can disrupt traffic. Secondly, traditional pedestrian counters require the presence of well-defined detection areas; in the case of pedestrian infrared counters, a blocking barrier on one side of the study space is required. The detection area of infrared sensors is difficult to define making it impractical for monitoring in open space facilities. Thirdly, the extreme temperature can impact the accuracy of traditional counting systems. Lastly, occlusion, which occurs when people walk or bike in groups, significantly reduces the accuracy of traditional point-based monitoring systems. The under-counting error associated with occlusion worsens as density increases, making traditional systems impractical for high-flow facilities.

More recently, computer vision solutions have emerged that use (visual spectrum) video sensors (Zangenehpour et al. 2015). These systems are typically mounted above a facility and are less prone to occlusion. However, they have some significant limitations such as poor performance under adverse weather conditions (rain or snow precipitation), low visibility conditions, and environments with shadows or glare. To address this issue, thermal video camera solutions have also emerged. However, they are very expensive (Fu et al. 2017). Another issue with image-based sensors is the data transfer and processing cost; video data needs to be streamed and processed on powerful computing servers. Image-based embedded systems for processing video data locally is expensive.

In recent years, Lidar (Light Detection and Ranging) technologies have been improved and show great potential in many transportation monitoring applications, including traffic monitoring of non-motorized facilities. Lidar devices emit laser beams at an object and then compute the distance to the object using the energy of the reflected beams received by the sensor. There are different implementations of Lidar systems based on their number of laser channels and their coverage area. For example, a one-dimensional laser scanner has one channel that covers a straight line. A two-dimensional (2D) Lidar includes an array of beams where each beam covers a straight line, and a set of beams covers a two-dimensional plane in space. Three-dimensional (3D) Lidar systems have two different types of solid and rotating Lidar sensors, which can scan their surrounding environment in 3D space (Tarko et al. 2018, De Silva et al. 2018, Pacala and Eldada 2017).

This paper investigates the performance of an automatic laser-based pedestrian counting system. The system addresses several limitations with existing counting technologies; the proposed real-time embedded system is not impacted by occlusion when monitoring facilities with very high volumes. More specifically, this paper proposes and tests a two-dimensional Lidar pedestrian counting system. This system serves as an upgrade from the previously implemented one-dimensional Lidar-based sensor. The proposed 2D system has several advantages over the one-dimensional system, including an extended coverage area; the ability to make multiple, simultaneous detections; enhanced accuracy in detection, especially when monitoring dense groups of objects.

6.3 LITERATURE REVIEW

The increasing demand for automatic pedestrian and cyclist counting for non-motorized facilities has led to developments and advancements in available technologies including point- and image-based systems. Some examples include passive infrared sensors for pedestrians, inductive loops and pneumatic tubes for bicycles, and more recently radar, 3D stereo camera, and video-based sensors. Recently, the Federal Highway Administration (FHWA) released a new edition of their Traffic Monitoring Guidebook, which provides detailed information about motorized and non-motorized traffic monitoring technologies and programs (Federal Highway Administration, 2016). Furthermore, the National Cooperative Highway Research Program (NCHRP) conducted a project to test several counting technologies. The study investigated the limitations and strengths of the alternative technologies and reported the accuracy of those that were tested. As one of the main limitations of traditional technologies, the report highlighted the poor performance of existing embedded pedestrian-counting systems under occlusion and high volumes (Board et al. 2017, Ryus et al. 2014). Although emerging technologies such as a stereo or video-based solutions have stronger performance, their (hardware and processing) costs make them less attractive. Embedded real-time video-based systems are also in the development stage.

Passive and active infrared sensors are the most popular types of sensors for pedestrian counting in outdoor environments. Passive infrared sensors detect pedestrians based on the changes in the heat emissions within their detection area. They are easy to install, have low power consumption, and a fast response rate. Nevertheless, their performance degrades in open spaces, under extreme temperatures, or in the presence of other sources of heat (e.g., vehicle engines and radiation from the sun). They are also incapable of dealing with occlusion on facilities with high pedestrian volumes (Greene-Roesel et al. 2008). NCHRP tested three different passive infrared-based sensors and reported a total error of 22.5% (measured as the average absolute percentage deviance – AADP) (Board et al. 2017).

Active infrared sensors can count pedestrians and cyclists, but they cannot classify them. An active infrared sensor consists of an emitter and a receiver. It should be mounted at the two opposite sides of the area under study, which makes it difficult to install at most cycling facilities. NCHRP tested an active infrared sensor on a shared pedestrian-cyclist facility, with an average hourly volume of 327 users, and reported an AADP of 7.3%, (Board et al. 2017, Ryus et al. 2014).

Ultrasonic-based detection and counting systems have not been widely used for non-motorized counting applications. However, in our previous work (Lesani et al. 2015)[1], the authors designed a low-cost ultrasonic system for pedestrian counting and compared it to an infrared sensor. The system demonstrated promising results in terms of real-time counting with acceptable accuracy. However, low-cost ultrasonic sensors have low sampling rates, operate for short distances (range measures four meters), and their waves diverge with distance (15-degree angle). This research on ultrasonic-based detection has led to further improvements and the development of a single beam Lidar sensor[2], which is a low-cost system that counts pedestrian volumes with high accuracy. Nonetheless, the single beam Lidar sensor has lower performance in environments with high pedestrian flows and large groups of people (Lesani et al. 2015).

Pneumatic tubes and inductive loop counters are the most common cyclists counting sensors. There are two types of pneumatic tube sensors: general-purpose counters (GPCs) and bicycle-specific counters (BSCs). Studies in (Nordback et al. 2011, Hyde-Wright and Krista Nordback PHD 2014, Nordback et al. 2016) evaluated a comparison between BSCs produced by the Eco-Counter and GPCs produced by MetroCount. The results in (Hyde-Wright and Krista Nordback PHD 2014) show that GPCs with long tubes show poor performance in cyclists counting, but for smaller lengths, GPCs reported a 94% weighted average accuracy. The accuracy of BCS sensors is between 94% and 95% for tube lengths between 4 and 27 feet. Nevertheless, the results in (Nordback et al. 2016) show that the mean percentage under-counting error (MPE) of BSCs is between 20% and 23%, and for GPCs the error is between 10% and 44%. NCHRP have also tested three different bicycle-specific tubes and one standard tube. BSCs reported AADPs of 10.8%, 16.6%, and 69.1%, and standard tubes reported an AADP of 17.1% (Ryus et al. 2014).

Inductive loops are electromagnetic-based counter systems and consist of a loop of wires. Although cycle-tracks and cycle lanes are ideal places for these sensors, factors such as detector sensitivity, pattern, and a number of loops have a direct effect on the accuracy of cyclist counting and directional speed estimating. A study on the installation of inductive loops has reported an

---

[1] Refer to *Appendix A* for more information.

[2] Discussed in Chapter 5

AAPD of 23% in shared facilities, and 7.6% in the separated pathway (Nordback et al. 2011). Additionally, NCHRP obtained an AAPD of 7.6% for embedded inductive loops and an AAPD of 10.5% for loops on the surface (Board et al. 2017, Ryus et al. 2014).

Recent advancements in computer vision algorithms and computing machines have enabled camera-based systems to count and classify pedestrians and cyclist (Li et al. 2012). However, they have some limitations including cost and weak performance at night and under extreme weather conditions. A recent study has compared a thermal camera with an MPE between -15% and 1%, and an infrared sensor with an MPE from -28% to 0% (Leykin and Hammoud 2006).

The laser-based system known as Lidar works by measuring the distance to the object. In addition to the distance data, the reflection value is reported by most of the Lidar sensors. Recent advancements in 2D and 3D Lidar sensors have made them useful in a wide range of applications in civil engineering. Airborne and terrestrial laser scanning have been used for documenting earth surface features or 3D models of buildings in the urban environment (Pu and Vosselman 2009, Yan et al. 2015). In transportation engineering, Lidar scanners are used for vehicle speed estimation or road infrastructure mobile scanning (Guan et al. 2015) and in autonomous vehicles. This paper aims to develop a 2D Lidar-based pedestrian counting system as an alternative to conventional counting systems.

6.4 SYSTEM HARDWARE AND MEASURES DEFINITION

The proposed system uses a 2D solid-state, 16-channel Lidar sensor from LeddarTech (Leddar M16). This sensor measures distances up to 50 meters with an angular resolution of 3 degrees between each channel and a sampling rate of 100 Hz.

Figure 6-1.a and Figure 6-1.b show the prototype and a photo of the hardware. The prototype includes the Lidar module that senses the distance from objects, a processing unit equipped with different communication modules for data telemetry purposes and a built-in camera for validation and ground truth data collection. Figure 6-1.c shows a sample of installation conditions. By adding a rotation angle (represented by θ), the system can fully cover a sidewalk. The data is processed in real-time using a low-cost 1.2GHz quad-core processor with a 2Gb RAM. The designed system can provide different communication protocols such as Ethernet, WiFi/Bluetooth for short-range communication, ZigBee/LoRA for long-range local connection between sensors and a cellular GSM network for long-range communication with the server. The power management unit can provide power from either a power grid and solar panel for permanent installations or from batteries for short-term installations.

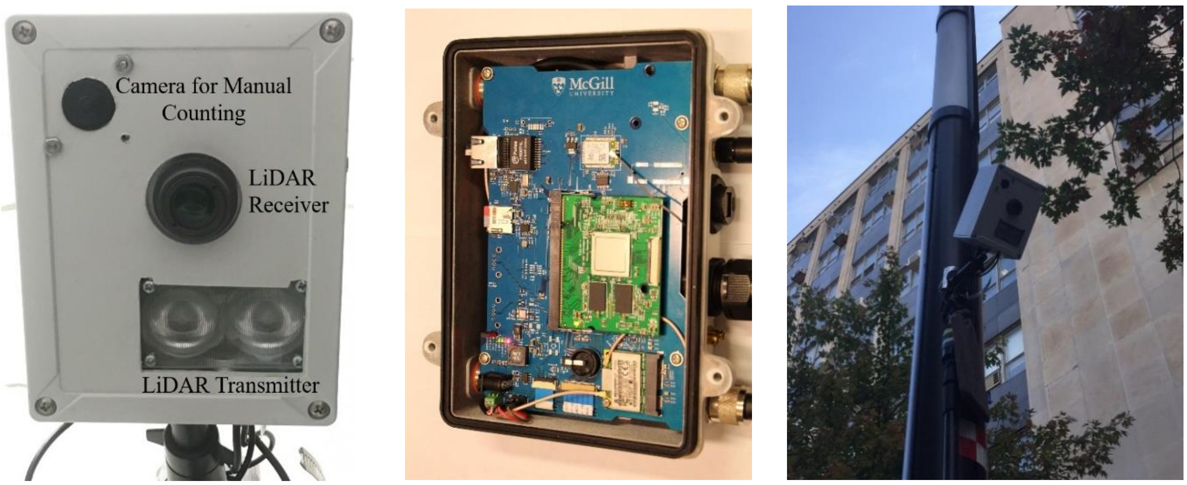

a) system prototype b) designed hardware c) sample installation

Figure 6-1. The system prototype, the designed hardware, a sample of installation, and a schematic of the processing unit.

Figure 6-2 shows the sensor configuration and setup. The key parameters used in the sensor measurements are defined as follows:

N) θ: angle of sensor rotation

O) h: height of sensor installation

P) α_1: total horizontal field of view (48 degrees)

Q) α_2: vertical field of view (7.5 degrees)

R) α_3: horizontal angle of each pixel ($48 \div 16 = 3$ degrees)

S) β_i: angle between the center and $i-th$ channels

T) $d_{i,t}$: distance measured by $i-th$ pixel (channel) at time t

U) d_t: vector of 16 measurements at time t, $d_t = [d_{1,t}, \ldots, d_{16,t}]_{1\times16}$

V) D_t: vector of raw data measurements including timestamp and d_t, $D_t = [t, d_t]_{1\times17}$

W) d_i^{max}: maximum distance measured by $i-th$ channel and when there are no moving objects in the detection area. ($d_{max} = [d_1^{max}, \ldots, d_{16}^{max}]_{1\times16}$).

X) Δd_{it}: the difference between the current distance, d_{it}, and the maximum distance d_i^{max}, and is calculated as: $\Delta d_{it} = d_{i,t} - d_{i-\max}$, and for all pixels: $\Delta d_t = d_t - d_{max}$.

Y) D_{tmp}: a matrix with 16 columns which holds the distance values when an object is in front of the sensor. Once there is no object for a predefined time, this matrix is processed and initialized to an empty matrix.

The rest of the parameters represented in this figure will be discussed in the following sections.

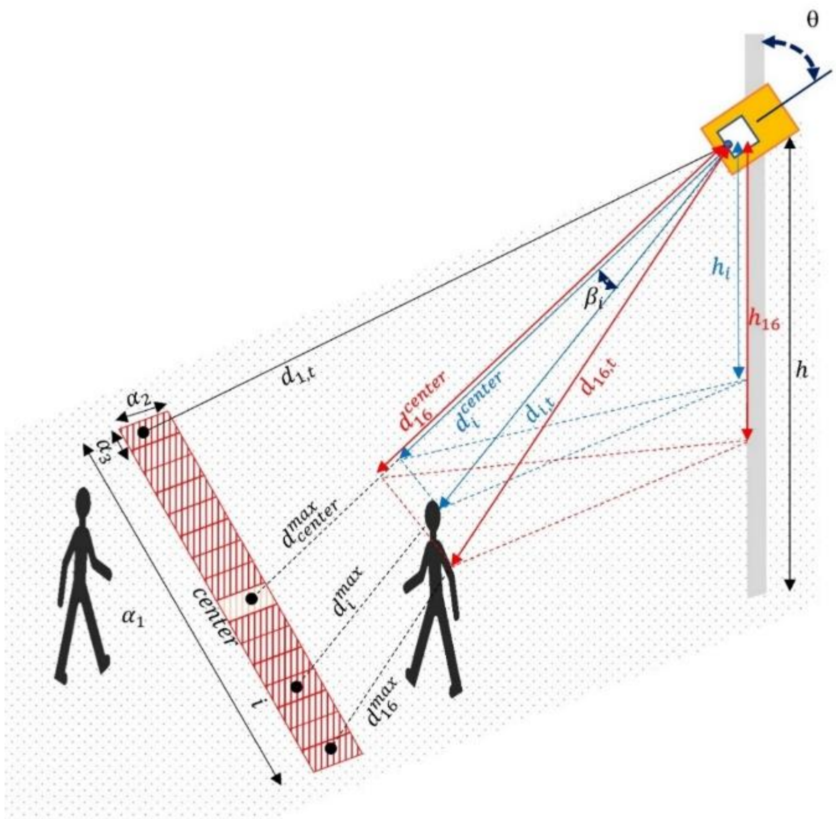

Figure 6-2. The definition of the field of view of the Lidar sensor

When there are no moving pedestrians in the detection zone, the sensor reports the maximum distance (to the background), which in some cases may be noisy. When the object passes the detection zone, the pixel values drop according to the distances between the sensor and the different parts of the object. Therefore, the object detection algorithm starts with the pattern analysis of the detection of the differences between the current distances value ($d_{i,t}$) and maximum observed distances (d_i^{max}).

6.5 PROPOSED METHODOLOGY

This section presents the developed methodology to process raw Lidar measurements for pedestrian detection, segmentation, direction definition, and counting. Figure 6-3 shows the flowchart of the methodology used to process raw data and report counts and directions.

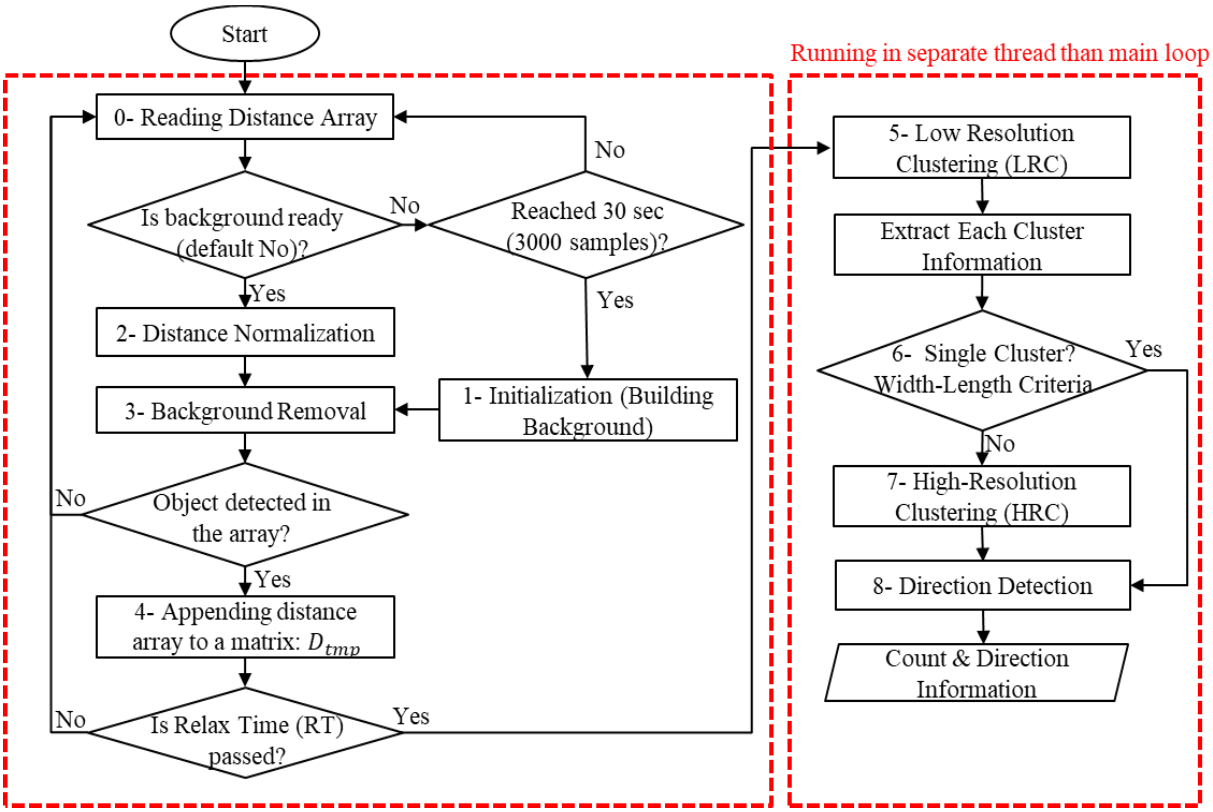

Figure 6-3. Flowchart of the methodology

6.5.1 Initialization

This step gives the initial raw distance measurements of each channel for the initialization time, e.g., 30 seconds, at the beginning of the algorithm (this is referred to as the initialization step). Data is then stored in a data array, $D_{0,30\text{sec}}$. In 30 seconds, this data array will include 3000 observations each consisting of a vector of 16 measurements:

$$D_{0,30\text{sec}} = [d_0; \quad \dots \quad d_{30sec}]_{16\times3000} \tag{1}$$

Then the median of each column (pixel) is calculated and the d_{max} vector ($d_{max} = [d_1^{max}, \ldots, d_{16}^{max}]_{1\times16}$) is built for background removal purposes. This array is compared with each new distance measurement to detect the objects and remove the background.

6.5.2 Data Normalization and background removal

The measured distance to the object depends on the height of the object and the index of the pixel measuring it. Therefore, the sensor records different distance values for an object when it is in different locations. The distance values of different pixels should be normalized for clustering purposes and for reconstructing the shapes of the objects. Figure 6-2 describes the parameters used for the normalization process. The user needs to define the central pixel, the pixel number that is facing the center of the sidewalk by measuring the minimum distance to the sidewalk.

First the projection of the distance measured by the $i-th$ channel, equivalent to the condition if the object where covered by the central pixel, is calculated as (2):

$$d_{i,j_{center}} = d_i \times \cos(\beta_i) \tag{2}$$

$$\beta_i = (i - \mathrm{j_{center}}) \times \frac{FOV_h}{I} \tag{3}$$

Where β_i is the angle between the center and i-th channels, $\mathrm{j_{center}}$ is the index of the center pixel, FOV_h is the horizontal field of view of the sensor (48°in this study), and I is the total number of pixels (16 in this study). Then the normalized vertical distance (h_i) of object detected by $i-th$ pixel is calculated as:

$$h_i = d_{i,j_{center}} \times cos(\theta) \tag{4}$$

Since the angle θ is independent of pixel ID, a rough estimation of it can give the required accuracy in calculating the vertical (normalized) distance between the sensor and object head.

6.5.3 Background Removal

The background removal step detects the presence of objects and constructs the object segment by comparing the current readings (d_t) of the sensor to the reference values. These reference values are the median of the measurements obtained in the initialization step. A threshold value, c, (in this study, c=0.3m) is defined for distance comparison, and filters out measurement noise. The sensor keeps the measurements of the triggered pixels and sets the output of the other pixels to a maximum value (the background or median value for that pixel), as follow:

Algorithm 1. Background Removal

1. At time t, define $\Delta d_{i,t} = \left| d_{i,t} - d_i^{max} \right|$
2. $if\ \sum_{i=1}^{16} \left(\Delta d_{i,t} > 0.3 \right) > 0$:
    print "Object Detected."
    where $\Delta d_{i,t}$ is less than $0.3m$, set the value of $d_{i,t}$ to $(1 + d_i^{\max})$ and update d_t

Append d_t to the matrix, D_{tmp} , defined as…

The first step of the algorithm compares the distance value of each pixel at time t with its reference value. If at least one pixel shows a difference greater than 0.3 m, then an object is present in that frame. In the second step of the above script, for all pixels that have not detected any object (i.e., $\left| d_{i,t} - d_i^{max} \right| < 0.3m$), their distance values are replaced by a predefined value (one meter more than the $i - th$ maximum distance). Then, the frame data is added to a new temporary variable called D_{tmp} for further processing.

6.5.4 Relax Time Concept

Relax Time (RT) is introduced for real-time implementation. After that the *Background Removal* algorithm detects the presence of an object, raw data is added to D_{tmp}, the temporary array. Once there are no more objects in the coverage area, a timer starts to count while the normalized distance data is being added to D_{tmp} until the timer reaches to a maximum RT value. Therefore, D_{tmp} has the information of at least one object. In this paper, a time interval of 1000 millisecond (based on experiments and by analysing at a set of detected samples) is considered. RT helps to avoid dividing an object into two different D_{tmp} frames, because of noisy or missing information.

Figure 6-4 illustrates two examples including photos of the site, raw distance data, and the results of the *Background Removal*. The raw distance values are multiplied by -1, for visualization purposes, which also transforms the local minimum points associated with the minimum distance to the head of the pedestrian to the local maximum values and changes the objective to a peak detection problem. The X-axis in the plots represents the pixel ID, the Y-axis is the epoch time in milliseconds, and the Z-axis shows the distance values (multiplied by -1).

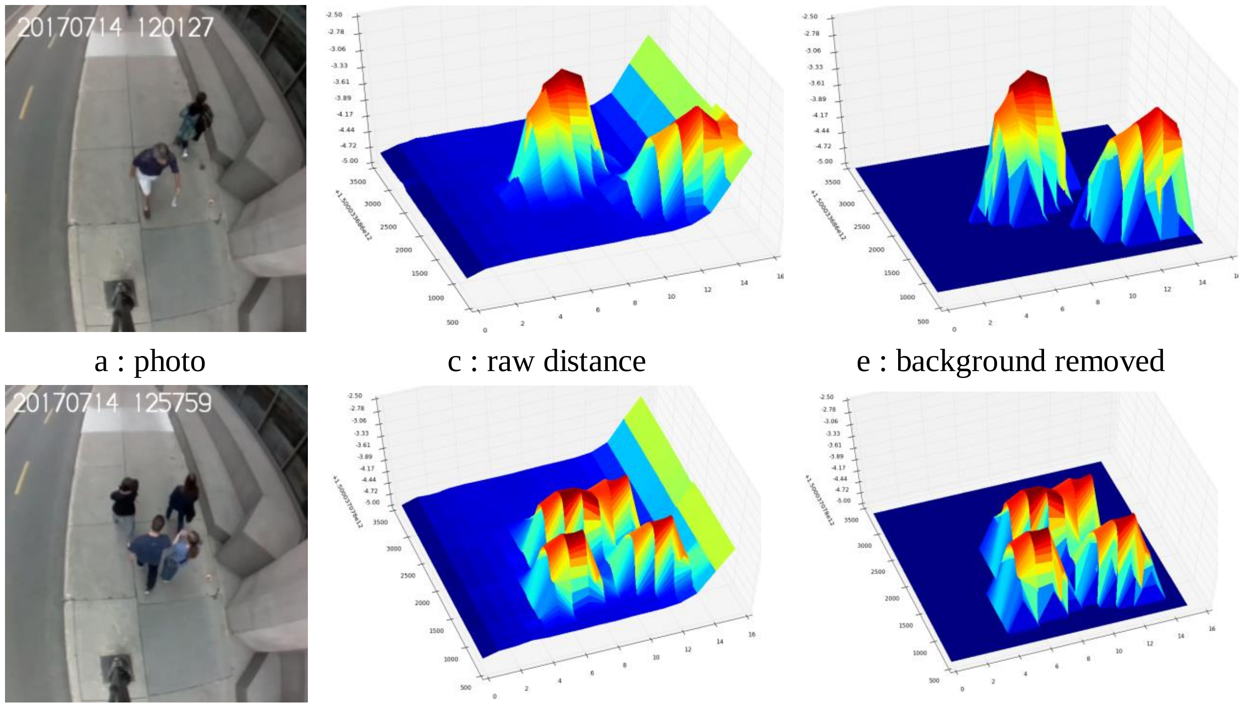

a : photo c : raw distance e : background removed

b : photo d : raw distance f : background removed

Figure 6-4. Site photos (a and b), the 3D plot of the raw distance data (c and d), and distance data with removed background (e and f)

In these two examples (Figure 6-4), the middle plots, (c and d), show the raw data (D_{tmp}) from the first detection of the object to the end of the Relax Time. Note that the wall on the right-side of the sidewalk has caused a sharp decrease in distance. Plots e and f show the same data after removing the background. The right-side plot in the first sample indicates two separate pedestrians. However, for the second example, the two pedestrians in the back are in close proximity to each other, thus their distance values are mixed and form one cluster. Circumstances in which pedestrians are in close proximity are challenging cases in counting applications.

6.5.5 Count Routine: Low-Resolution Clustering

A proposed sub-routine, called the *Low-Resolution Clustering (LRC)* routine, helps to cluster the D_{tmp} into sub-sets with a single pedestrian or group of pedestrians walking closely. The travel direction detection is the main reason for separating "*single cluster*" from "*grouped cluster*." The details of the steps are provided below:

Algorithm 2. **LRC routine**

1: Find local maximum points of the distance columns of $-\mathbf{D_{tmp}}$ as the peak of clusters (peak_local_max routine in Python),
2: Put cluster points at the local maximum points from previous points (ndimage.label in Python),
3: Find $\mathbf{labels}$ (a matrix of $\mathbf{n} \times \mathbf{16}$ label elements) of the different pedestrian clusters by applying the watershed algorithm to the distance columns of $\mathbf{D_{tmp}}$ (watershed routine in Python).

This routine starts with a peak detection algorithm, where the peak_local_max routine in Python, applied to the distance columns of -D_tmp, finds the candidate pixels representing the head of the pedestrian. Then the ndimage.label routine, also in Python, puts cluster labels at detected peaks. After that, the Watershed clustering algorithm is used to segment groups of pedestrians into different sub-clusters. The watershed transformation is a simplified image segmentation technique (Meyer 1994). Any grayscale image can be viewed as a topographic surface where high intensity denotes peaks and hills while low intensity denotes valleys. The idea or behind the watershed transformation is as follows. You start filling every isolated valley (local minima) with different colored liquid (labels). As the liquid rises, depending on the peaks (gradients) nearby, liquid from different valleys, with different colors, will start to merge. To avoid that, you build barriers in the locations where liquid merges. You continue the work of filling liquid and building barriers until all the peaks are under water. Then the barriers you created gives you the segmentation result.

The distance matrix is considered as a mono-color image and then Watershed segmentation is applied to it. The output, the labels matrix, is a matrix with the same size where the cells with zero values represent the background, and others show the clusters ID (pedestrian ID).

6.5.6 Count Routine: Width-Length Criteria

Width-Length Criteria determines whether the cluster corresponds to one pedestrian or to a group of people based on comparing *lengths* (number of time frames that an object is present at the coverage area) and *width* (number of pixels that object covers) of each cluster with predefined threshold values of 50 frame numbers and 5 pixels respectively. Then if at least one dimension of the cluster is larger than its threshold value, it is considered as the "*grouped object.*" Subsequently, those "*single object*" clusters are given to a direction detection algorithm, and those "*grouped* *object*” cluster are processed in another sub-routine called *High-Resolution Clustering* (HRC) for further analysis.

6.5.7 Count Routine: High-Resolution Clustering (HRC)

The peak detection algorithm implemented in the LRC routine uses a square-search window (same size in the pixel and the time axis). However, because of the low pixel resolution and high sampling rate of the sensor, the square search window can result in either detecting many noisy peaks for one object (when using a small size search window) or combining two objects if they are close to each other (when using a large size search window). The proposed *High-Resolution Clustering* (HRC) routine has the same steps as the LRC routine, but it uses a custom size for the search window. Since the HRC routine has more computing complexity, it is reasonable to perform the LRC first and then apply HRC to “grouped clusters” instead of the all detected objects.

The window size is defined based on monitoring some samples of the detected single and grouped clusters and plotting their distance patterns (based on looking at data and experimental parameter setting). The selected *length* of the search window (in the time axis) is equal to 25 rows. The size of this window is such that the two pedestrians walking back to back are not closer than 25 samples (with a 10 milliseconds sample-rate of the sensor, the gap period between two pedestrians will be equal to 0.25 second). The selected *width* (number of pixels) of the search window is based on at least one-pixel gap between the head of two pedestrians. This value is the minimum required gap for identifying the two separate objects. Therefore, the search window will be a rectangle with a size of 25×3. The *maximum_filter* toolbox (in *scipy.ndimage.filters* python library) provides a fast peak detection algorithm based on a customized window size. The summary of HRC routine is as follow:

Algorithm 3. **HRC Routine**

1: Define $\boldsymbol{Z_i}$ as the distance columns of $\boldsymbol{D_{tmp}}$, where $\boldsymbol{labels}$ is equal to the $\boldsymbol{i-th}$ candidate cluster

2: Find the local maximum mask of $\boldsymbol{Z_i}$ as the peak of the $\boldsymbol{i-th}$ cluster with a search window of $\boldsymbol{25 \times 3}$ by using maximum_filter in Python,

3: Apply morphological operation including the binary_erosion routine in Python and the logical AND to find the exact position of the eligible local maximum values, 4: Put cluster points at the eligible local maximum points from step 3 by using ndimage.label in Python and make the matker_HRC matrix,

5: Find $\boldsymbol{labels}$ of the different pedestrian cluster by applying the watershed algorithm to $(-\boldsymbol{Z_i})$ which is done by the watershed routine in Python.

First, the distance data of the $i-th$ candidate cluster (Z_i) is extracted from the clusters outputted by *Width-Length Criteria*. Then the *peak_local_max* routine in Python finds a local maximum mask with a search window of 25×3. After that, a set of morphological operations is applied to the obtained maximum mask to get the exact position of the maximum pixels representing the head of the pedestrians. The next (fourth) step is marking each peak and creating a labelled matrix called $markers\_HRC$. Then the *Watershed* algorithm does the second clustering by having the initial clustered data frame and the location of the peaks.

Figure 6-5 shows the outputs of the LRC and HRC routines for a given sample in detail. The first row shows the four different clusters formed by the LRC routine: two single pedestrian clusters (1 and 4) and two clusters with grouped pedestrians (2 and 3). Then the clusters with multiple pedestrians are given to the HRC routine. Plots in the 2nd and in the 4th rows show the outputs of the local maximum, binary erosion and peak detection algorithms respectively. Plots in the 3rd and 5th rows illustrate the sub-clusters formed by the HRC routine.

6.5.8 Direction Detection

The sensor installation, with an angle of θ (around 30°), creates specific distance patterns for pedestrians moving in different directions. Figure 6-6 presents two examples of distance patterns over space and time. When the object is moving from the left to the right (Figure 6-6.a), the distance values show the maximum value during t_1 (ground). When the head of the pedestrian arrives at the detection zone of the sensor at t_2, the distance value drops sharply to a minimum value. Once the object moves forward, the distance increases smoothly until the timestamp t_7, when the pedestrian leaves the detection zone. For the right to left direction, Figure 6-6.b is an example of an inverted pattern. Figure 6-6.c and Figure 6-6.d show real 3D examples of the distance patterns of two objects in opposite directions over time.


Site Snapshot

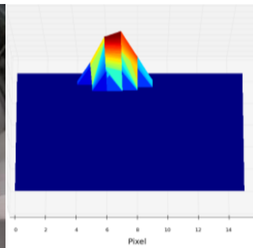
1st LRC single cluster

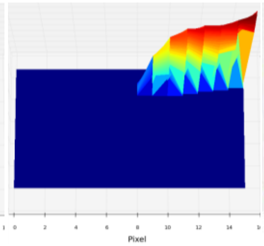
2nd LRC grouped cluster

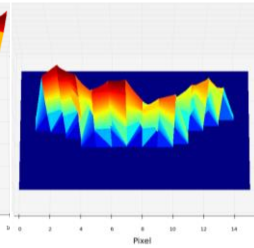
3rd LRC grouped cluster

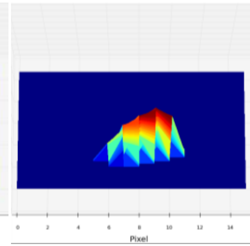
4th LRC single cluster

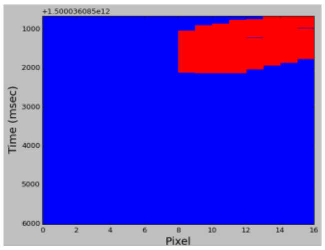
2nd LRC cluster – maximum filter

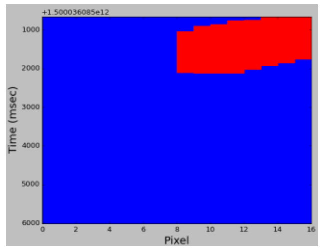
2nd LRC cluster – morphological erosion

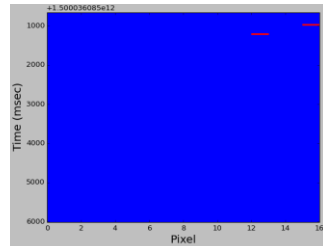
2nd LRC cluster – peaks

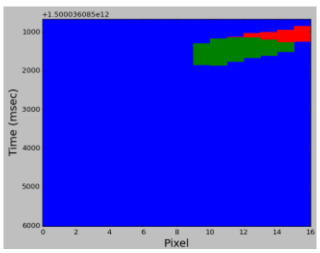
HRC output of 2nd LRC cluster

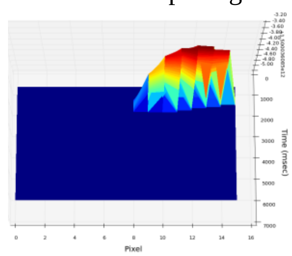
1st HRC sub-cluster of 2nd LRC cluster

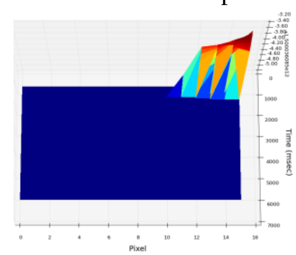
2nd HRC sub-cluster of 2nd LRC cluster

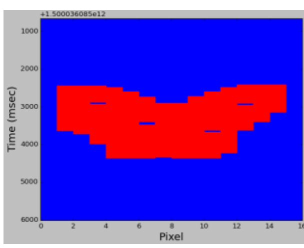
3rd LRC cluster – maximum filter

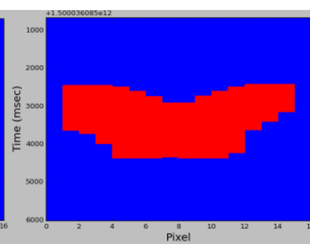
3rd LRC cluster – morphological erosion

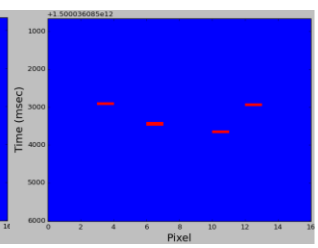
3rd LRC cluster – peaks

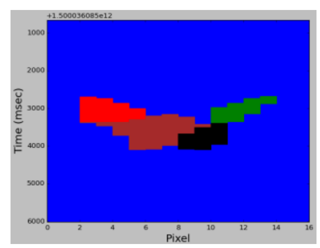
HRC output of 3rd LRC cluster

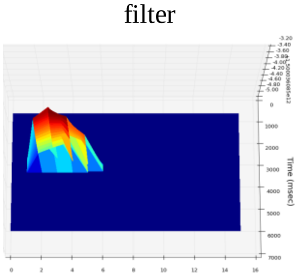
1st HRC sub-cluster of 3rd LRC cluster

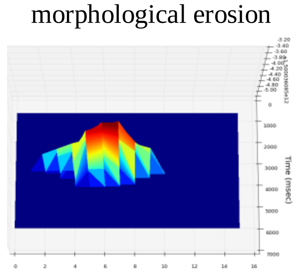
2nd HRC sub-cluster of 3rd LRC cluster

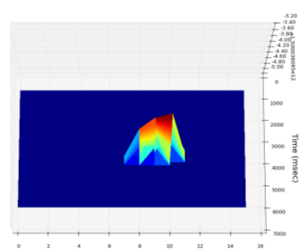
3rd HRC sub-cluster of 3rd LRC cluster

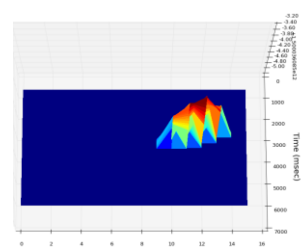
4th HRC sub-cluster of 3rd LRC cluster

Figure 6-5. The detailed output of the LRC and HRC routines (8 pedestrians)

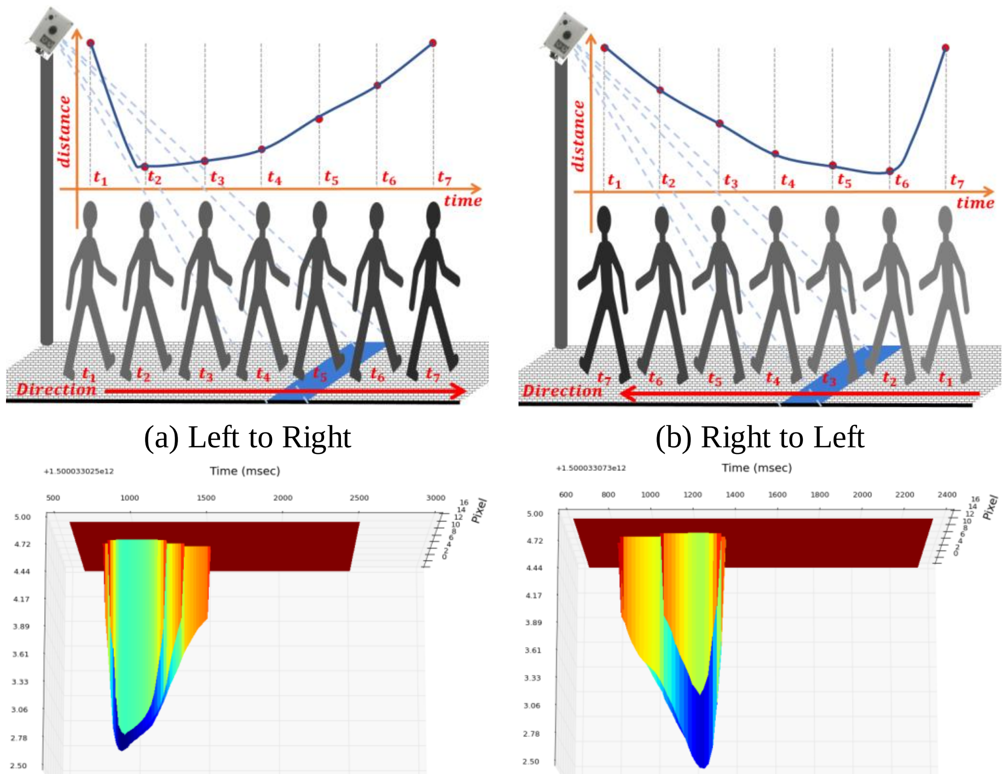

(a) Left to Right (b) Right to Left

(c) sensor data (L to R) (d) sensor data (R to L)

Figure 6-6. Distance patterns for two different directions

Based on the described patterns, three different measures are used to identify the direction of the object:

1. $count_p$ and $count_n$ - the number of positive and negative slopes at each column (pixel),
2. ave_p and ave_n - the average of the positive and the negative slopes,
3. $index\_peak$ and $center$ - the location of the detected cluster peak in comparison to the center of the cluster. Note that in the provided sample, for the left to right, $index\_peak$ is equal to 2 and $center$ is equal to 4.

For the "*single object*" clusters, comparing the positions of the center and the peak in a specific pixel that peak has been detected at, can accurately identify the direction:

- $if\ center < index\_peak$:
- $direction = LR = Left\ to\ Right$
- $elif\ center > index\_peak$:

- $direction = RL = \ Right\ to\ left$

For "*grouped object*" clusters and in some cases people who are walking closely in a group, the shape of the detected cluster by the HRC routine might be distorted. Therefore, the following steps have been used to identify the direction of each sub-cluster:

- $if\ count_p > count_n: direction = LR;\ else: direction = RL$
- $if\ ave_p < ave_n: direction = LR; else: direction = RL$
- $if\ center < index_{peak}: direction = LR; else: direction = RL$

The column which the cluster peak exists ($index\_peak$) and left and right columns of it is used to estimate the direction. For each of these three columns, three different direction criteria are used. Therefore, there are nine different directions for each cluster, and the most repeated direction is assigned as the final cluster direction.

6.6 SYSTEM PERFORMANCE EVALUATION

This section discusses the performance of the system. The sensor was installed at two different sidewalks in Montreal (near McGill University campus): I) sidewalk of the Robert-Bourassa Boulevard (between Sherbrooke Street and Milton street); II) sidewalk of Milton Street (between University street and Aylmer street). For the second location, the sensor was installed close to a controlled intersection with traffic lights at the entrance of McGill University. Therefore, at the beginning of the green phase, a high volume of pedestrians passes through the coverage area and makes it a complicated condition for counting multiple pedestrians. Table 6-1 summarizes the information about the facilities and the overall outcomes of the developed system. The duration of data collection was 4 hours and 21 minutes for the first site and 4 hours and 1 minute for the second site. Both sites had a high volume of pedestrians at the periods of installation.

For the evaluation of the proposed system, aggregate and disaggregate error measures have been calculated. The aggregate error compares the total number of pedestrians counted by the sensor with the observed (ground truth) pedestrians in the video. In the aggregate error, the over-counting and the under-counting errors can cancel out. The disaggregate error evaluates the detection of pedestrians individually. Based on these two concepts several error measurements can be derived from the manual and automatic counts.

Accuracy or the True Positive Rate (TPR) is calculated by dividing the total number of correct counts by the total manual counts. Precision is the ratio of the total correct counts to the total sensor counts. Under-counting and over-counting errors are the ratios of a number of falsely rejected (negative) counts and falsely accepted (positive) counts to total manual counts, respectively. Finally, direction error is the ratio of total false direction detection to total manual counts.

Testing results for the 2 locations are reported in Table 1. In the first site, the manual count is equal to 1,585. The developed sensor reported 1,553 pedestrians, with 1,543 being correctly counted, 10 (0.64%) being over-counted, and 42 (2.6%) being under-counted. It incorrectly reported the direction of 17 pedestrians (1.07%). Similar results were obtained in the second location, where the manual count was equal to 3578 pedestrians. The second facility was more crowded and challenging than the first one. However, the proposed system reported 3,555 pedestrians, with 3,532 being correctly counted, 23 (0.65%) being over-counted, and 46 (1.29%) being under-counted. It incorrectly reported the direction of only 19 pedestrians (0.5%).

The accuracy of the proposed system is 97.4% and 98.7% for the first and the second facility respectively. Furthermore, its precision also suggests high performance and has a value of 99.4% for the first location and 98.7% for the second location. These two measures illustrate the promising results of the proposed system.

Table 6-1 also assesses the overall performance of the system by considering the over-count, under-count, and direction detection errors in 15-minute time intervals and for different directions. Three error measures have been calculated including the *Average Percentage Deviation* (ADP), average of the over and under-counting errors, the *Average Absolute Percentage Deviation* (AADP), the average of absolute value of false alarms and rejections, and the *Weighted AAPD* (WAAPD) where the weights are ratios of the pedestrian volume in 15-minute intervals to the total value. WAAPD gives importance to the time-intervals with higher pedestrian volume. The negative APD values show that the under-counting is the primary source of error. However, some over-counting errors diminish the effects of the under-counting. The total AAPD is 4.3% and 1.6% for the first and second sidewalks respectively.

Table 6-1. Summary of results for both facilities

<table>
<tr><td>Sites:</td><td colspan="3">Robert-Bourassa Boulevard</td><td colspan="3">Milton</td></tr>
<tr><td>Start Time</td><td colspan="3">11:45:21</td><td colspan="3">14:22:35</td></tr>
<tr><td>End Time</td><td colspan="3">16:06:48</td><td colspan="3">18:23:42</td></tr>
<tr><td>Total Duration (hours)</td><td colspan="3">04:21:27</td><td colspan="3">04:01:07</td></tr>
<tr><td>Sidewalk Width (meters)</td><td colspan="3">4</td><td colspan="3">3</td></tr>
<tr><td>Device Mounting Height (meters)</td><td colspan="3">4</td><td colspan="3">4</td></tr>
<tr><td colspan="7">Counts</td></tr>
<tr><td>Manual Counts (Ground Truth)</td><td colspan="3">1585</td><td colspan="3">3578</td></tr>
<tr><td>Sensor Counts (True Positive+ False Positive)</td><td colspan="3">1553</td><td colspan="3">3555</td></tr>
<tr><td>Correct Sensor Count (True Positive)</td><td colspan="3">1543</td><td colspan="3">3532</td></tr>
<tr><td>Sensor Over Count (False Positive)</td><td colspan="3">10</td><td colspan="3">23</td></tr>
<tr><td>Sensor Under Count (False Negative)</td><td colspan="3">42</td><td colspan="3">46</td></tr>
<tr><td>Sensor Direction Error</td><td colspan="3">17</td><td colspan="3">19</td></tr>
<tr><td colspan="7">Errors Measures</td></tr>
<tr><td>Accuracy (True Positive Rate)</td><td colspan="3">97.35%</td><td colspan="3">98.71%</td></tr>
<tr><td>Precision (Positive Predictive Value)</td><td colspan="3">99.36%</td><td colspan="3">99.35%</td></tr>
<tr><td>Aggregated Error</td><td colspan="3">2.02%</td><td colspan="3">0.64%</td></tr>
<tr><td>Under Counting Error (False Negative Rate)</td><td colspan="3">2.65%</td><td colspan="3">1.29%</td></tr>
<tr><td>Over Count Error (False Discovery Rate)</td><td colspan="3">0.64%</td><td colspan="3">0.65%</td></tr>
<tr><td>Direction Error</td><td colspan="3">1.07%</td><td colspan="3">0.53%</td></tr>
<tr><td colspan="7">Detail Direction Error</td></tr>
<tr><td>Direction</td><td>L-R[1]</td><td>R-L[2]</td><td>Total</td><td>L-R</td><td>R-L</td><td>Total</td></tr>
<tr><td>Average Percentage Deviation (APD)</td><td>-2.5%</td><td>-5.8%</td><td>-4.0%</td><td>-1.7%</td><td>-1.3%</td><td>-1.5%</td></tr>
<tr><td>Average Absolute Percentage Deviation (AAPD)</td><td>3.6%</td><td>5.8%</td><td>4.3%</td><td>2.1%</td><td>1.3%</td><td>1.6%</td></tr>
<tr><td>Weighted (WAAPD)</td><td>3.0%</td><td>4.8%</td><td>3.5%</td><td>1.9%</td><td>1.1%</td><td>1.5%</td></tr>
<tr><td colspan="7">1. L-R: Left to Right
2. R-L: Right to Left</td></tr>
</table>

Figure 6-7.a and Figure 6-7.b show the match between manual and automatic counting results during several time intervals and different directions for both sidewalks. In Figure 6-7.a, there is an increase in the error between 14:30:00 and 15:30:00. By reviewing the provided video footages of this period, it turned out that rainfall had occurred in that time and most of the pedestrians were carrying an umbrella, and for those people that used a shared umbrella, the sensor counted one

pedestrian. In Figure 6-7 (b), for time intervals between 14:30:00 and 15:30:00, the error is slightly more than the other intervals. By reviewing video footage, it was evident that there are some situations where two large groups of pedestrians are passing in different directions simultaneously. However, there were several situations where pedestrians were walking opposite each other simultaneously, and the sensor was able to detect their direction correctly and simultaneously.

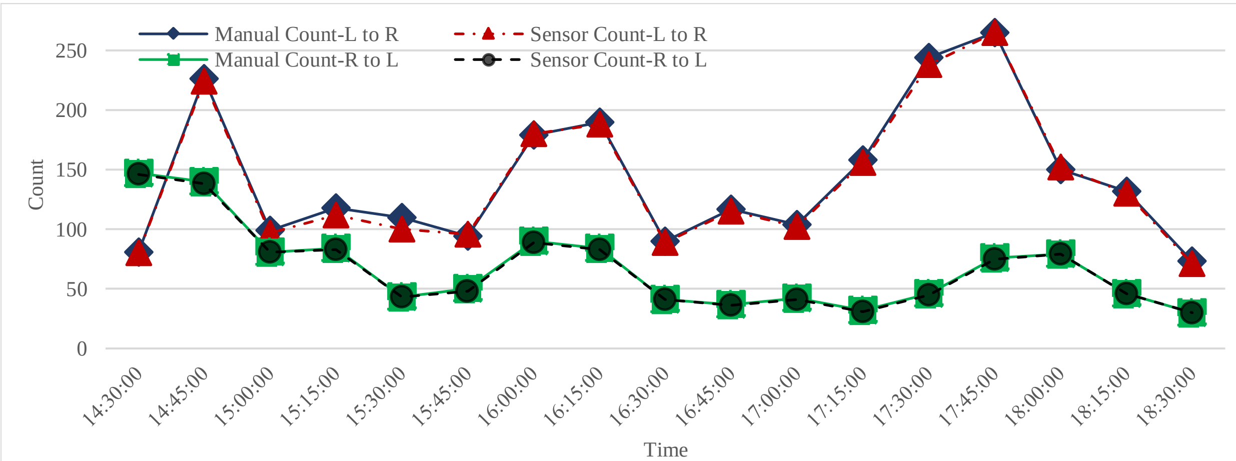

(a) Sidewalk of the Robert-Bourassa Boulevard

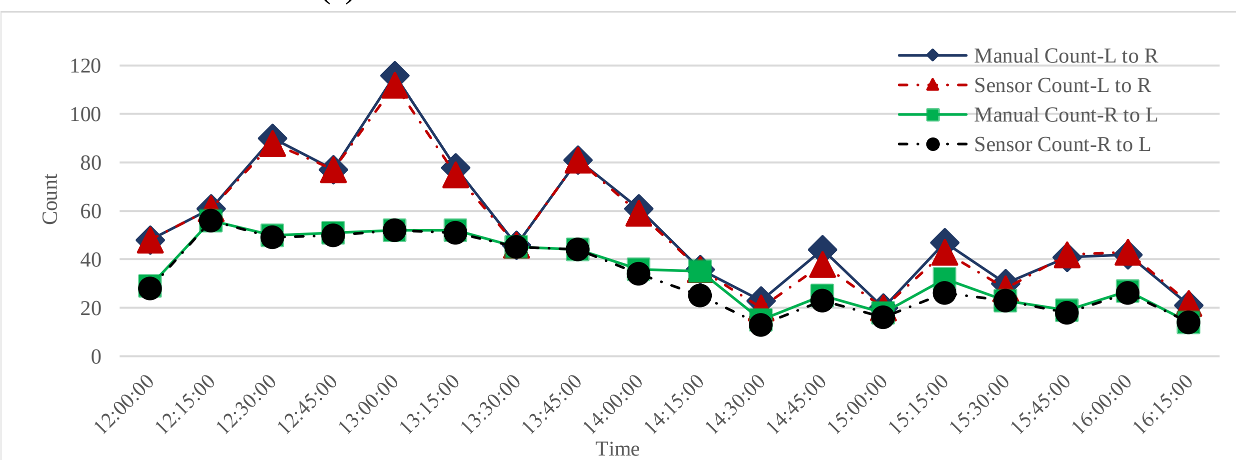

(b) Sidewalk of the Milton Street

Figure 6-7. Manual and Sensor Counts in 15-minutes Time Intervals

6.7 CONCLUSION AND FUTURE WORK

This work reports the development and testing of a Lidar-based real-time pedestrian counting system. The system is based on a sixteen-laser channel sensor measuring the distance to objects every 20 milliseconds. First, the background-removal routine filters out the distances with respect to the background and gives the distances to the foreground objects. Then, two proposed clustering routines named LRC and HRC are implemented providing single and group clusters, and counts. Finally, the direction identification algorithm helps determine the direction of travel for each individual pedestrian. Among other advantages, the proposed directional pedestrian counting system operates in real time and different weather conditions. Algorithms require minimum calibration and no training. The system can also handle occlusion and high volume conditions. This highly accurate pedestrian monitoring system would be useful in a variety of transportation applications such as network planning and management, safety analysis, traffic light optimization, pedestrian warning system (smart pedestrian signs), etc.

As part of this work, the performance of the system is evaluated at two different counting locations (sidewalks) by comparing sensor counts and manual counts from video data at aggregate and disaggregate (15-min interval) levels. These sidewalks are close to McGill University and have high pedestrian flows, with people traveling in dense groups.

Among other results, the disaggregate accuracy of the system was 97.4% and 98.7% for the first and second sidewalks respectively. Over-counting errors for both sites were 0.7%, and under-counting errors were 2.7% and 1.3%, respectively. Additionally, considering the direction detection error along with under-counting and over-counting, results show an APD of -4% and -1.5%, and an AAPD of 4.3% and 1.6% for the first and second counting locations.

The validation results of the system show the first promising application of 2D Lidar technology for monitoring pedestrian facilities. Its accuracy in real-time monitoring is high compared to other solutions available on the market, such as camera-based systems, which are expensive and very sensitive to lighting condition and infrared-based (or side-based) technology which has low counting accuracy due to occlusion.

The developed system can be easily installed and requires a simple calibration process. However, it has some limitation, including the coverage area. For covering wider sidewalks, it is necessary to increase the height of installation. However, this will cause the horizontal resolution to be degraded and, thus, pedestrians that are passing between beams may not be detected. Using a 2D Lidar sensor with a higher number of channels can address this limitation. Pedestrians that carry an umbrella and other items that cover multiple individuals results in under-counting. This limitation which has been observed and reported in this paper seems to be one of the challenges for all pedestrian counting systems that are installed above a facility. Another limitation is the detection of children when they are close to an adult. Their distance pattern will be entirely mixed with that of the adult and make it difficult to detect and count them separately.

In future work, the proposed system will be tested on more pedestrian facilities. The proposed data analysis will be applied to bike facilities to count the number of cyclists, and eventually to mixed mode applications with classification capability where pedestrian and cyclists have a shared facility. Higher 2D resolution Lidar sensors will be also tested in different environments.

6.8 REFERENCES

Board, T.R., National Academies of Sciences, E. and Medicine (2017) Methods and Technologies for Pedestrian and Bicycle Volume Data Collection: Phase 2, The National Academies Press, Washington, DC.

De Silva, V., Roche, J. and Kondoz, A. (2018) Fusion of Lidar and camera sensor data for environment sensing in driverless vehicles.

FHWA (2016) Federal Highway Administration, US Department of Transportation, October 2016.

Fu, T., Stipancic, J., Zangenehpour, S., Miranda-Moreno, L. and Saunier, N. (2017) Automatic traffic data collection under varying lighting and temperature conditions in multimodal environments: thermal versus visible spectrum video-based systems. Journal of advanced transportation 2017.

Greene-Roesel, R., Diogenes, M.C., Ragland, D.R. and Lindau, L.A. (2008) Effectiveness of a commercially available automated pedestrian counting device in urban environments: Comparison with manual counts.

Guan, H., Li, J., Yu, Y., Chapman, M. and Wang, C. (2015) Automated road information extraction from mobile laser scanning data. IEEE Transactions on Intelligent Transportation Systems 16(1), 194-205.

Hyde-Wright, A. and Krista Nordback PHD, P. (2014) Counting bicyclists with pneumatic tube counters on shared roadways. Institute of Transportation Engineers. ITE Journal 84(2), 32.

Lesani, A., Miranda-Moreno, L.F., Fu, T. and Romancyshyn, T. (2015) Development and Testing of an Ultrasonic-Based Pedestrian Counting System.

Leykin, A. and Hammoud, R. (2006) Robust multi-pedestrian tracking in thermal-visible surveillance videos, pp. 136-136, IEEE.

Li, S., Sayed, T., Zaki, M., Mori, G., Stefanus, F., Khanloo, B. and Saunier, N. (2012) Automated collection of pedestrian data through computer vision techniques. Transportation Research Record: Journal of the Transportation Research Board (2299), 121-127.

Meyer, F. (1994) Topographic distance and watershed lines. Signal processing 38(1), 113-125.

NCHRP National Cooperative Highway Research Program Report, Transportation Research Board.

Nordback, K., Kothuri, S., Phillips, T., Gorecki, C. and Figliozzi, M. (2016) Accuracy of bicycle counting with pneumatic tubes in Oregon. Transportation Research Record: Journal of the Transportation Research Board (2593), 8-17.

Nordback, K., Piatkowski, D.P., Janson, B.N., Marshall, W.E., Krizek, K.J. and Main, D.S. (2011) Using inductive loops to count bicycles in mixed traffic. Journal of Transportation of the Institute of Transportation Engineers.

Pacala, A. and Eldada, L. (2017) Three-dimensional lidar sensor based on two-dimensional scanning of one-dimensional optical emitter and method of using same, Google Patents.

Pu, S. and Vosselman, G. (2009) Knowledge based reconstruction of building models from terrestrial laser scanning data. ISPRS Journal of Photogrammetry and Remote Sensing 64(6), 575-584.

Pucher, J. and Buehler, R. (2017) Cycling towards a more sustainable transport future, Taylor & Francis.

Pucher, J., Buehler, R. and Seinen, M. (2011) Bicycling renaissance in North America? An update and re-appraisal of cycling trends and policies. Transportation Research Part A: Policy and Practice 45(6), 451-475.

Ryus, P., Ferguson, E., Laustsen, K.M., Prouix, F.R., Schneider, R.J., Hull, T. and Miranda-Moreno, L. (2014) Methods and technologies for pedestrian and bicycle volume data collection, Citeseer.

Tarko, A., Romero, M., Ariyur, K., Bandaru, V. and Lizarazo, C. (2018) Detecting and tracking vehicles, pedestrians, and bicyclists at intersections with a stationary Lidar, Statens väg-och transportforskningsinstitut.

Ussery, E.N., Carlson, S.A., Whitfield, G.P., Watson, K.B., Berrigan, D. and Fulton, J.E. (2018) Transportation and Leisure Walking Among US Adults: Trends in Reported Prevalence and Volume, National Health Interview Survey 2005–2015. American journal of preventive medicine 55(4), 533-540.

Yan, W.Y., Shaker, A. and El-Ashmawy, N. (2015) Urban land cover classification using airborne Lidar data: A review. Remote Sensing of Environment 158, 295-310.

Zangenehpour, S., Miranda-Moreno, L.F. and Saunier, N. (2015) Automated classification based on video data at intersections with heavy pedestrian and bicycle traffic: Methodology and application. Transportation Research Part C: Emerging Technologies 56, 161-176.

Chapter 7: Conclusion and Future Work

7.1 GENERAL CONCLUSION

With a significant growth of the cities and the issues related to urban mobility and the environment, local governments are constantly looking for solutions to improve the urban mobility of their citizens. There are recent initiatives to build smart-city or ITS platforms, which monitor the network with an array of sensors, collect and centralize the data on cloud systems, and analyze them. ITS is considered to be the main part of smart city initiatives that can help with congestion and all the related issues. In this context, there is great attention from governments and policymakers into encouraging active (or non-motorized) mobility, as a sustainable solution to deal with the negative impacts of the car-oriented mobility (e.g., traffic congestion, climate change, and air pollution issues). Considering pedestrian and cyclists as the main part of active mobility, the need for monitoring their activity is also crucial. Therefore, smart transportation systems require multi-sensory, multi-mode monitoring system to collect necessary information.

In this research, we develop a set of automated real-time solutions that can work independently or can be integrated into a platform to monitor multimodal traffic networks, in particular, non-motorized modes, and generate information such as travel time (speeds) and volumes in bicycle and pedestrian environments. More specifically the proposed solutions include two types of systems, a between-point monitoring system using WiFi and BT technologies and fixed-point systems using Lidar technology. Our solutions support different types of wired and wireless communication protocols including short range (Bluetooth), medium range (WiFi), long range and low power consumption (LoRA) and to cloud connection over LTE networks. These protocols provide flexibility to embed our solutions to any smart city and IoT platforms with minimum modification. Also, the designed sensors are non-intrusive with minimum calibration requirements and can be used for either short-term or long-term data collections.

Our developed WiFi-Bluetooth scanning system was presented in Chapter 3 along with its testing in a network with two modes, pedestrians, and cyclists. A framework for classifying the objects and extrapolating the pedestrian volume from WiFi traces was developed. Four different classifiers were calibrated and tested, ranging from simple classifiers based on speed threshold values to more complex classifiers using fused-statistical logit models. The average error percentages using logit models with speed data and time-seen (separate models) as variables were 14% and 16%, respectively. However, with a combined model, including both speed and time-seen duration, the method showed much better results with an average classification error percentage of 3.7%. Additionally, the use of WiFi traces to extrapolate pedestrian flow was explored. The results show, with a simple developed extrapolation function, the flow estimated by WiFi traces could accurately track the pattern of the pedestrian flow coming from manual counts. As part of this work, the performance of the two technologies (Bluetooth and WiFi) was compared in terms of detection rates. From this, it was concluded that Bluetooth technology underperforms in non-motorized transportation networks; with WiFi technology being the most appropriate for monitoring networks with low-speeds. Since the main goal of this thesis was developing systems applicable in the multi-modal traffic network, the use of the developed WiFi-Bluetooth system was extended to the vehicular traffic network. Despite the low detection rate of Bluetooth technology in non-motorized networks, the literature shows this technology can provide accurate information about the traffic patterns in vehicular networks. The low detection rate of Bluetooth technology in the non-motorized network indicates that most of the detected Bluetooth devices in a mixed network (pedestrian, cyclist and vehicles) can be associated with vehicles. This could lead to the development of monitoring systems that take the best of the two technologies by computing vehicle (travel times) metrics using Bluetooth data, and, then use WiFi traces for other modes. The next step was to test the performance of the WiFi-Bluetooth scanner in monitoring traffic in the vehicular network.

In Chapter 4 the work was extended to arterial traffic monitoring. The initial findings show that the detection rates of WiFi technology are higher than Bluetooth. However, when just one pair of sensors is considered for analysis, the Bluetooth technology captures more trips between two sensors. This finding comes from the fact that WiFi devices are discoverable when they are broadcasting probe signals, and it happens randomly between one to two-minute intervals. In this case, if the device passes any sensor outside of broadcasting interval, the devices are not detected. Implementing a network of sensors can help to solve this issue. On the other hand, when the Bluetooth is in discoverable mode, it is very likely that any sensor in the network can capture it.

Finally, the combination of the two technologies could help in increasing the precision of the travel time (speed) estimates. Analysis on travel time estimation using two technologies, considering a pair of sensors shows an average speed estimation error of 8.6 %, 11.1 %, and 5.8 % for Bluetooth, WiFi, and the mixed system, respectively. When comparing Bluetooth with WiFi data, it is observed that more accurate travel time estimations are obtained - because of the higher detection rate of Bluetooth when just one pair of sensors is used and because the Bluetooth data has less noise.

The importance of between-point monitoring systems in multi-modal traffic networks was shown in chapters 3 and 4. However, automated counting technologies are also a key element of an integrated monitoring system for non-motorized transportation. Much more attention has been directed towards motorized counting technologies with less focus in non-motorized monitoring systems. In chapter 5 and 6, we developed two innovative solutions to count the number of pedestrians and cyclists in non-motorized facilities. In Chapter 5, a new monitoring solution is proposed using a single beam (1D) Lidar technology to accurately count pedestrians or cyclists, and measure each road-user direction, in different environments. The current solutions for counting pedestrians or cyclists are either expensive to implement on large scale or suffer from low accuracy. The main cyclist is counting solutions, including loop detectors, need to be embedded in the pavement, which increases maintenance and installation costs and is not suitable for temporary data collection. The infrared-based pedestrian counting also suffers from low accuracy on high volume facilities and has specific installation requirements.

To address the main issues with current technological solutions, our proposed solution benefits from Laser-based range finding sensors to measure the distance to the objects with narrow beams which helps to resolve the occlusion problem in many cases. The high sample rate of a Lidar sensor helps to accurately count the objects and identify the direction. Furthermore, the system maintains high accuracy on high-volume facilities. With the proposed solution, the detection area is adjustable by the sensor user, which provides flexibility over infrared-based solutions. Also, the low power consumption design of the system can help collect data for more than two weeks on a single battery charge.

The sensor has been tested in different traffic conditions and non-motorized traffic facilities. The results show that in 80% of 15-min automated counting samples, the error was between 0-5% and 0-2% for pedestrian and cyclists counting respectively. Despite the performance of the single beam Lidar, it was observed that in conditions with very high pedestrian volumes, the occlusion problem of pedestrians walking in groups and side by side, can cause a drop in system accuracy.

To address this issue in more congested pedestrian networks, a novel technology is proposed in Chapter 6 based on a 2-dimensional Lidar system. The details of the developed systems are provided in this Chapter along with the results of the test. This solution is designed to be installed in available posts to monitor the area from above. It helps easily resolve the occlusion problem when the facility is very congested and wide. Using, 2D-Lidar technology, the shape of the objects can be constructed accurately. This feature helps classify road users in mixed networks. The results show that the proposed system has accurately counted more than 97% of people at the disaggregated level, with less than 1.1% direction identification error. The results reveal that the over-count error is less than 0.7%, and the counter had missed 1.3% and 2.7% of pedestrians for two selected sites (undercount error). At the aggregated level (15-minutes intervals), the average absolute percentage deviations (AADP) are 1.6% and 4.3% with a weighted AAPD of 1.5% and 3.5% for the selected sidewalks. The higher power consumption of the system is a limitation of the proposed solution which requires either solar panel or access to the City power grid for long term data collection.

7.2 FUTURE WORK

In our case studies, the WiFi-Bluetooth sensor can be used in pedestrian cyclists facilities or vehicular networks. As part of the future work, the sensor can be used in multi-modal traffic networks with pedestrian, bicycle and vehicle flows. In that case, the classification framework needs to be extended to cover all modes. A mode-classification based on Bluetooth data on a mixed network can help to extend our WiFi-based classifier for networks with pedestrians, cyclists and vehicles.

The use of the wireless received signal strength indicator (RSSI) could be also investigated as an extra source of information for classification purposes in complex networks. The study also shows the potential of using WiFi traces for flow estimation purposes. However, more complex estimation models could improve the accuracy of the system estimates.

A single beam Lidar sensor has been tested to count the directional flow of pedestrians and cyclists. The evaluation results show a high correlation between the count results and the ground truth flow. As a future work, a non-linear correction factor could be investigated to improve the accuracy of pedestrian counting systems in a high pedestrian volume. Also as a part of the future work, speed/density estimation features can be added to the counting system. This could help study the level of service of bike facilities and generate flow-speed-density curves. The sensor can also be used to implement green waves on bike facilities using estimates of the gaps between cyclists in real-time and feed this information to traffic light controllers.

The findings on 2D based solution show the shape of the object can be extracted accurately. This feature could be used for classification of the object and extend the application to mixed mode networks including vehicular traffic. 3D Lidar solutions could be also investigated for very complex networks. This solution would provide more details about the objects in both vertical and horizontal views.

7.3 PUBLICATIONS

7.3.1 Referred Journals and Patent Applications

Asad Lesani, Luis Miranda-Moreno, “Development and Testing of a Real-Time WiFi-Bluetooth System for Pedestrian Network Monitoring, Classification and Data Extrapolation”, IEEE Transactions on Intelligent Transportation Systems.

Asad Lesani, Ehsan Nateghinia, Luis Miranda-Moreno, “Designing a 2D Lidar Based Real-Time Pedestrian Counting System for High-Volume Conditions”, to be submitted for publication Transportation Research Part C: Emerging Technologies.

Asad Lesani, Luis Miranda Moreno, “Pedestrian/cyclists counting system using Lidar technology”, Patent application, Disclosure Number D2018-0070

7.3.2 Conference Papers

Asad Lesani, Ehsan Nateghinia, Luis Miranda-Moreno, "*Development and Evaluation of a 2D Lidar Real-Time Pedestrian Counting System for High-Volume Conditions*" , 97th Annual Meeting of the Transportation Research Board.

Asad Lesani, Anthony Andreoli, Luis F. Miranda-Moreno, "*Development and Testing of an Laser-Based Automated Pedestrian/Cyclist Counting System"*, 96th Annual Meeting of the Transportation Research Board.

Taras Romancyshyn, Asad Lesani, Luis F. Miranda-Moreno, "*Monitoring Signalized Intersection Performance with Bluetooth and Wifi Duration Data"*, 96th Annual Meeting of the Transportation Research Board

Asad Lesani, Luis F. Miranda-Moreno, "*Development and Testing of a Real-Time WiFi-Bluetooth System for Pedestrian Network Monitoring and Data Extrapolation"*, 95th Annual Meeting of the Transportation Research Board, January 2016

Asad Lesani, Taras Romancyshyn, Luis F. Miranda-Moreno, "*Arterial Traffic Monitoring Using an Integrated WiFi-Bluetooth System"*, 95th Annual Meeting of the Transportation Research Board, January 2016

Taras Romancyshyn, Asad Lesani, Luis F. Miranda-Moreno, *"The Effect of Weather on Travel Speed from Bluetooth Sensor Data"*, 95th Annual Meeting of the Transportation Research Board, January 2016

Asad Lesani, Luis F. Miranda-Moreno, Ting Fu, Taras Romancyshyn, *"Development and Testing of an Ultrasonic-Based Pedestrian Counting System",* 94th Annual Meeting of the Transportation Research Board, January 2015

Stewart Jackson, Asad Lesani, Luis Miranda-Moreno, *"Towards a WIFI system for traffic monitoring in different transportation facilities", 93rd Annual Meeting of the Transportation Research Board, January 2014*

Appendix A

As a part of this research, the authors have developed and tested a pedestrian counter based on Ultrasound technology. This initiative was an attempt to address the shortcomings of the current commercial counting solutions[3].

This section provides some information about the sensor hardware and software components and some test results. In the end, we briefly discuss why authors replace Ultrasonic sensors with Lidar technology as the range finder sensor in their solution.

The design of the sensor involves two aspects: hardware design and software design. Hardware design includes integrating all necessary elements to have a real-time automated pedestrian counting system. The methodology of how pedestrian counts can be obtained from the raw output of the ultrasonic sensor is described in the software design section.

A.1 HARDWARE DESIGN

The hardware of the designed system consists of three different parts: a sensory system, a microprocessor (which is the core of the system) and a robust data logger system. All of the three different parts are explained in this subsection.

A.1.1 Sensory System

An ultrasonic sensor is used to measure the distance between the sensor and passing objects. The ultrasonic sensor works based on the concept of ultrasound wave speed in the air. The sensor transmits an ultrasound wave in the air for a predefined time (around 5 microseconds) and then listens to the echo of the wave. Based on the transmitting and receiving time difference and knowing the speed of a sound wave in the air, the distance between objects can be measured.

The ultrasonic sensor has some advantages in comparison with other technologies in the market designed to measure distance. In particular, the transmitter and receiver of the ultrasonic sensor can be mounted on the same board. Also, because the ultrasound wave is independent of weather

[3] for more detailed review on the current available solutions refer to chapters 1,2 and 5

condition and environment light, the accuracy of the measurement should be reliable regardless of the weather conditions even in hot and sunny summer days; the condition that affects the performance of the infrared-based sensors the most.

A.1.2 Microprocessor

The microprocessor is the most important part of the system hardware. The microprocessor can be programmed in some programming languages. In this project, an AVR based micro-controller is used to implement the pedestrian counting methodology and interface all other parts of the system. Additionally, the pedestrian counting method can be relatively easily implemented with this type of micro-controller.

A.1.3 Data Logger

The data logger consists of the following parts:

- Real Time Clock Module, to keep the data time stamped
- GSM modem, to keep the system working in real-time and send data to the server every 15 minutes
- SD card, to save all the data on an SD card in case the GSM modem internet connection is lost

It is worth mentioning that once the system components are built, they are integrated into a solid water-proof enclosure. Figure 7-1.a provides a picture of the system hardware. Moreover, Figure 7-1.b shows the sensor with the enclosure installed at one of the testing sites.

a) System hardware   b) Installation infrared and ultrasonic

Figure 7-1. Pictures of the System

A.2 SOFTWARE DESIGN

The methodology and necessary steps to implement an automated pedestrian counting are described in this section.

A.2.1 Distance Measurement

In this step, the microcontroller actuates the ultrasonic sensor to send the ultrasound wave to the environment for a duration of 5 microseconds. After this time, the processor listens for the echo of the ultrasound wave and based on the time difference between transmitting and receiving the ultrasound wave and its speed, the distance between the sensor and a passing object is measured.

A.2.2 Noise Reduction Measurement

In some cases, the ultrasonic sensor cannot get the ultrasound wave echo of the object in the meantime. Therefore, the distance to the object is measured as the maximum range of the sensor (e.g., 3. meters for this sensor, it can be changed by the user such as to cover a limited area like at crosswalks). To solve this issue, an algorithm is required to eliminate this noise from the output of the system. The one used in this system is based on the moving average concept. At first, a window of samples is defined and used to calculate the average of samples within that window. The window size is defined considering the sample rate, pedestrians average speed, and their body width (from trial and error; the 5 last samples were considered). The algorithm replaces the noisy data at each window with the minimum value of the samples within that window. Figure 7-2 shows a simplified example of noisy data and the output from the noise reduction technique.

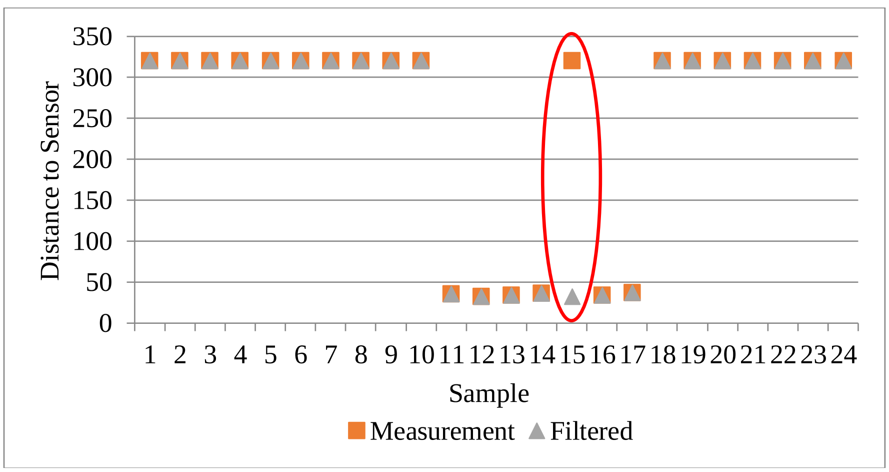

Figure 7-2. Noisy Distance Measurement and Filtered Data

A.2.3 Object Detection

The distance measurements is then classified based on the distance thresholds. When the processor gets a new measurement it checks the distance value with the value of the last sample. If the difference is more than the predefined threshold (e.g., 35 cm), then a new class of distance is started. The mentioned threshold was considered based on the average body width of the people. If a smaller value is obtained, things like bags, or even a moving hand of a person can be considered as a new group. On the other hand, if it is considered to be bigger, two people passing in parallel will be underestimated.

When a new distance group is started, then the mean value of all distance samples in the last group is calculated. Also, the number of the distance measurement samples in each class is counted for future processing.

Figure 7-3 shows an example of the distance measurements for a few seconds when two pedestrians passed the sensor sight line. As depicted in Figure 7-3, the object detection process in cases when objects (pedestrians) pass one by one is straightforward. However, in some cases, objects such as pedestrians walking their bikes or pedestrian hands and bags can be considered as a new class. The average value of the distance samples in this type of class will be very close to the average of the previous or next class but, the number of samples will be much smaller than the sample class belonging to the pedestrian body. So, some thresholds can be defined on the average value and the number of the samples in each class of measurement to eliminate over-counting.

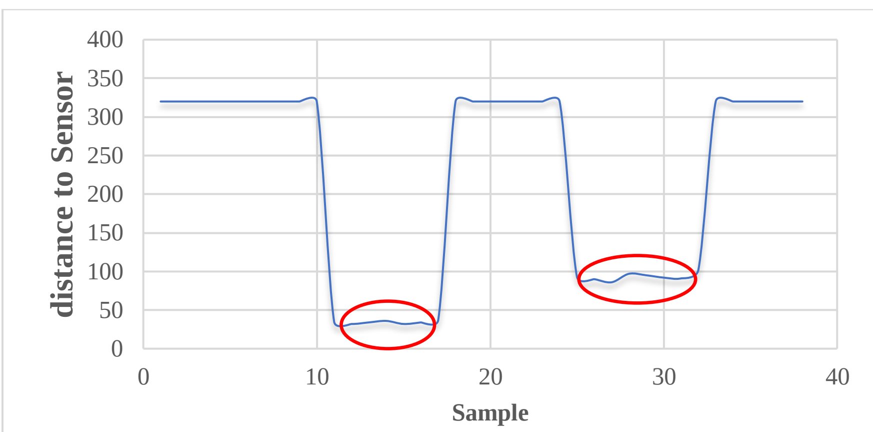

Figure 7-3. Sample of Measurement for Two Objects

In addition to the aforementioned issue, there are situations in which pedestrians pass side by side without any detectable gap between them. Figure 7-4 illustrates this situation. To be able detect these patterns (objects walking almost in parallel), another threshold for the mean value for each sample class needs to be defined. As explained before, each sample class refers to a group of samples that are tightly close. So, if the differences between the mean values of two subsequent sample classes are more than the threshold value, the second class is detected as new object.

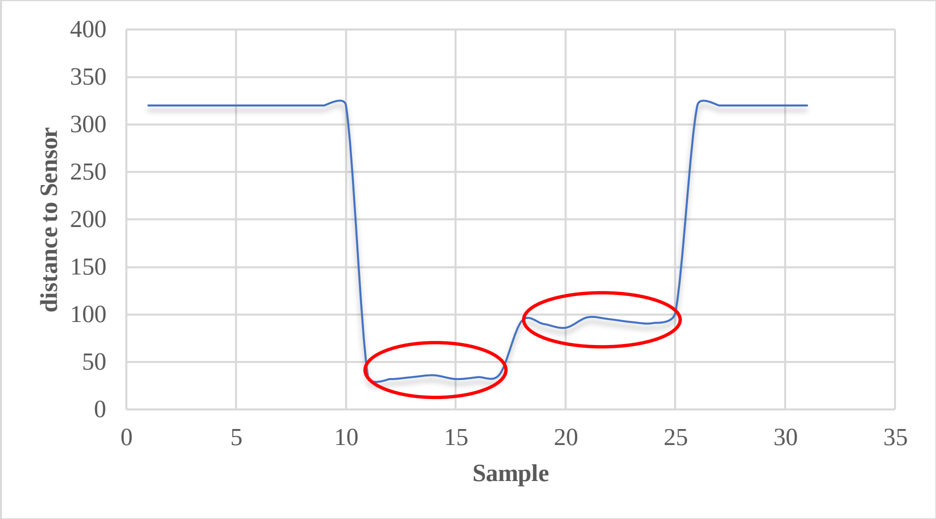

Figure 7-4. Distance Samples in Case Two Pedestrians Passing Almost Parallel

A.2.4 Decision Making

In this step, based on the defined rules on the mean values and number of distance samples in each class, the algorithm decides whether or not the passing object is a pedestrian. If the rules are satisfied, the object is counted as a pedestrian and the counter value is increased. In order to have a better view of the pattern in each class, the decision making is done based on the information from the last four classes. This information helps to check if the two subsequent patterns with close distance mean values belong to the same pedestrian or two separate pedestrians.

After doing so, the processor gets the time from the real-time clock module and sends the counter value to the server every 15 minutes (it can be changed by user). Then, the counter value is reset to zero.

Figure 7-5 provides the flow chart of the pedestrian detection methodology described above.

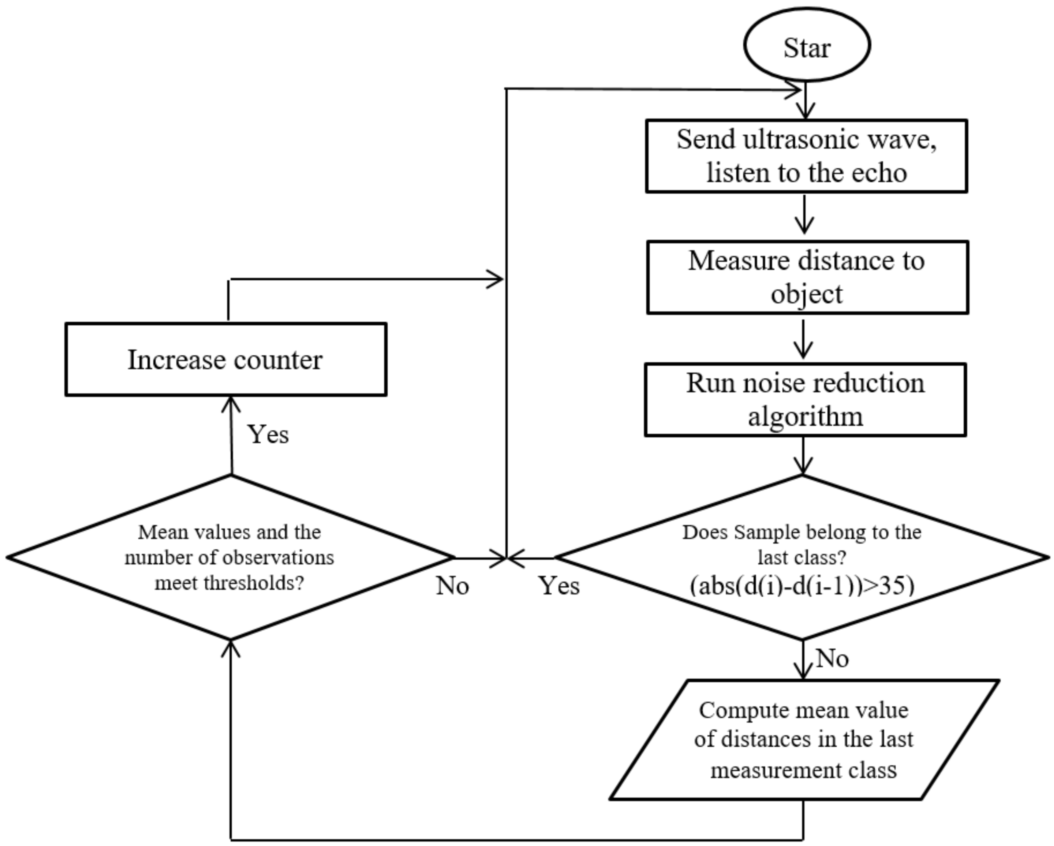

Figure 7-5. Flow chart for Pedestrian Detection Methodology

A.2.5 Performance Measures

In order to evaluate the performance of the system, the following testing protocol was applied:

Selection of Testing Sites: In this case sidewalks with different volume intensities, as well as different pedestrian flow patterns such as people walking in groups, were the subjects of interest.

Sensor installation: Sensors were installed on existing infrastructure (posts). In parallel with the sensor, a video camera on a mast was installed. In one of the testing locations, an infrared sensor (pyro box contact) from Eco-Counter (http://www.eco-compteur.com) was also installed.

Data Processing and Analysis: After several hours of data collection with the two systems and the video camera, counts for every 15-min interval were obtained for each sensor. Video data was processed manually and defined as the “ground truth”. For this purpose, plots and error measures were obtained. The error and deviation between the sensor and ground truth counts are computed using the Absolute Percentage Deviation (AAPD):

$$error_i = \frac{A_i - G_i}{G_i} \quad (1)$$

$$AAPD = \frac{1}{n}\sum_{i=1}^{n}\left|\frac{A_i - G_i}{G_i}\right| \quad (2)$$

where A_i is the automated count for time i (15min in this case), and G_i is the manual count for time i.

A.3 SYSTEM EVALUATION

This section presents the approach that was used to evaluate the performance of the ultrasonic-based counting system using the protocol defined previously. As a first step, three different sites with different widths and volume conditions were selected. For each site, one or two days of data collection were conducted from which video data was also recorded to obtain manual counts. These 3 sites are described as follows:

A.3.1 Site selection

Site 1 - Milton Street – site with pedestrians walking in groups. The ultrasonic sensor was first installed on Milton Street, in Montreal, at a site located a few blocks east of McGill University, on the southern sidewalk. This location was chosen because of its relatively high flow of pedestrians, most of which are university students either heading to or away from the university. It is not difficult to observe pedestrians walking in groups, which is a condition that is critical for automatic counting with traditional sensors such as infrared.

Site 2 – Sherbrooke Street – site without a wall. The second site was located on Sherbrooke Street West, near the main gate of McGill University, Montreal. The sidewalk was selected because of its high pedestrian traffic, as well as for its lack of a wall in the proximity. The width of the sidewalk is more than the first site and there is no wall on one side of the sidewalk. A limitation of an infrared sensor is that sidewalks in which the sensor is installed should have a wall or a clear physical-delimitated area. Open spaces or inexistence of a wall can deteriorate the performance of this type of sensor.

Site 3 – University Street – site with stop-and-going flow conditions. The third site is located at the intersection if University Street and Saint Catherine. This site was selected because of its high pedestrian traffic given its proximity to a commercial area and for the retail exhibit windows that cause stop-and-going flow conditions. Pedestrians often stop to look at retail exhibits causing over-counting issues. However, this site has a well-defined counting area with a wall.

site 1 site 2 site 3

Figure 7-6. Snapshot of the selected sites

A.3.2 Results

The general results of the three sites are presented in Table 7-1. From this table, one can observe that the errors percentage varied between 0.9 and 24.7 for the ultrasonic sensor and between 0.8 and 42.1 for the infrared sensor over the 3 test sites. In addition, AADP for the ultrasonic and infrared sensors ranged from 6.4 to 12.3 and 4.6 to 19.4, respectively. These results clearly show the potential of using Ultrasonic technology in our counting solution.

Table 7-1 Summary statistics of tests per site

Measure		Site 1		Site 2		Site 3	
Error (%)	Infrared	Min	-	Min	0.9	Min	0.8
		Max	-	Max	42.1	Max	9.9
	Ultrasonic	Min	1.7	Min	3.7	Min	0.9
		Max	24.7	Max	18.6	Max	27.2
AADP (%)	Infrared	-		19.4		4.6	
	Ultrasonic	12.3		9.9		6.4	

The initial findings clearly show the potential of this counting system with a very interesting performance on sidewalks with low to high volumes (from 200 to 800 pedestrians per hour). The under-counting error, due mainly to occlusion, varies between 0 to -20% in 98% of the cases. Based on the results, the error increases slightly with volumes, with a power or linear function, which can be used to generate correction functions. These functions can be used to improve the counting estimates (reduce error) in congested sidewalks.

The proposed system could help in handling the limitations of infrared technology, such as the requirement of an obstruction, such as a wall, or well-defined detection area. In open areas or wide sidewalks without walls, the definition of the counting area is a challenge for infrared sensors. In this condition, the accuracy of the infrared-based sensor is deteriorated. In the proposed ultrasonic system, the coverage area can be set by the user, so it can be used at different locations including open spaces. Additionally, the ultrasonic technology is not sensitive to temperature as opposed to an infrared-based sensor which can be significantly affected on hot-sunny days.

Although the result shows promising performance in terms of real-time counting with acceptable accuracy, with further development and testing of the proposed solution, we found some limitations as presented below:

- The Ultrasound range finder sensors have a fairly low sample rate (less than 10 sample per second). This limits the sensor's performance when the objects are moving fast or cases of occlusion. Additionally, low sample rates makes it impossible to detect the direction of the objects.
- The range of the sensors are limited to less than 4 meters, which makes it limited to narrow sidewalks.
- The ultrasound waves diverge by increasing the distance (15- degree angle), which reduces the accuracy when people are walking in a group.

To address these issues, authors benefit from high sample rate, accurate Lidar sensors with very narrow beams.